Aus der
Klinik für Hämatologie, Onkologie und klinischen Immunologie
der Heinrich-Heine-Universität Düsseldorf
Direktor: Universitätsprofessor Dr. med. R. Haas

# Molekulare Charakterisierung und Therapieformen bei Lungenkarzinomen

## Habilitationsschrift

zur Erlangung der Venia legendi für das Fach
Innere Medizin
der Hohen Medizinischen Fakultät
der Heinrich-Heine-Universität Düsseldorf

vorgelegt von

Dr. med. Ulrich-Peter Rohr
aus Berlin-Tempelhof

2005

## Inhaltsverzeichnis


**Zusammenfassung** **03**

**1. Einleitung** **05**

**2. Einsatz des adeno-assoziierten Virus Typ 2 (AAV-2) als Vektor zur Gentherapie beim nichtkleinzelligen Lungenkarzinom (NSCLC)** **09**

2.1. Lebenszyklus des AAV-2-Wildtyps und Herstellung von rekombinanten AAV-2-Partikeln 09

2.2 Tropismus von AAV-2 in humanen Zellen und Lungenkarzinomzellinien 12

2.3 Quantifizierung von rAAV-2-Partikeln 15

2.4 Einsatz von rAAV-2 bei NSCLC-Zelllinien 18

**3. Identifizierung neuer prognostischer Faktoren bei Patienten mit kleinzelligem Lungenkarzinom (SCLC)** **19**

3.1 Die prognostische Bedeutung des c-kit Rezeptors bei Patienten mit SCLC 19

3.2 Die prognostische Bedeutung des Tumorsuppressorgens FHIT bei Patienten mit SCLC 22

**4. Molekulare Charakterisierung der Lungenkarzinome im Vergleich mit normalem Lungengewebe** **25**

**5. Schlussfolgerung und Ausblick** **31**

**6. Literatur** **36**

**7. Abkürzungsverzeichnis** **40**

**8. Danksagung** **42**

**9. Zusammengefasste Publikationen** **43**

## Zusammenfassung

Ziel der vorliegenden Arbeit war die molekulare Charakterisierung von primären Lungenkarzinomen, die Identifizierung neuer prognostischer Faktoren sowie die Etablierung eines neuen Vektorsystems, dem adeno-assoziierten Virus Typ-2 (AAV-2) zur Genersatztherapie beim Lungenkarzinom.

Da wir nachweisen konnten, dass ein neues Vektorsystem, rAAV-2, einen hohen Tropismus für Lungengewebe hat, untersuchten wir die histologischen Subtypen von Lungenkarzinomen hinsichtlich ihrer möglichen Empfänglichkeit für einen rAAV-2-vermittelten Gentransfer. Es zeigte sich dabei eine hohe Affinität von rAAV-2 ausschließlich zu den nicht-kleinzelligen Lungenkarzinomen (NSCLC), da diese den Rezeptorbesatz aufwiesen, die rAAV-2 zur effektiven Infektion benötigen. Vor der Durchführung von funktionellen Experimenten entwickelten wir eine real-time PCR Methode zur Qantifizierung von genomischen und infektiösen Titern der rekombinant hergestellten AAV-2-Partikel. Für die funktionellen Untersuchungen verwendeten wir einen neuen, therapeutischen rAAV-2-Vektor, der das humane Wildtyp-p53-Gen enthält (rAAV-2-p53). Dieser therapeutische Vektor zeigte in-vitro eine signifikante Hemmung des Zellwachstums von NSCLC-Zelllinien. Weiterhin erhöhte rAAV-2-p53 die Sensitivität von Tumorzellen gegenüber dem Chemotherapeutikum Cisplatin. Die präklinischen Vorarbeiten betrachteten wir als Vorraussetzung für einen Einsatz des AAV-2-Vektorsystems im Rahmen einer klinischen Studie zur Behandlung von Patienten mit nicht-kleinzelligem Lungenkarzinom.

Zur individuellen Prognose des Krankheitsverlaufes für Patienten mit Lungenkarzinom und der Wirksamkeit einer bestimmten Therapie ist die Identifizierung pathophysiologisch relevanter Gene entscheidend. Die Fortschritte in der Erforschung prognostischer und prädiktiver Faktoren sind beim NSCLC mit Identifizierung von p53, k-ras oder EGFR-1 bereits erkennbar. Demgegenüber sind die Erkenntnisse von prognostisch relevanten Signalwegen beim SCLC gering. In meiner Arbeit stelle ich 2 pathophysiologisch relevante Gene vor. Dabei handelt es sich um den c-kit-Rezeptor und das „fragile histidine triad“ (FHIT)-Tumorsupperssorgen, deren Proteinexpression in 88 % bzw 62 % aller SCLC-Primärtumore immunhistochemisch nachweisbar ist. Die klinische Relevanz liegt darin, dass Patienten mit Expressionsverlust jedes einzelnen dieser beiden Gene eine signifikant schlechtere

Überlebenswahrscheinlichkeit haben. Somit ist es möglich eine Patientengruppe zu identifizieren, die einer modifizierten Therapieform bedarf.

Eine molekulare Charakterisierung der Lungenkarzinome ist durch Oligonukleotid-Mikroarray-Technologie möglich. So verglichen wir das Genexpressionsprofil von primären Lungentumoren mit normalem Lungengewebe. Mittels computerunterstützter Normalisierung und Multiklassenanalyse der Daten gelang es, 944 signifikante Gene bei SCLC und NSCLC zu identifizieren, die gegenüber dem Normalgewebe der Lunge differentiell exprimiert waren. In Abhängigkeit vom histologischen Subtyp zeigten sich Unterschiede bei solchen Genen, die an der Regulation von Proliferation und Zelladhäsion beteiligt sind. Weiterhin wiesen die Lungentumore ein individuelles Muster von Genen auf, die für Strukturproteine kodieren. Die differentielle Genexpression erlaubt eine diagnostische Unterscheidung der unterschiedlichen histologischen Lungenkarzinomentitäten auf molekularer Ebene. Darüber hinaus wurden für SCLC sowie die Adeno- und Plattenepithelkarzinome der NSCLCs Gene identifiziert, die erfolgversprechende Kandidaten für eine zielgerichtete Therapie sind.

## 1. Einleitung

Das Lungenkarzinom steht als Todesursache durch Krebs bei Männern an erster und bei Frauen an dritter Stelle. So starben in Deutschland im Jahre 2000 39.000 Menschen an einem Lungenkarzinom. Selbst mit der derzeit besten chemotherapeutischen Behandlung mit einer Kombination aus Cisplatin und einem weiteren Zytostatikum wie Vinorelbine oder Gemcitabine liegt die mediane Überlebenszeit für Patienten mit fortgeschrittenem Lungenkarzinom bei 9-11 Monaten (Schiller, 2001; Schiller, 2002). Die neue Generation von Zytostatika, wie z.B. die Taxane, führte zu keiner Verbesserung des Gesamtüberlebens der Patienten (Schiller, 2002). Um die Therapie auf eine pathophysiologische Grundlage zu stellen, bedarf es eines besseren Verständnisses der molekularen Karzinogenese der Lungentumoren. Im Gegensatz zu anderen soliden Tumoren, wie z.B. dem kolorektalen Karzinom, ist über den Prozess der Entwicklung einer normalen Zelle des Lungengewebes zum invasiven Lungenkarzinom nur wenig bekannt. Dabei gilt es zu beachten, dass unter dem Begriff Lungenkarzinom verschiedene histologische Entitäten zusammengefasst werden, die charakteristische Unterschiede aufweisen. So unterscheidet man histologisch zwischen kleinzelligen und nicht-kleinzelligen Lungenkarzinomen, wobei letztere in großzellige Karzinome, Plattenepithelkarzinome und Adenokarzinome unterteilt werden. Diese Klassifikation spiegelt auch eine unterschiedliche Prognose wider, wobei je nach histologischem Phänotyp die genetischen Veränderungen unterschiedlich sind. So ist das Tumorsuppressorgen (TSG) p16 bei 30-70 % der Patienten mit NSCLC inaktiv, während ein weiteres Tumorsuppressorgen, das Retinoblastom-(RB) Gen, nur in 15-30 % der Fälle verändert ist (Forgacs, 2001). Dem gegenüber beobachtet man bei Patienten mit SCLC in über 90 % ein abnormales RB-Gen, während das TSG p16 intakt ist (Wistuba, 2001). Von besonderem therapeutischen Interesse sind Gene, die in Tumoren von Patienten mit SCLC und NSCLC in gleicher Weise verändert sind. Tatsächlich zeigen beide Subgruppen in karyotypischen Untersuchungen eine Reihe von identischen Chromosomenaberrationen (Girard, 2000). Ein Locus mit der höchsten Deletionsrate liegt auf Chromosom 17p, wo das Tumorsuppressorgen p53 kodiert wird. Das p53 Protein hat eine Schlüsselrolle für die Aufrechterhaltung der genomischen Integrität wobei Schäden der zellulären DNA einen Anstieg in der Konzentration von p53 zur Folge haben. Dadurch kommt es in einem zweiten

Schritt zu einem Anstieg proapoptotischer, zellzyklusarretierender und DNA-reparaturregulierender Gene (Levine, 1997). Angesichts der exponierten Stellung von p53 ist es möglich, in das gesteigerte Wachstumsverhalten der Lungentumorzelle einzugreifen. Als Gentransfersysteme werden virale und nicht-virale Vektoren verwendet, von denen insbesondere virale Vektoren für die klinische Anwendung eine Rolle spielen. An ein virales Vektorsystem, welches in-vivo Verwendung finden soll, wird eine Vielzahl von Anforderungen gestellt. Neben einer fehlenden Pathogenität für den Menschen sollte die Lungenkarzinomzelle möglichst selektiv und unabhängig vom Zellzyklus durch den Vektor infiziert werden. Postinfektös sollte der replikationsunfähige Vektor intrazellulär persistieren, damit das therapeutische Gen über einen langen Zeitraum transkribiert und translatiert werden kann. Ein solches Vektorsystem, welches diesen durch seine Eigenschaften diesen Voraussetzungen nahe kommt, leitet sich vom Wildtyp des adeno-asoziierten Virus Typ 2 (wt-AAV-2) ab. Das zu den Parvoviren gehörende, replikationsunfähige DNA-Virus, das die Zielzelle unabhängig vom Zellzyklus infiziert, ist erst nach Superinfektion mit einem zweiten Virus aus der Herpes- oder Adenovirusfamilie in der Lage, sich zu replizieren. Darüber hinaus führt AAV-2 beim Menschen zu keiner Erkrankung (Berns, 1990; Monahan, 2002). Das therapeutische Potential dieses Vektorsystems wurde bereits in klinischen Studien gezeigt, in denen die Sicherheit und Effektivität von rekombinant hergestellten AAV-2 (rAAV-2) als Gentransfersystem zur Behandlung von Patienten mit zystischer Fibrose (Moss, 2004) und Hämophilie B (Wang, 2005) nachgewiesen werden konnte. Eine Brücke zur Krebstherapie eröffnete sich durch die Erkenntnisse, dass eine Infektion mit wt-AAV-2 einen tumorhemmenden Einfluss auf die Entstehung des Zervixkarzinoms hat (Smith, 2001) und die Sensitivität von Sarkom- und Karzinomzellen für eine Chemotherapie erhöht (Duverger, 2002; Schwarzbach, 2002). Eines unserer Ziele war es, dieses Vektorsystem für die Behandlung von Patienten mit Lungenkrebs zu entwickeln und einzusetzen. Dazu untersuchten wir den Tropismus von AAV-2 für normales Lungengewebe und Lungenkarzinome. Für funktionelle Experimente benutzten wir eine Methode, um genomische und infektiöse rAAV-2-Titer unabhängig vom therapeutischen Gen zu ermitteln. Danach entwickelten wir den therapeutischen rAAV-2-p53-Vektor, der die DNA für das p53 trägt. Danach analysierten wir die funktionellen Effekte von p53 auf Zelllinien von nicht-kleinzelligen Lungenkarzinomen. Zusätzlich führten wir funktionelle Tests mit dem Chemotherapeutikum

Cisplatin durch, um zu sehen, ob rAAV-2-p53 die Chemosensitivität von Tumorzellen erhöhen kann.

Neben p53 ist bei Lungenkarzinomen von einem Verlust von weiteren, bisher unbekannten Tumorsuppressorgenen auszugehen. Neben den bereits beschriebenen drei chromosomalen Regionen mit den höchsten Deletionsraten existiert ein weiterer Locus mit Verlust am kurzen Arm von Chromosom 3, der bei 90-100 % der Tumoren von Patienten mit SCLC und 50-80 % der Tumoren von Patienten mit NSCLC vorhanden ist (Wistuba, 2001). Als Kandidat für ein potentielles Tumorsuppressorgen in dieser Region gilt das „fragile histidine triad“ (FHIT)-Gen, eine Dinukleotidhydrolase auf Chromosom 3p14. In Tumorzellen wurde durch Gentransfer des FHIT-Gens in-vitro- und in-vivo Apoptose eingeleitet und Tumorwachstum verhindert (Roz, 2002; Ji, 1999). Neben der Rolle als Tumorsuppressorgen war die Expression dieses Genes bei Tumoren von Patienten mit NSCLC im Stadium I mit einem besseren medianen Überleben assoziiert (Toledo, 2004). Somit galt die Expression von FHIT als prognostischer Faktor für diese Patienten. Somit war ein weiterer wesentlicher Aspekt meiner Arbeit die Identifikation von neuen, molekularen Prognosefaktoren bei kleinzelligen Lungenkarzinomen. Hierzu bauten wir eine Gewebebank für Patienten mit SCLCs auf, deren Krankheitsverlauf im weiteren sorgfältig dokumentiert wurde. Mittels immunhistochemischer Färbemethoden bestimmten wir die Expression von FHIT und überprüften einen möglichen Zusammenhang mit dem Überleben der Patienten. Neben dem Tumorsuppressorgen FHIT untersuchten wir auch die Expression des c-kit-Rezeptors. Da der c-kit Rezeptor auf 79-88% der kleinzelligen Lungenkarzinome exprimiert wird (Hibi, 1991), spielt er für die Pathophysiologie von SCLCs eine wichtige Rolle (Rygaard, 1993). Diese Hypothese wird unterstützt durch die Expression des „stem cell factors“ (SCF) in 57-76 % aller untersuchten SCLC-Zelllinien, da SCF der Ligand von c-kit ist und im Sinne einer autokrinen Schleife die Zellproliferation erhöht (Hibi, 1991). Zur Prüfung der prognostischen Relevanz bestimmten wir mittels Immunhistochemie die Expression dieses Rezeptors bei Patienten mit SCLC und prüften in Univariat- und Multivariatanalysen, ob c-kit ein unabhängiger Prognosemarker ist.

Da mit den bisherigen Methoden nur einzelne Gene hinsichtlich ihrer prognostischen Relevanz untersucht werden konnten, suchten wir nach einer Möglichkeit, einen größeren Anteil des Transkriptoms der Lungentumorzelle zu betrachten. Dies ist mit Hilfe der Microarray-Technologie möglich, wobei für Patienten mit Plattenepithelkarzinomen in der

Kopf-Halsregion die prognostische Relevanz der Methodik gezeigt werden konnte (Hanna, 2001). So ließen sich mit Hilfe der cDNA Array Diagnostik sechzig tumor-assoziierte Gene identifizieren, deren Expression eine Vorhersage erlaubte, ob der Tumor auf eine Strahlentherapie ansprechen würde. Der dritte Teil meiner experimentellen Arbeit beschäftigt sich daher mit der Entwicklung und Nutzung einer Methode zur molekularen Charakterisierung von Lungenkarzinomen. Dabei isolierten wir zunächst das Tumorgewebe aus Bronchoskopieproben mittels „Laser-Capture Mikrodissektion“. Damit konnten wir mittels der Affymetrix-GeneChip-Technologie ein 8793 Gene umspannendes Expressionsprofil von primären humanen Lungenkarzinomen erstellen. Wir ermittelten die Genexpressionsprofile der Tumoren von 20 Patienten mit NSCLC und 9 Patienten mit SCLC. Diese Profile verglichen wir mit denen aus 5 Proben von Patienten ohne Lungentumor. Auf diese Weise gelang es uns, 944 Gene zu identifizieren, die von Adenokarzinomen, Plattenephitelkarzinomen und kleinzelligen Karzinomen der Lunge im Vergleich zu normalen Lungengewebe differentiell exprimiert werden. Auf der Grundlage dieser Ergebnisse konnten wir eine Datenbank zur molekularen Klassifikation der Lungentumore aufbauen. Neben der damit geschaffenen neuen Klassifikation haben wir einen Einblick auf neue Aspekte in der Pathophysiologie des jeweiligen histologischen Subtyps gewonnen.

## 2. Einsatz des adeno-assoziierten Virus Typ 2 (AAV-2) als Vektor zur Therapie beim nichtkleinzelligen Lungenkarzinom (NSCLC)

### 2.1. Lebenszyklus des AAV-2-Wildtyps und Herstellung von rekombinanten AAV-2-Partikeln

Der AAV-2-Wildtyp (wt-AAV-2) gehört zu der Gruppe der humanen Parvoviren und besteht aus 4679 Basen einer Einzelstrang-DNA, die von einer Kapsidhülle umgeben ist. Mit seiner Größe von 22nm gehört es zu den kleinsten bekannten infektiösen Viren. Trotz der hohen Seroprävalenz von wt-AAV-2 von 80 % in der Bevölkerung ist das Virus mit keiner Erkrankung assoziiert (Monahan, 2002).

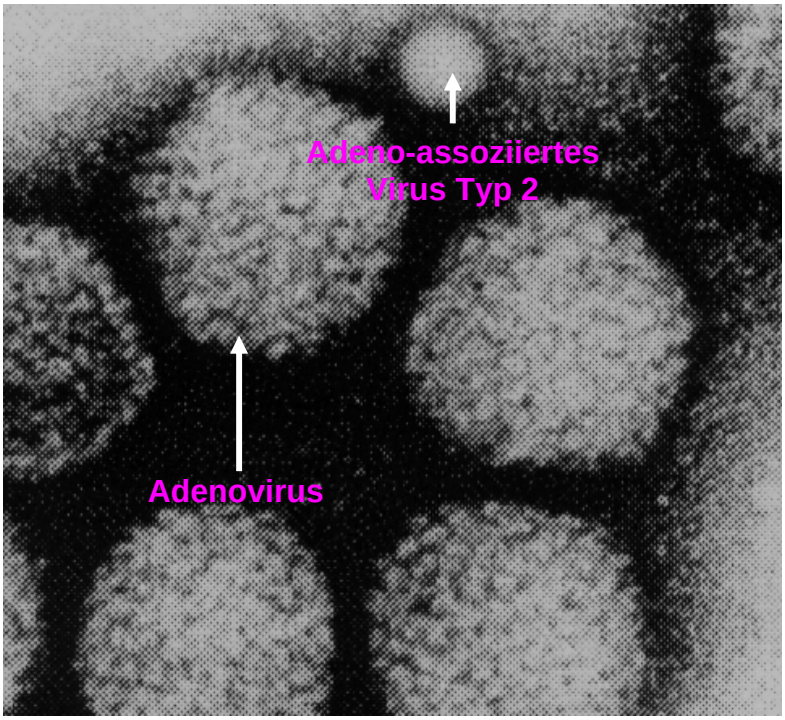


**Abb. 1: Größenvergleich von Adenovirus und adeno-assoziiertem Virus Typ-2 in 250.000facher Vergrößerung** (Quelle: Prof. Steward McNulty, Vetenary Sciences Division, Queen´s University, Belfast, GB, www.qub.ac.uk).

Das Genom von wt-AAV-2 kodiert für zwei Proteine *rep* und *cap*. Das nicht strukturbildende Rep-Protein dient der viralen Replikation und chromosomalen Integration, während das Cap-Protein die Virushülle bildet, welche die DNA umgibt und die ikosaedrische Struktur von AAV-2 formt. Im AAV-2-Genom wurden drei Promotor p5, p19 und p40 identifiziert. Die Transkripte des p5 und p19 Promotors bilden durch alternatives Splicen die vier Rep-Proteine Rep40,

Rep52, Rep68 und Rep78. Die Transkripte des p40 Promotors bilden die 3 Hüllstrukturproteine von AAV-2, VP1, VP2 und VP3, die im stöchiometrischen Verhältnis von 1:1:10 gebildet werden. Das AAV-2-Genom wird flankiert durch die „Inverted Terminal Repeats“ (ITR), die aus 145 Basenpaaren an jeder Endseite des Genoms bestehen. Die ITRs sind wichtige Elemente für die Verpackung, Replikation, Transkription und Integration von AAV-2 in der Wirtszelle.

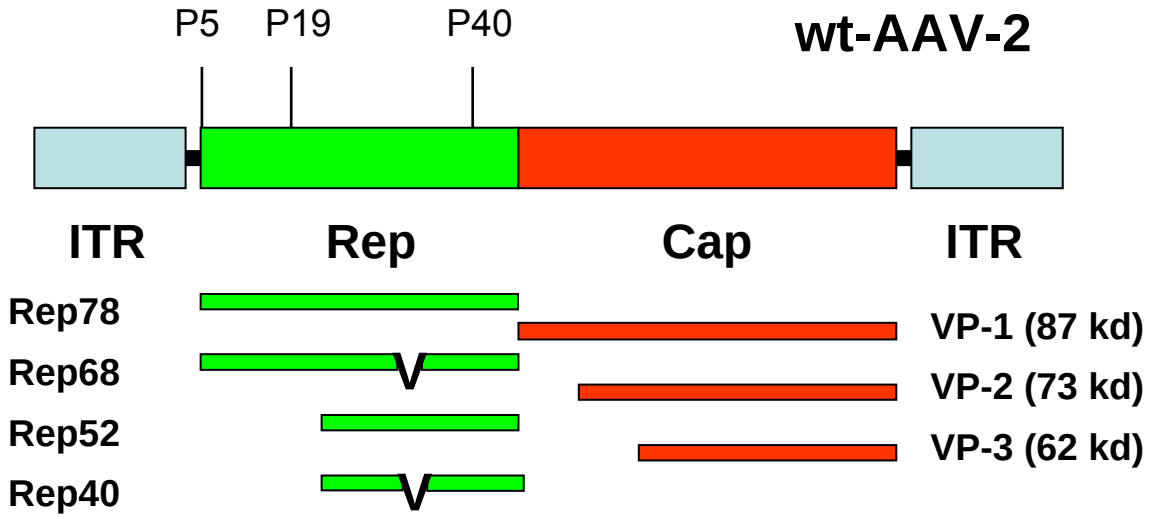


**Abb. 2: Genomische Anordnung und Organisation des wt-AAV-2.**

wt-AAV-2 ist ein Dependovirus und benötigt die Hilfe eines weiteren Virus zur eigenen Replikation. Als Helferviren wurden Mitglieder aus den Familien der Herpesviren und Adenoviren identifiziert. In Abwesenheit der Helferviren integriert sich das AAV-2-Genom in eine zwei Kilobasen umfassende Stelle im langen Arm von Chromosom 19 (19q13.3). Diese Rep 68 und Rep78 vermittelte, zielgerichtete provirale Integration in das Wirtschromosom ist ein bislang einzigartiges Phänomen bei Viren, die eukaryote Zellen infizieren können. Wenn eine latent durch wt-AAV-2-infizierte Zelle durch ein Adeno- oder Herpesvirus superinfiziert wird, kommt es, nach Exzision der proviralen DNA aus dem Wirtschromosom 19, zur Replikation und Verpackung des wt-AAV-2-Genoms. Die durch das Helfervirus bedingte Zelllyse führt schließlich zur Freisetzung der neugebildeten AAV-2-Viren (Vihinen-Ranta, 2004).

Am Beginn meiner Arbeit stand die Herstellung von rekombinanten AAV-2-Partikeln (***Ref. A***). Diese rAAV-2-Partikel sollten ohne Superinfektion eines Helfervirus produziert werden, um ein reines rAAV-2-Vektorprodukt zu erhalten und eine Rekombination mit anderen Viren zu vermeiden. Aufbauend auf den Arbeiten von Hörster (1999), Grimm (1998) und Samulski, (1989), die zur Klonierung des Vektorplasmids pAAV-gfp-AR6- und des Helferplasmids pDG führten, verwendeten wir diese zwei Plasmide zur Produktion von rekombinanten rAAV-2-Partikeln. Das Vektorplasmid pAAV-gfp-AR6- enthielt das Markergen für das „Enhanced Green Fluorescent Protein (EGFP)“ und als therapeutisches Gen die HIV-1 gerichtete Antisensesequenz AR6. Flankiert wurden die Gene von den ITRs des AAV-2-Klons psub201, während der „immediate-early“ Promoter des humanen Zytomegalievirus als Promotor diente. Das Helferplasmid pDG enthielt alle Verpackungs- und adenoviralen Helfervirusgene Rep, Cap bzw. E2A, E4, VA, die zur rAAV-2-Partikelproduktion benötigt werden. Vektor- und Helferplasmid transfizierten wir mittels Kalziumphosphatpräzipitation in die Produktionszelllinie 293T. Nach Ernte, Aufreinigung und Konzentration der gebildeten rAAV-2-Vektoren bestimmten wir durchflusszytrometrisch die Höhe des infektiösen Titers. Nach Infektion der Zelllinie HeLa mit dem EGFP transgenen rAAV-2-Vektor bestimmten wir den prozentualen Anteil an grün fluoreszierenden HeLa-Zellen, wobei der infektiöse rAAV-2-Titer, je nach Vektorpräparation, zwischen $4x10^8$ und $2x10^9$ / ml lag. Um für die weiteren Zellexperimente einen einheitlichen Vektortiter zu erhalten, führten wir alle aufgereinigten Vektorpräparationen zu einer Gesamtsuspension mit einem Titer von $6x10^8$ rAAV-2-Partikeln pro Mililiter zusammen. Unsere Untersuchungen zeigten, wie es durch die Verwendung der Plasmide pAAV-gfp-AR6- und pDG möglich ist, ohne eine Superinfektion von Adenoviren oder Herpesviren infektöse rAAV-2-Partikel in hoher Konzentration und Reinheit herzustellen.

## 2.2 Tropismus von AAV-2 in humane Zellen und Lungenkarzinomzellinien

Nach der Herstellung von infektiösen rAAV-2-Partikeln wandten wir uns der Frage zu, ob AAV-2 ein geeignetes Vektorsystem für einen Gentransfer in Zellen aus der Lunge oder Lungenkarzinomen ist. Ergebnisse über die Empfänglichkeit unterschiedlicher Gewebe für AAV-2 waren bisher für verschiedene Tiere und Zelllinien bekannt. Diese Resultate sind zunächst jedoch nicht auf primäre, humane Zellen übertragbar. Deshalb untersuchten wir den Tropismus von rAAV-2 beim Menschen an „gesunden" Zellen. Hierzu wurden neun unterschiedliche, primäre Zelltypen neuroektodermaler, mesenchymaler oder endodermaler Herkunft mit rAAV-2 transduziert. (***Ref. A***). Wir inkubierten infektöse, virale rAAV-2-EGFP-Partikel mit den primären humanen Zellen und analysierten den viral vermittelten Transfer des EGFP-Gens mittels Durchflusszytometrie. Von den neun untersuchten primären humanen Zelltypen wiesen Bronchialepithelzellen, arterielle Endothelzellen sowie glatte und quergestreifte Skelettmuskulatur die höchsten Transduktionsraten zwischen 34,3 % und 81,6 % auf. Geringere Transduktionsraten zwischen 4,3 % und 19,5 % fanden wir bei Chondrozyten, Haarfollikelzellen und Fibroblasten, während CD34-positive, hämatopoietische Blutstamm-und Vorläuferzellen sowie Melanozyten für einen AAV-2-vermittelten Gentransfer resistent waren.

Da das Bronchialepithel der Lunge zu den empfänglichsten humanen Zellen für rAAV-2 gehörte, interessierte uns als nächstes das Verhalten von Zellen aus Lungenkarzinomen gegenüber AAV-2. Wir untersuchten daher zehn Lungenkarzinomzelllinien hinsichtlich der Effizienz eines AAV-2-vermittelten Gentransfers (***Ref. D***). Bei NSCLC-Zelllinien zeigte sich eine hohe Empfänglichkeit für rAAV-2 mit einer Transduktionseffizienz zwischen 64,4 % und 98,9 %. Im Gegensatz dazu waren SCLC-Zelllinien nahezu resistent mit Transduktionsraten zwischen 1,1 % und 5,9 %.

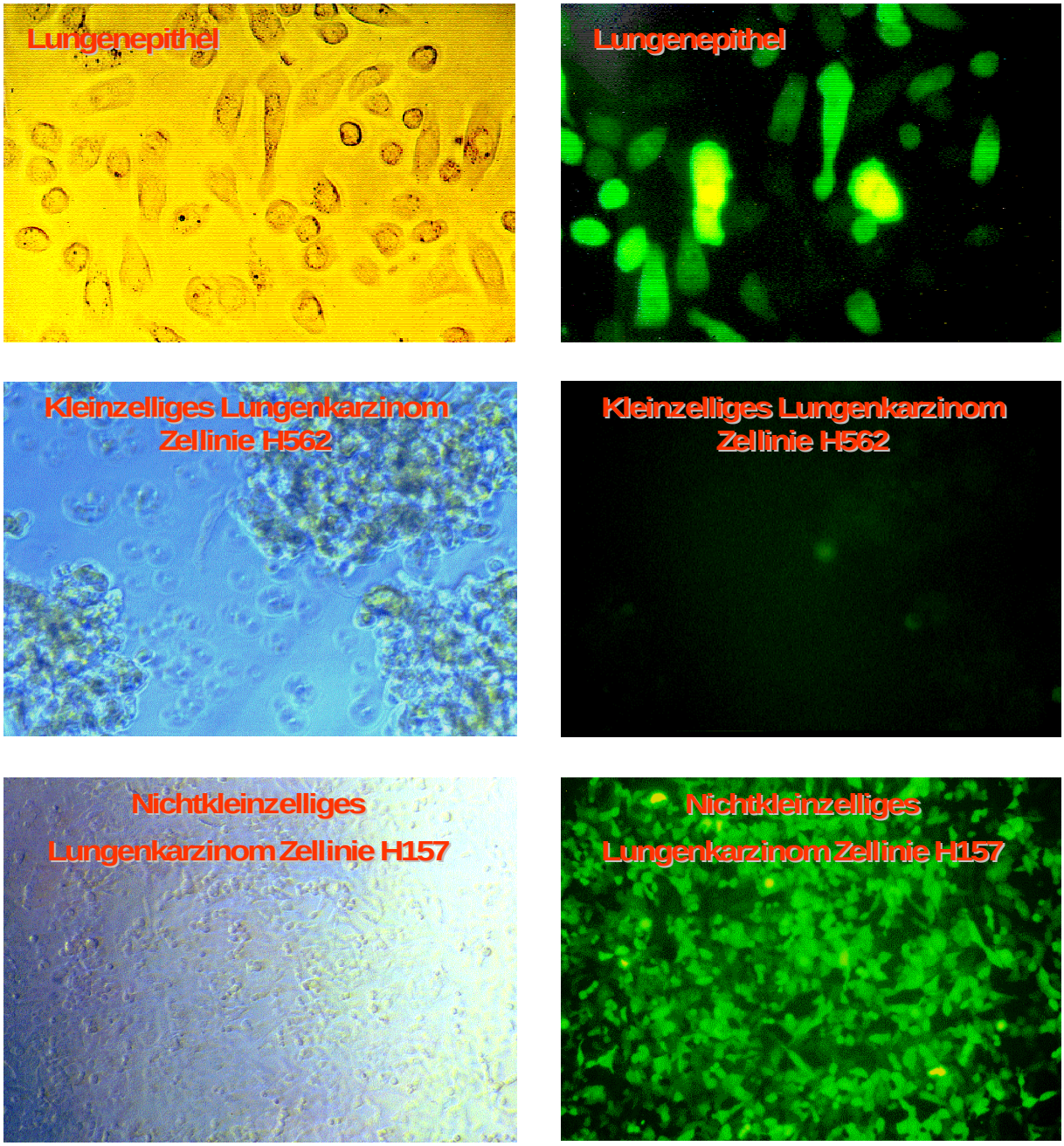


**Abb. 3: Unterschiedlicher Tropismus von rAAV-2 in Lungenepithel, kleinzellige und nichtkleinzellige Lungenkarzinome.**

Als Grund für die unterschiedlichen Transduktionsergebnisse zwischen den verschiedenen primären humanen Zellen und den Lungenkarzinomzellinien vermuteten wir einen unterschiedlichen Rezeptorbesatz der Zellen, der für die Bindung und Internalisierung von rAAV-2 von Bedeutung ist. Die AAV-2-Infektion wird initiiert durch die Bindung an ein ubiquitär vorkommendes membranassoziiertes Heparansulfat-Proteoglykan, während der

Eintritt von AAV-2 in die Zelle durch mindestens einen der bisher bekannten Korezeptoren, dem „fibroblast growth factor receptor-1“ (FGFR-1) und Integrin αVß5, vermittelt wird. Wir untersuchten daher mittels Immunhistochemie und Durchflußzytometrie die Expression von FGFR-1 und αVß5 auf den benignen und malignen Zellen. Es zeigte sich, dass die Zellen bzw. Zelllinien, die hohe Transduktionsraten für rAAV-2 aufwiesen, beide AAV-2-Korezeptoren exprimierten. Im Gegensatz dazu konnte keiner der beiden AAV-2-Korezeptoren auf den Zelltypen bzw. Zelllinien nachgewiesen werden, die niedrige Transduktionsraten aufwiesen oder für einen AAV-2-vermittelten Gentransfer resistent waren (***Ref. A und Ref. D***).

Insbesondere zeigten die Experimente, dass rAAV-2 ein effektiver Vektor für einen Gentransfer in nicht-kleinzellige Lungenkarzinome ist. Der Grund dieser hohen rAAV-2-Transduktionsrate basiert auf der Expression beider AAV-2-assoziierter Korezeptoren auf der Zelloberfläche von nicht-kleinzelligen Lungentumoren. Diese Ergebnisse können als Grundlage zur Weiterentwicklung des Vektorsystems und funktioneller Experimente zur Hemmung des Zellwachstums von Tumoren dieser Entität dienen.

## 2.3 Quantifizierung von rAAV-2-Partikeln

Neben der Auswahl einer geeigneten Zielzelle ist es für gentherapeutische Ansätze mit dem rAAV2-Vekor wichtig, den viralen Titer bestimmen zu können. Die bisherige Virusquantifizierung beruhte darauf, das grün-fluoreszierende Markergen für EGFP mittels rAAV-2-vermitteltem Gentransfer in die Zelle einzuschleusen. Mittels des durchflusszytometrisch bestimmten prozentualen Anteils grün fluoreszierender Zellen konnte der infektiöse virale Titer bestimmt werden.

Für gentherapeutische *in-vivo* Studien bedarf es keines Markergens, sondern nur des therapeutischen Gens. Deshalb ließ sich die oben beschriebene Methode zur Bestimmung des viralen Titers nicht verwenden. Wir entwickelten daher eine quantitative „real-time“ PCR-Methode (qPCR), um den genomischen rAAV-2-Titer zu bestimmen (***Ref. B***). Als Zielsequenz für die PCR-Primer wurde die CMV-Promotorsequenz im rekombinanten AAV-2-Genom gewählt, da der CMV-Promotor bei Gentherapiestudien beim Menschen am häufigsten verwendet wurde. Mit Hilfe des rAAV-2-Vektorplasmids erstellten wir durch serielle Verdünnungen eine DNA-Standardeichkurve, welche fünf Logarithmusstufen umfasst. Um die unbekannte Kopienzahl der bei der Vektorpräparation entstehenden rAAV-2-Partikel zu ermitteln, setzten wir die PCR-Kurve der rAAV-2-Partikel in Beziehung zur DNA-Standardeichkurve. Basierend auf der Menge an viraler Einzelstrang-DNA in der Probe berechneten wir so den genomischen Virustiter. Zur Validierung der neuen Methode haben wir die qPCR ermittelten rAAV-2-Titer mit der bisher verwendeten durchflusszytrometrischen Standardmethode verglichen. Zwischen den Ergebnissen von 42 verschiedenen, über fünf log Stufen umfassenden rAAV-2-Titern, die mit beiden Methoden bestimmt wurden, zeigte sich ein signifikanter ($p<0.0001$) Korrelationskoeffizient von 0,85.

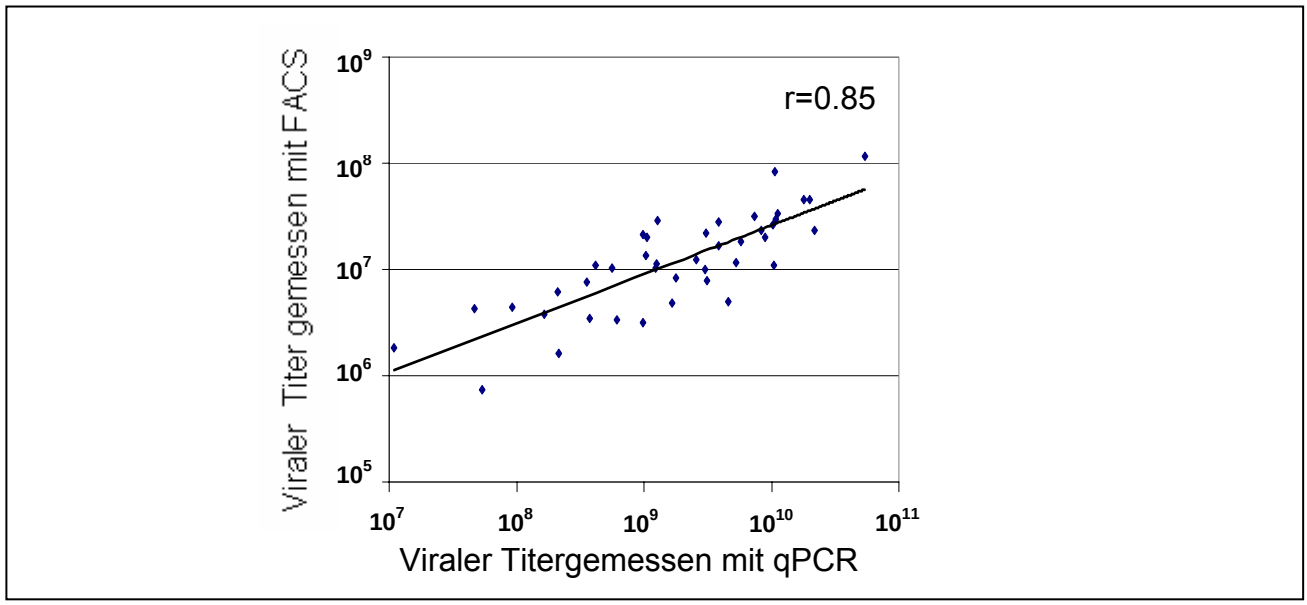


**Abb. 4: Vergleich der rAAV-2-Titer gemessen mit der durchflusszytometrischen Standardmethode (FACS) im Vergleich zur neuen qPCR.** Insgesamt wurden 42 unterschiedliche rAAV-2-Proben, die als Punkte dargestellt sind, miteinander verglichen. Der Korrelationskoeffizient r nach Pearson betrug 0,85.

Weiterhin konnten wir im Vergleich der beiden Methoden zeigen, dass die Rate von genomischen zu infektiösen rAAV-2-Partikeln im Mittel bei 253:1 lag. Innerhalb von 42 Viruspräparationen kamen somit auf einen infektiösen rAAV-2-Partikel 253 Partikel, die durch fehlerhafte Hüllproteine oder Rezeptoren nicht in der Lage sind, eine Zelle zu infizieren. Die hohe Standardabweichung dieser Ratio (SD±241) macht deutlich, wie sehr die Ratio zwischen genomischen und infektiösen Partikeln (mit <10:1 bis >800:1), je nach Qualität der individuellen viralen Vektorherstellung, variieren kann.

Für funktionelle Experimente mit rAAV-2-Vektoren, die aus verschiedenen Präparationen stammen, ist der infektiöse Vektortiter also relevanter als der genomische Titer, da nur infektöse Vektoren einen Gentransfer vermitteln. Unser nächstes Ziel war daher die Weiterentwicklung der qPCR zur Quantifizierung der genomischen *und* infektiösen rAAV-2-Titer (***Ref. C***). Die Methode basiert auf dem Lebenszyklus des wt-AAV-2. Nach Infektion der rAAV-2-permissiven Zelllinie HeLa mit dem rAAV-2-Virus wurde diese lysiert. Die funktionell inaktiven, einsträngigen DNA-haltigen viralen Partikel zerstörten wir mit einer spezifischen, enzymatischen S1-Einzelstrang-DNAse-Verdauung. Die verbliebenen, transkriptionell aktiven doppelsträngigen rAAV-2-Kopien quantifizierten wir mit der oben beschriebenen qPCR-Methode. Zur Validierung der neuen Methode wurden 40 rAAV-2-Präparationen mit zwei

anderen Standardmethoden auf ihren infektiösen viralen Titer hin untersucht und die Ergebnisse der drei Methoden miteinander verglichen. Als Standardmethoden dienten der standardisierte, aber zeit- und materialaufwändige „Infectious Center Assay“ (ICA) sowie der bereits oben beschriebene durchflusszytrometrische Nachweis der EGFP-Expression. Zwischen den gemessenen infektiösen Titern der qPCR und der durchflusszytometrischen Methode zeigte sich ein signifikanter ($p<0,001$) Korrelationskoeffizient von 0,87. Auch im Vergleich zur zweiten Standardmethode, dem ICA, fanden wir eine signifikante ($p<0.001$) Korrelation von 0,8 zu den gemessenen infektiösen Titern der qPCR.

Somit konnten wir eine Methode etablieren, mit der die genomischen und infektiösen Titer von rAAV-2-Präparationen ohne Markergen einfach und valide bestimmt werden konnten. Diese Methode erleichtert weitere therapeutisch ausgerichtete, rAAV-2-vermittelte Gentherapieexperimente.

## 2.4 Einsatz von rAAV-2 bei NSCLC-Zelllinien

Nach Identifizierung von Zellen von nicht-kleinzelligen Lungenumoren als geeignetes Zielgewebe und Etablierung einer Methode zur Quantifizierung von genomischen und infektiösen rAAV-2-Titern, versuchten wir einen gentherapeutisch wirksamen rAAV-2-Vektor zu klonieren und an NSCLC-Zelllinien zu erproben (***Ref. D***). Zur Wiederherstellung der pro-apoptotischen p53 Funktion in p53-deletierten oder -mutierten NSCLC-Zelllinien stellten wir einen rAAV-2-Vektor (rAAV-2-p53) her, der die Wildtyp p53-cDNA enthält. Nach Bestimmung des genomischen Titers des neuen p53-kodierenden, rekombinanten AAV-2 infizierten wir die Zelllinien H1299, H23 und H157 von Patienten mit NSCLC unterschiedlicher Histologie. In Abhängigkeit der verwendeten Konzentration von 30 - 600 genomischen rAAV-2-p53-Partikeln pro Zelle ließ sich das Tumorzellwachstum der untersuchten NSCLC-Zelllinien um 44 % bis 71,7 % hemmen. Als Kontrolle für diese Experimente verwendeten wir einen rAAV-2-Vektor, der die cDNA für das EGF-Protein enthielt und keinen Effekt auf die Tumorzellproliferation hatte. Die durch den rAAV-2-p53 Vektor vermittelte Hemmung des Zellwachstums war im Vergleich mit dem rAAV-2-EGFP-Kontrollvektor mit einer vierfach höheren Apoptoserate in der Tumorzelle vergesellschaftet.

Danach untersuchten wir, ob die rAAV-2-vermittelte Wiederherstellung von p53 in der Tumorzelle die Chemosensitivität für Cisplatin, eines in der Behandlung von Patienten mit Lungenkarzinomen sehr häufig verwendeten Zytostatikums, erhöhen kann (***Ref. D***). In Kombinationsexperimenten von rAAV-2-p53 und Cisplatin konnten wir nachweisen, dass durch den Synergismus von rAAV-2-p53 und Cisplatin eine additive bzw. über-additive Wachstumshemmung induziert wird. Diese lag in Abhängigkeit von der verwendeten Zelllinie, zwischen 81% und 91%. Die Tumorzellen, die die Kombinationstherapie überlebten, waren selbst unter optimalen Wachstumsbedingungen in ihrem klonogenen Langzeitwachstum signifikant gehemmt. Im Gegensatz dazu erzielten wir keine zusätzliche Wachstumshemmung durch die Kombinationsbehandlung von Cisplatin und rAAV-2-Kontrollvektor im Vergleich zu Zellen, die nur mit Cisplatin behandelt wurden.

Diese Experimente zeigen, dass rAAV-2-Vektoren ein geeignetes Transfersystem für nichtkleinzellige Lungenkarzinome sind und damit potentiell für einen therapeutischen Einsatz in Frage kommen.

# 3 Identifizierung neuer prognostischer Faktoren bei Patienten mit kleinzelligem Lungenkarzinom (SCLC)

## 3.1 Die prognostische Bedeutung des c-kit Rezeptors bei Patienten mit SCLC

Um neue prognostische Gene bei Patienten mit SCLC zu identifizieren, untersuchten wir die Expression von potentiell relevanten Genen auf Proteinebene. Ein interessanter Vertreter ist der c-kit Rezeptor, der von 79 % bis 88 % der untersuchten Zelllinien von Patienten mit kleinzelligem Lungenkarzinom exprimiert wird. Da 57 % bis 76 % der SCLC-Zelllinien neben dem c-kit Rezeptor auch den aktivierenden Liganden, den „stem cell factor“ (SCF), exprimieren, lässt sich über ein autokrines Wachstumssignal beim SCLC spekulieren (Hibi, 1991). Durch die Autostimulation des Rezeptors kommt es zur Phosphorylierung von Tyrosinresten am intrazellulären Anteil des c-kit Rezepors, die ihrerseits als Bindungsstellen für intrazelluläre Signalproteine fungieren. Zu diesen zählen Vertreter der jak/stat, ras/raf und pdk1/akt-Signalkaskaden, durch die verschiedenste Zellfunktionen wie Proliferation, Adhäsion, Chemotaxis und Apoptose vermittelt werden (Heinrich, 2002).
Um den Anteil an c-kit positiven kleinzelligen Tumoren zu bestimmen und die prognostische Bedeutung dieses Rezeptors für Patienten mit SCLC zu ermitteln, untersuchten wir 203 Primärtumoren von Patienten mit kleinzelligem Lungenkarzinom auf eine c-kit Expression (***Ref. E***) und fanden diese auf 87,7 % aller Tumore. Bei den Patienten war eine fehlende c-kit-Expression mit einem signifikant (p=0,0084) schlechteren Überleben verbunden. Unabhängig von der Stärke der c-kit Expression lag das mittlere Überleben bei den c-kit-positiven Patienten bei 358 ($\pm$49) Tagen, während die Patienten, deren Tumor kein c-kit exprimierte, bei 151 ($\pm$15) Tagen lag. Weiterhin korrelierte der Anteil c-kit exprimierender Tumorzellen mit der Überlebenszeit des Patienten. Patienten, deren Tumor mehr als 75 % c-kit positiver Zellen aufwies, hatten ein mittleres Überleben von 424 Tagen. Hingegen sank das mittlere Überleben auf 295 Tage für die Patienten, deren Tumor zwischen 25 % - 75 % c-kit positiver Tumorzellen aufwies. Die schlechteste Prognose mit einem mittleren Überleben von 164 Tagen hatten die Patienten, deren Tumor keine oder einen Anteil von unter 25 % c-kit positiver Zellen hatte. Neben der univariaten Analyse mit dem Kaplan-Meier Modell führten wir auch eine multivariate Analyse durch. Neben der TNM-Klassifikation und dem

Performance-Status des Patienten war der Anteil der c-kit positiven Tumorzellen ein unabhängiger prognostischer Parameter.

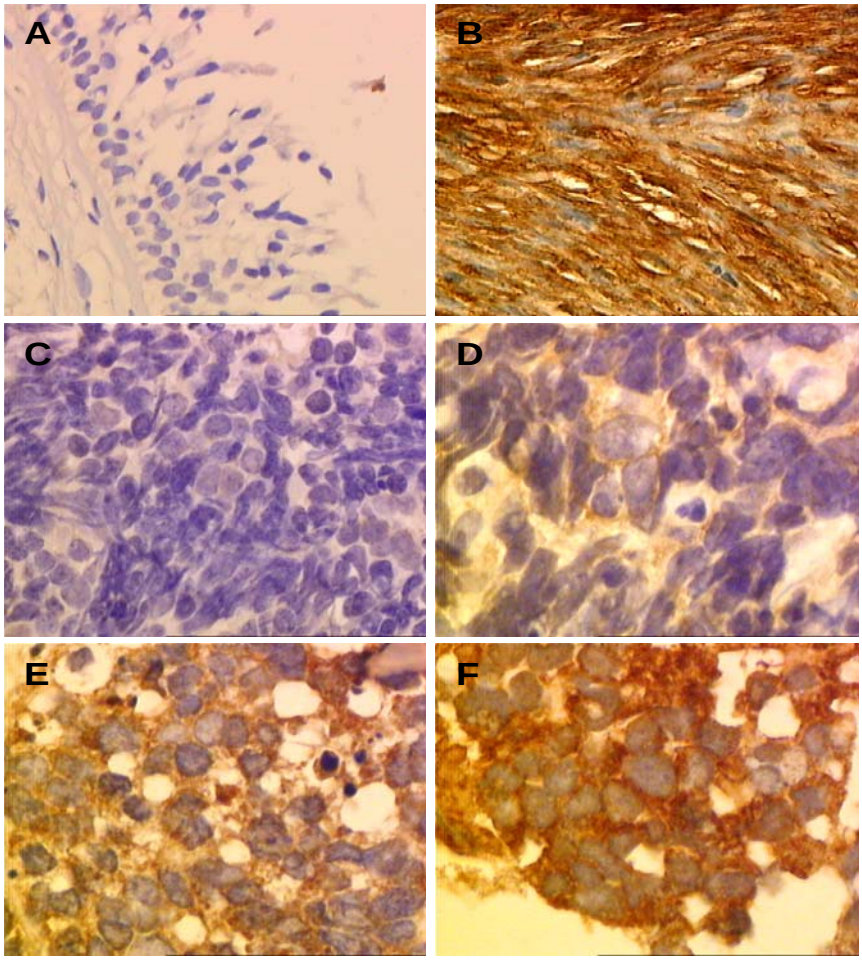


**Abb. 5: Differentielle Expression des c-kit-Rezeptors bei kleinzelligen Karzinomen der Lunge.** A: Bronchialepithel. B: Als Positivkontrolle wurde ein Gastrointestinaler Stromazelltumor (GIST) verwendet, der eine hohe Expression des c-kit Rezeptors aufweist. C: SCLC mit fehlender c-kit Expression. D, E, F: SCLC mit schwacher, inermediärer und starker immunhistochemischer c-kit-Färbereaktion.

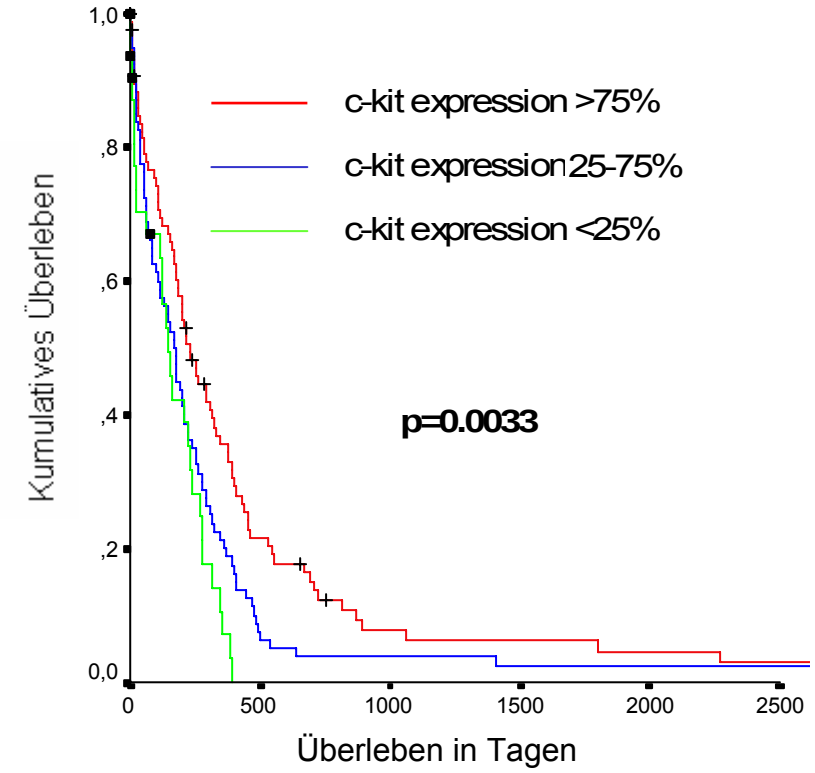


**Abb. 6: Abhängigkeit des Gesamtüberlebens des Patienten mit SCLC von der Anzahl c-kit-exprimierender Tumorzellen.**

Diese Daten belegen die prognostische Relevanz des c-kit Rezeptors bei Patienten mit SCLC. Da sich die Prognose der Patienten mit dem Anteil positiver c-kit Tumorzellen verbessert, ist von einer Hemmung des Rezeptors kein therapeutischer Effekt zu erwarten. Diese Einschätzung ist nicht rein spekulativer Natur, wenn man sich das Ergebnis einer klinischen Phase II Studie bei Patienten mit SCLC betrachtet, die mit dem Tyrosinkinase-Inhibitor (TKI) Imatinib (Glivec™) behandelt wurden. Der TKI inhibiert neben anderen Tyrosinkinasen auch die intrazelluläre c-kit-Kinasedomäne. Die 12 mit Imatinib behandelten Patienten wiesen alle einen Krankheitsprogress auf (Krug, 2005), was darauf schließen lässt, dass eine Hemmung des Rezeptors Wachstum und Expansion der Tumorzellen fördert.

## 3.2 Die prognostische Bedeutung des Tumorsuppressorgen FHIT bei Patienten mit SCLC

Eine Gemeinsamkeit zwischen kleinzelligen und nichtkleinzelligen Lungenkarzinomen ist der chromosomale Verlust bestimmter Genabschnitte, die somit bei der Pathophysiologie dieser Tumore eine Rolle spielen könnten. Einer dieser Abschnitte ist der kurze Arm des Chromosoms 3, wobei 90 bis 100 % der Patienten mit SCLC und 50 bis 80% der Patienten mit NSCLC mindestens ein Allel der Regionen 3p25, 3p21.3 und 3p14 verloren haben (Wistuba, 2001). Das „fragile histidine triad“ (FHIT) Gen, welches in der 3p14.2 Region liegt, könnte daher bei der Entstehung von Lungenkarzinomen eine Rolle spielen. Obwohl der exakte Signalweg für das aus 146 Aminosäuren bestehende 16,8 kDa große Protein FHIT unbekannt ist, geht man davon aus, dass es als Signalmolekül in der p53 assoziierten Apoptose und Zellzykluskontrolle involviert ist. Um die prognostische Relevanz von FHIT als mögliches Tumorsuppressorgen zu beleuchten, untersuchten wir 225 paraffin-eingebettete Primärtumoren von Patienten mit kleinzelligem Lungenkarzinom im Zusammenhang mit deren Überleben (***Ref. F***). Eine FHIT Expression fand sich bei 61,8% der SCLC Tumoren. Patienten ohne Nachweis des FHIT Proteins hatten eine signifikant (p=0,0061) kürzere mediane Überlebenszeit von 157 Tagen. Im Vergleich dazu lebten Patienten, deren Tumore FHIT exprimierten, im Median 210 Tage.

Darüber hinaus bestimmten wir den Anteil FHIT positiver Tumorzellen und korrelierten diesen Wert mit der Überlebenszeit des Patienten. Hatten die Tumoren der Patienten einen Anteil an FHIT positiven Tumorzellen von weniger als 25 %, so lag deren mediane Überlebenszeit bei 155 Tagen. Demgegenüber hatten die Patienten, in deren Tumor mehr als 25 % der Zellen FHIT positiv waren mit 217 Tagen eine signifikant (p=0,0016) längere Überlebenszeit. In der multivariaten Analyse nach dem Cox-Regressionsmodell war der Anteil FHIT positiver Tumorzellen unter 11 klinischen Variablen ein unabhängiger prognostischer Faktor für Patienten mit kleinzelligem Lungenkarzinom.

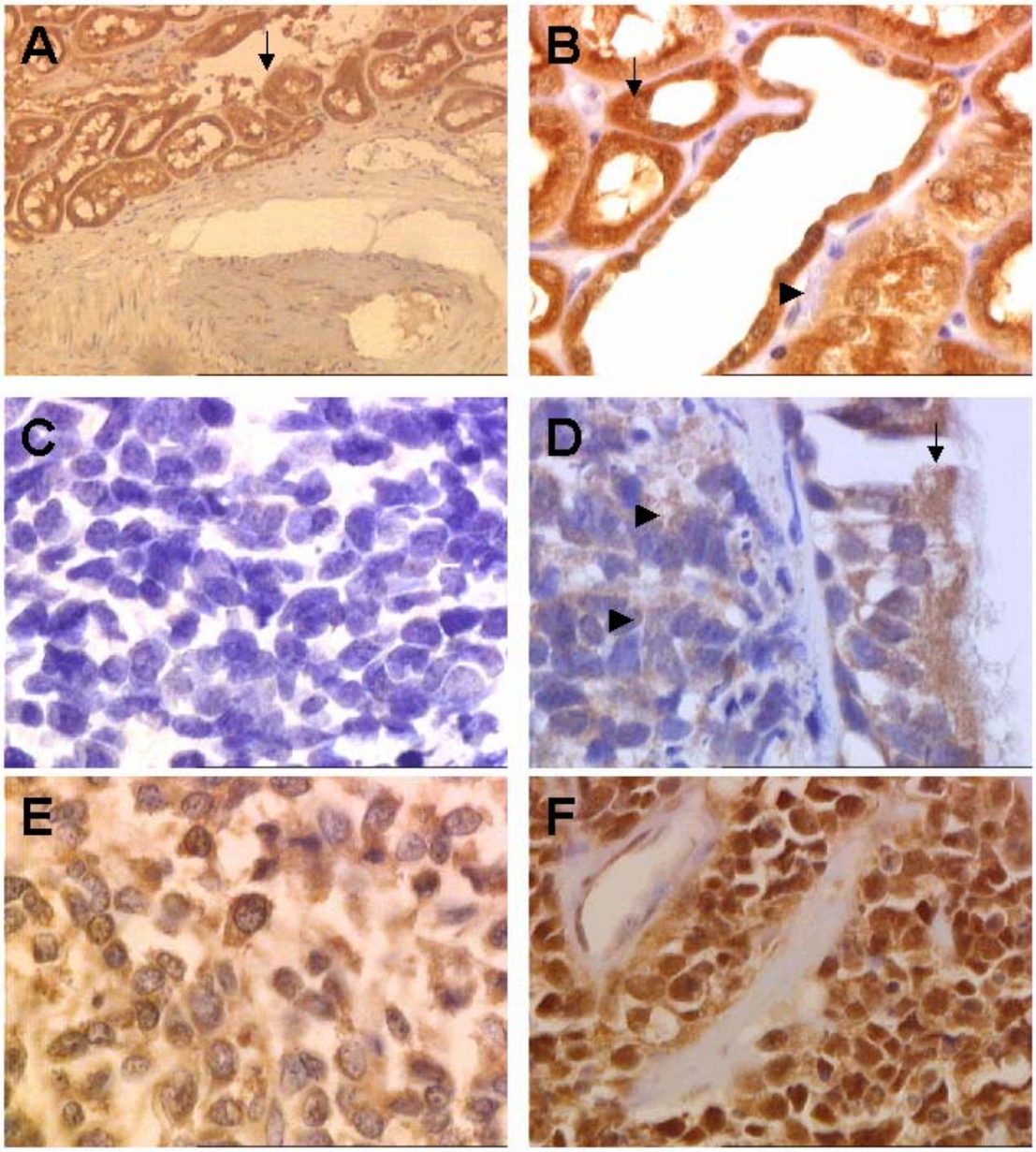


**Abb. 7: Differentielle FHIT-Expression bem SCLC.**
A, B: Kontrollfärbungen am Nierengewebe. Die Pfeile zeigen die als Positivkontrolle dienenden Nierentubuli. Die Pfeilspitze in B zeigt das als Negativkontrolle dienende Bindegewebe zwischen den Nierentubuli. C: SCLC ohne FHIT-Expression. D, E, F: SCLC mit schwacher, mittlerer und starker immunhistochemischer Färbereaktion für FHIT. Die Pfeilspitzen in D zeigen die schwache FHIT-Expression in Tumorzellen, der Pfeil zeigen eine ebenfalls schwache Färbereaktion am physiologischen, mehrschichtigen Flimmerepithel der Lunge.

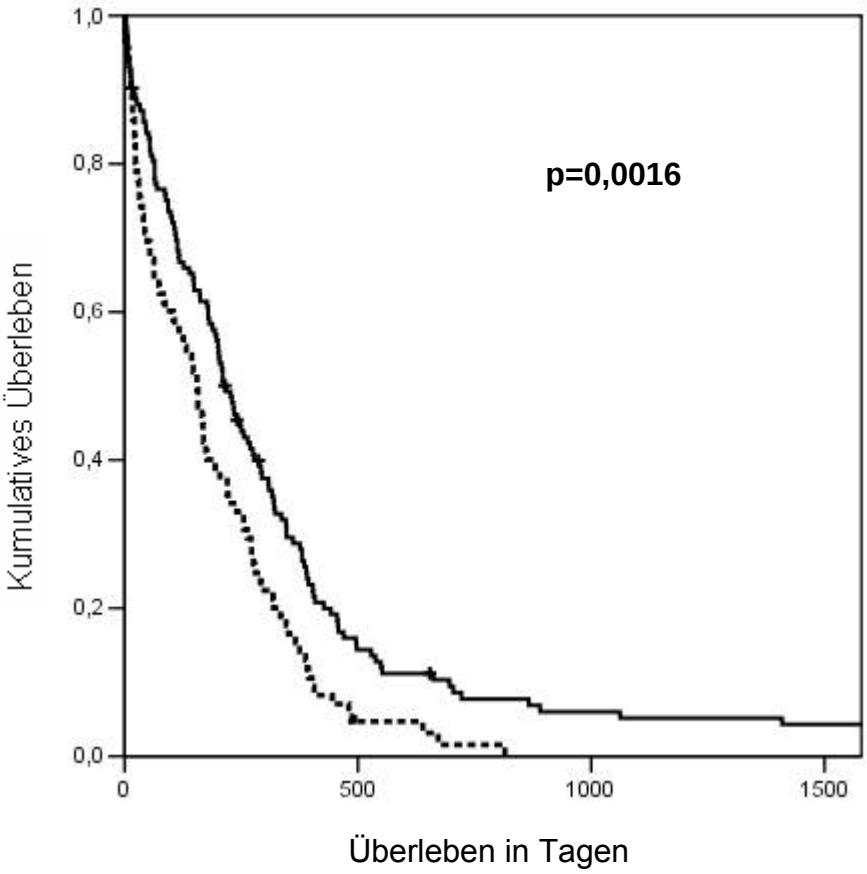


**Abb. 8: Abhängigkeit des Überlebens der Patienten mit SCLC von der Anzahl FHIT-exprimierender Tumorzellen**.
Die gestrichelte Linie zeigt die Überlebenskurvenj von Patienten, deren Tumore ≤ 25 % FHIT positiver Zellen aufwiesen. Die durchgezogene Linie beschreibt die Überlebenskurve für die Patienten mit SCLC, deren Tumore aus > 25 % FHIT positiver Zellen bestanden.

Diese Ergebnisse lassen den Schluss zu, dass FHIT bei SCLC möglicher Teil eines zellzyklusregulierenden Tumorsuppressors sind. Neben der Bedeutung des FHIT-Gens als einem neuen prognostischen Marker bei Patienten mit SCLC könnte es zu einem potentiellen Kandidatengen für eine Genersatztherapie mit einem viralen Vektor werden.

## 4. Molekulare Charakterisierung von Lungentumoren im Vergleich zu normalem Lungengewebe

Nachdem wir die prognostische Bedeutung von c-kit und FHIT gefunden hatten, wollten wir uns in einem nächsten Schritt einen umfassenderen Einblick in die molekulare Pathogenese von Lungenkarzinomen verschaffen. Durch die Isolierung von Tumorzellen aus einem Gewebeverband mittels der lasergestützten Mikrodissektion (Laser Capture Microdissection, LCM) und der Genexpressionsanalyse von Tumorzellen mit Hilfe von Oligonukleotid-Mikroarrays benutzten wir zwei Methoden.

Dazu untersuchten wir 29 Proben von primären Lungenkarzinomen, wobei es sich um 20 NSCLCs (10 Adenokarzinome und 10 Plattenepithelkarzinome) und 9 SCLCs handelte. Als Kontrollgruppe wurden 5 Proben aus dem Lungengewebe von Patienten ohne Lungenkarzinom verwendet, die aus anderen Gründen bronchoskopiert wurden.

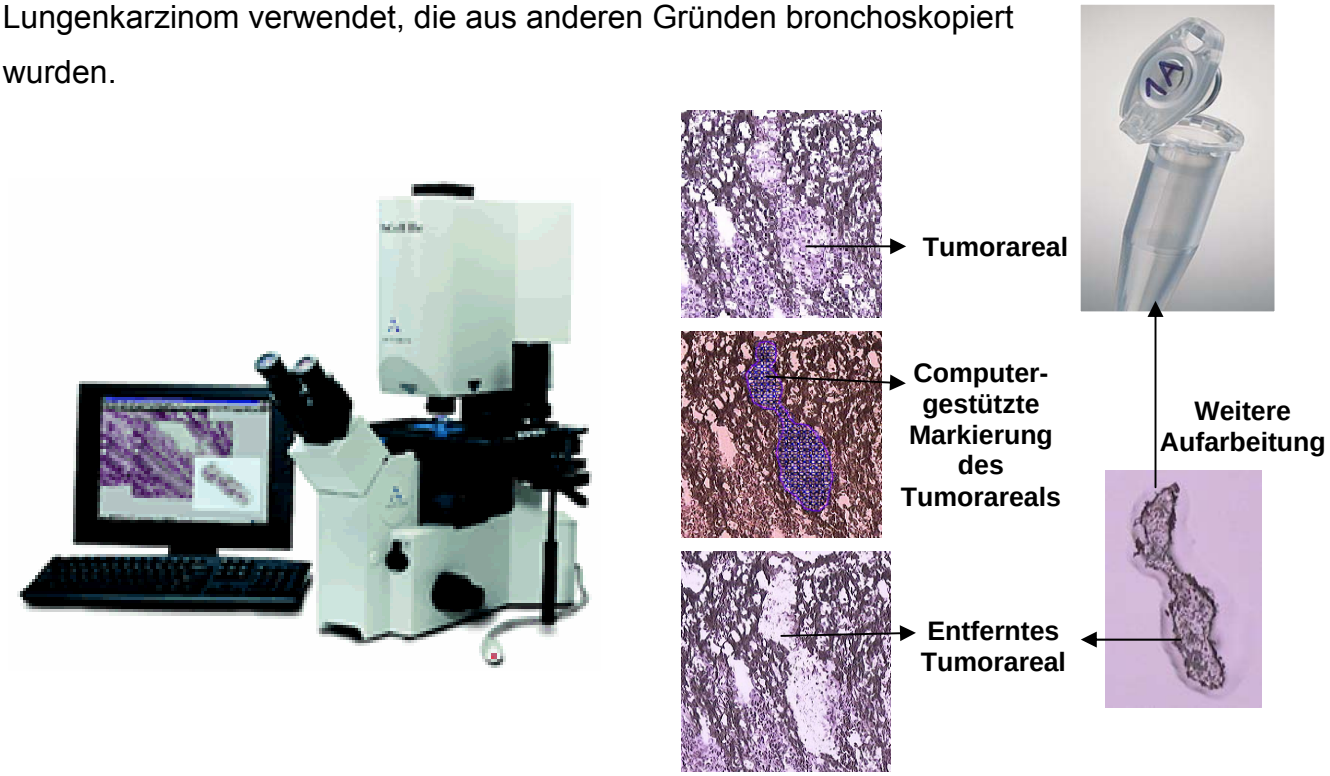


**Abb. 9: Methode der Laser-Capture Mikrodissektion.**
Mittels computergestützter Software wird das unter dem Mikroskop identifizierte Tumorareal markiert, isoliert und zur weiteren Aufarbeitung aus dem restlichen Gewebeverband entfernt.

Von den Biopsaten, die während der Bronchoskopie gewonnen wurden, fertigten wir zunächst 8 µm dicke Kryoschnitte an. Nach Fixation, Dehydratation und Färbereaktion

isolierten wir dann aus den Tumorarealen Gewebe für die Untersuchung der Genexpression mittels LCM.

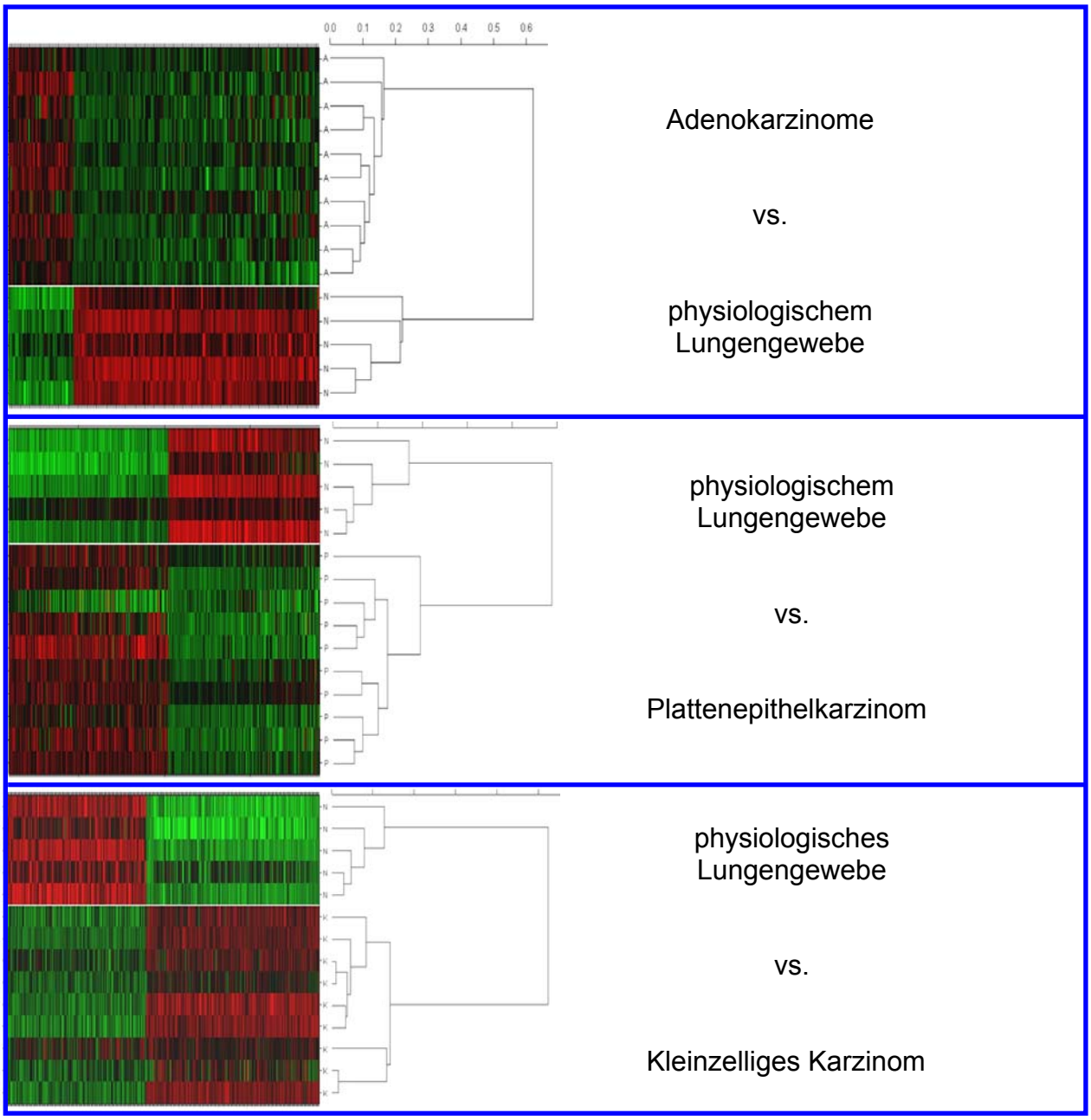


**Abb. 10: Unterschiede im Genexpressionsprofil zwischen normalem Lungengewebe und Adenokarzinomen, Plattenepithelkarzinomen und kleinzelligen Karzinomen der Lunge**

Dazu extrahierten wir aus den Tumorzellen die RNA, welche nach einer bioanalytischen Qualitätskontrolle amplifiziert und mit Oligonukleotid-Arrays der Firma Affymetrix hybridisiert

wurde. Auf diesem Array sind 8793 charakterisierte Gene aufgetragen. Die computergestützte Auswertung der Expressionsdaten umfasst nach der Normalisierung mittels „variance stabilizing transformation“ die Multiklassenanalyse auf der Grundlage der „significance analysis of microarrays“ (SAM) zur Identifikation von signifikant unterschiedlich exprimierten Genen. Die hierarchische Clusteranalyse erlaubte anhand der Genexpressionsprofile eine Unterscheidung zwischen Lungentumoren und Normalgewebe der Lunge. Im Vergleich zum Normalgewebe fanden wir für das kleinzellige Lungenkarzinom, das Plattenepithel- und das Adenokarzinom der Lunge insgesamt 404, 335 bzw. 205 Gene, die bei einer geschätzten Fehlerrate (false discovery rate) von < 2,6 % mindestens um den Faktor 2 differentiell exprimiert waren. Zum besseren pathophysiologischen Verständnis wurden diese Gene ihren biologisch-funktionellen Gruppen zugeordnet.

In Abhängigkeit vom histologischen Subtyp zeigten sich bemerkenswerte Unterschiede zwischen den histologischen Subtypen der Lungenkarzinome. Bei den Plattenepithelkarzinomen waren 22 % aller signifikant differentiell exprimierten Gene solche, die an der Steuerung der Tumorzellproliferation beteiligt sind. Diese Gene waren, verglichen mit dem Normalgewebe, zwischen 2,1 und 5,7 fach überexprimiert. Drei dieser Gene, die der Gruppe der Cykline angehören, sind Schlüsselgene innerhalb des Zellzykluses. Die im Plattenephithelkarzinom im Vergleich zu normalem Lungengewebe überexprimierte „cyklin-dependent kinase 4“ führt direkt oder indirekt über Kompexbildung mit Cyklin D2 oder Cyklin D3, die ebenfalls überexprimiert sind, zur Phosphorylierung des Tumorsuppressorgens Rb. Durch das phosphorylierte und somit inaktivierte Rb kann die Tumorzelle den ersten Checkpunkt zwischen G1 und S-Phase passieren. Das Fortschreiten in die S zur G2-Phase bzw. von der G2-Phase in die mitotische M-Phase der Zelle wird durch die Cykline A2 und B2 vermittelt, die bei Plattenepithelkarzinomen ebenfalls beide überexprimiert wird.

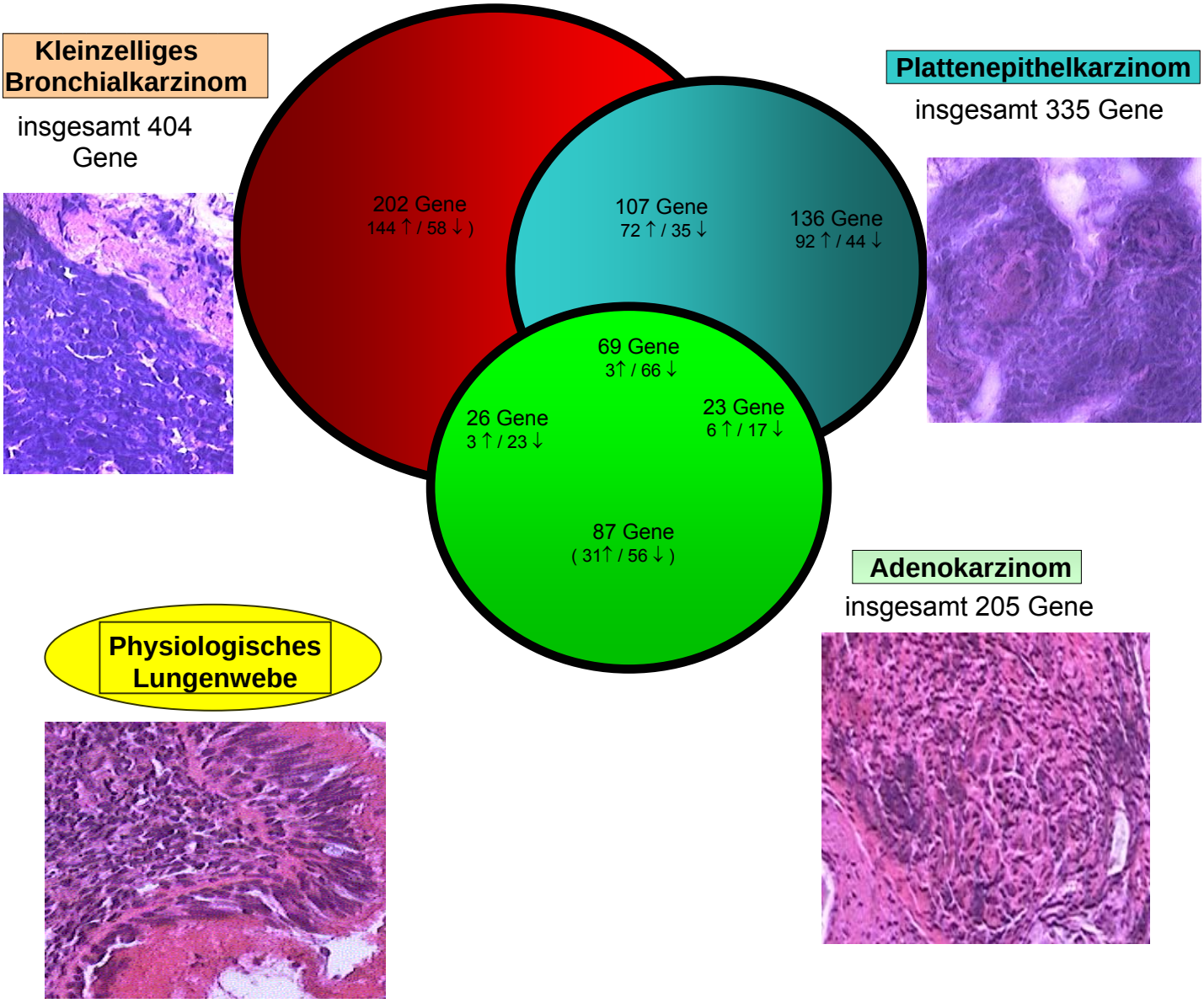


**Abb. 11: Verteilung der 944 signifikanten, differentiell exprimierten Gene der Lungentumore im Vergleich zum physiologischen Lungengewebe.**
Pfeile nach oben bzw. unten symbolisieren die Anzahl der Gene, die in dieser Entität gegenüber der Kontrolle über- bzw. unterexprimiert sind.

Im Vergleich zu den Plattenepithelkarzinomen lag der Anteil proliferationsassoziierter Gene bei den Adenokarzinomen lediglich bei 1%, während 9% aller signifikanten Gene beim Adenokarzinom die Zelladhäsion regulierten. Hier zeigte sich, im Vergleich zur Kontrolle, ein Muster von differentiell über- oder unterexprimierten Zelladhäsionsmolekülen, welche die Invasivität und Metastasierung der Lungenkarzinome beeinflussen. Die drei Gene ICAM-1,

Integrin beta-2 und alpha-3 waren beim Adenokarzinom im Vergleich zu Normalgewebe zwischen 2,1 und 5,8 fach überexprimiert, während acht Gene, zwei davon aus der Familie der Cadherine, zwischen 2,1 und 12,3 fach herunterreguliert waren. Die differentielle Expression von Adhäsionsmolekülen moduliert das invasive Wachstum einer Tumorzelle, wobei die erhöhte Expression von Integrin alpha-3 das Metastasierungspotential bei Lungenkarzinomen steigert (Gogali, 2004). Weiterhin ist die reduzierte Expression der kalziumabhängigen Cadherine, die eine Zell-Zell-Adhäsion vermitteln, mit Tumorprogression, Metastasierung und ungünstiger Prognose bei gastrointestinalen Tumoren und urogenitalen Tumoren assoziiert (Kase, 2000).

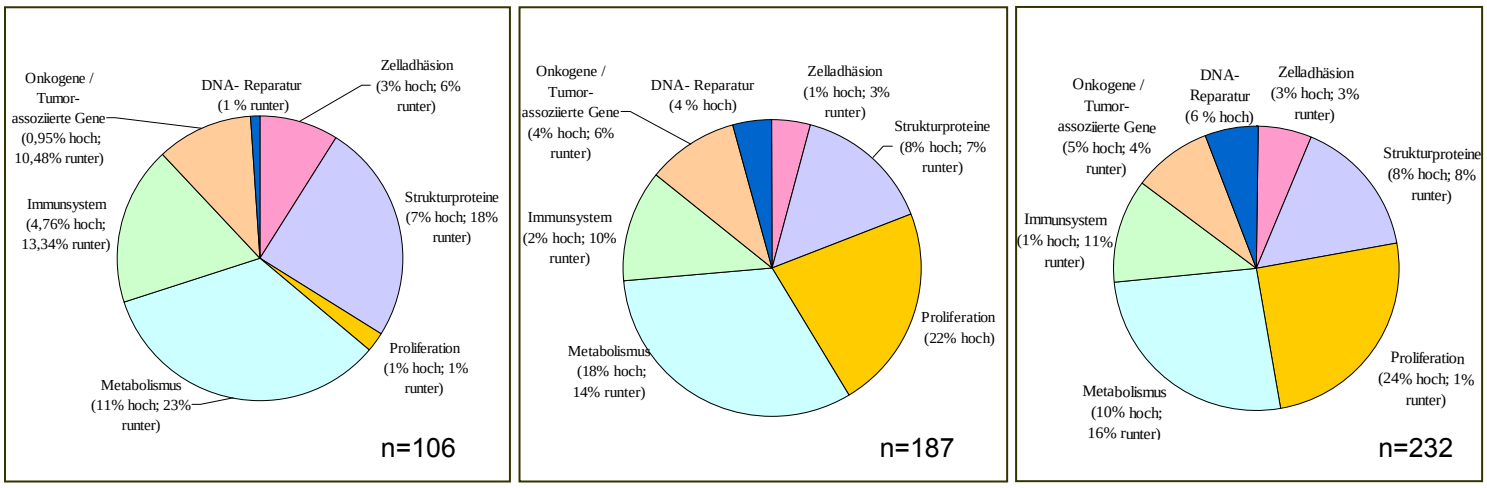


**Abb. 12: Einteilung der signifikant differentiell exprimierten Gene in sieben biologisch relevante, funktionelle Gruppen.** DNA- Reparatur und Proliferation nimmt vom Adenokarzinom zum kleinzelligen Lungentumor hin zu. Veränderungen der Gene bezüglich Metabolismus, Zelladhäsion, Immunsystem und Strukturproteine sind bei allen drei Subtypen zu finden.

Kleinzellige Lungenkarzinome zeigten ihre ontogenetische Verwandtschaft zu neuronal differenziertem Gewebe dadurch, dass elf Gene gegenüber normalem Lungengewebe überexprimiert waren, wie beispielsweise das synaptosomal-assoziierte Protein, Synaptotagmin sowie das synaptotagmin-bindende Protein. Die Relevanz dieser Proteine für die Pathophysiologie des kleinzelligen Lungenkarzinoms ist bisher nicht beleuchtet worden.

In der Zusammenschau erlauben diese Ergebnisse einen tieferen Einblick in pathophysiologische Vorgänge der Kanzerogenese für die histologischen Subtypen der Lungenkarzinome. Mit Hilfe der Cluster-Analyse lassen sich diese nun molekular klassifizieren. Die Identifizierung von einzelnen Genen innerhalb der funktionellen Gengruppen bietet weiterhin die Grundlage für die Entwicklung neuer Substanzen, die für die Therapie möglichst spezifisch für den jeweiligen Subtyp des Lungenkarzinoms sind.

## Schlussfolgerungen und Ausblick

Durch genetische Aberrationen kann es zu einem Ausfall von Tumorsuppressorgenen oder einer Überexpression von Onkogenen kommen, die zur unkontrollierten Proliferation von Tumorzellen führt. Mittels viraler Vektoren ist es prinzipiell möglich, auf molekularer Ebene durch Gentransfer gezielt in das Wachstumsverhalten einzugreifen. Die bis dato am häufigsten verwendeten viralen Vektoren für eine Gentherapie beim Menschen basieren auf Adenoviren und Retroviren. Beide Vektosysteme haben jedoch den entscheidenden Nachteil, per se Krankheiten auszulösen. So können adenovirale Vektorsysteme beim Menschen eine schwere Immunantwort, das sogenannte „systemic inflammatory response syndrome“ (SIRS) auslösen, welches zum Multiorganversagen führt (Hollon, 2000). Retroviren integrieren nach Infektion nach dem Zufallsprinzip in das Genom der Zielzelle, was zu Insertionsmutationen und so zu malignen Erkrankungen führen kann. In einer französischen Studie kam es durch Gentransfer mit retroviralen Vektoren bei 2 von 11 Patienten mit schwerer Immundefizienz (SCID) zu der Entwicklung eines T-Zell-Lymphoms (Check, 2003).
Das in unserer Arbeitsgruppe etablierte, auf dem adeno-asoziierten Virus Typ 2 basierende Vektorsystem, ist im Vergleich zu den adeno- und retroviralen Vektorsystemen ein „junges“, dessen Potential erst seit etwa 10 Jahren genutzt wird. Die Eigenschaften von wt-AAV-2 weckten besonderes Interesse im Hinblick auf eine mögliche Krebstherapie. So konnte durch einen direkten tumorhemmenden Effekt einer wt-AAV-2-Infektion das Risiko für das Auftreten eines Zervixkarzimoms gesenkt werden. Weiterhin ließ sich die Sensitivität von Karzinom- und Sarkomzelllinien gegenüber verschiedenen chemotherapeutischen Substanzen durch eine Wildtypinfektion steigern und Nebenwirkungen von Chemotherapien vermindern. Die fehlende Humanpathogenität, niedrige Immunogenität von AAV-2 und schließlich der von uns gezeigte Tropismus für nicht-kleinzellige Lungenkarzinome ermutigten uns, dieses Vektorsystem für einen gentherapeutischen Einsatz zur Therapie von Patienten mit Lungenkarzinom beim Menschen weiterzuentwickeln. Nachdem wir mit der Virusquantifizierung die Grundlagen für experimentelle Untersuchungen beim Lungenkarzinom geschaffen hatten, galt es zu untersuchen, ob therapeutische rAAV-2-Vektoren zur Behandlung von NSCLCs geeignet sind. Dazu konstruierten wir einen neuen rAAV-2-p53-Vektor, welcher das human Wildtyp-p53-Gen kodiert. Wir wählten als

therapeutisches Gen p53, da seine apoptoseinduzierenden Eigenschaften in Lungenkarzinomen bereits hinlänglich bekannt sind. Mit Hilfe des Vektors konnten wir zeigen, dass es im Vergleich mit dem EGFP kodierenden rAAV-2-Kontrollvektor zu einer p53-vermittelten Wachstumsinhibition aller untersuchten NSCLC-Zelllinien kam. Der inhibitorische Effekt von p53 beruhte dabei auf einer gesteigerten Apotoserate in den Lungenkarzinomzelllinien. Da die Arbeiten von Duverger (2002) und Schwarzbach (2002) gezeigt hatten, dass die Sensitivität von Tumorzellen durch wt-AAV-2 alleine oder den zusätzlichen Einsatz von chemotherapeutischen Substanzen erhöht werden kann, untersuchten wir, ob rekombinante AAV-2-Vektoren auch diese Eigenschaften aufweisen. Wie die Ergebnisse unserer Experimente zeigten, hatte der rekombinante AAV-2-Vektor die Fähigkeit des Wildtyps verloren, Tumorzellen in An- oder Abwesenheit eines Chemotherapeutikums zu sensibilisieren. Wahrscheinlich beruht dies auf der Entfernung des Replikationsproteins *rep* aus dem Genom des Wildtyps, was für die Herstellung rekombinanter AAV-2-Partikel eine unverzichtbare Voraussetzung ist. Trotz der fehlenden Sensibilisierung von Tumorzellen durch rAAV-2 konnten wir durch die kombinierte Behandlung von Cisplatin und dem therapeutischen rAAV-2-p53-Vektor eine additive oder überadditive Wachtumshemmung beim NSCLC erreichen. Selbst die überlebenden Tumorzellen waren trotz optimaler Wachstumsbedingungen in ihrer Fähigkeit signifikant beeinträchtigt, Tumorkolonien auszubilden. Grundsätzlich ist das AAV-2-Vektorsystem also für eine Gentherapie von Patienten mit NSCLCs geeignet. Die Übertragung solcher in-vitro Experimente in eine Krebsbehandlung beim Menschen ist jedoch aus verschiedensten Gründen problematisch und unterscheidet sich stark vom gentherapeutischen Einsatz von somatischen Erkrankungen einzelner Gene wie zum

Beispiel bei einem Enzymdefekt. Bei Patienten mit Hämophilie B, bei denen der Gerinnungsfaktor IX vermindert ist, ließen sich Faktor IX-Gen-enthaltende rAAV-2-Partikel erfolgreich in den Muskel transduzieren. Der im Muskel produzierte Gerinnungsfaktor wurde anschließend kontinuierlich ins periphere Blut sezerniert. Bei einer gentherapeutische Krebstherapie würde der intravenös applizierte rAAV-2-Vektor aufgrund seiner von uns gezeigten Affinität zu Endothelzellen und glatten Gefäß-Muskelzellen nicht am eigentlichen Wirkort, dem Lungentumor, ankommen. Daher müsste ein therapeutischer rAAV-2-Vektor direkt intratumoral appliziert oder per Aerosol inhaliert werden (Moss, 2004). Alternativ

könnten die Rezeptoren von rAAV-2 so modifiziert werden, dass ein selektiver Tropismus nur noch für Lungentumorzellen besteht. Eine Oberflächenmodifikation zur Schaffung einer Vektorspezifität für eine Tumorzelle ließ sich bereits für Zellen von Patienten mit chronischer lymphatischer Leukämie (CLL), die normalerweise resistent gegenüber wt-AAV-2 sind, erfolgreich demonstrieren (Girod, 1999; Buning, 2003).

Neben der Identifizierung von prädiktiven Markern bildete die Suche und Identifikation von prognostisch relevanten Genen den zweiten Schwerpunkt meiner Arbeit. Beim kleinzelligen Lungenkarzinom ist bereits zu einem frühen Zeitpunkt mit einer Fernmetastasierung zu rechnen. Nur in den limitierten Krankheitsstadien I-II ist eine Operation als kurative Therapie möglich und nach wie vor wird die Frage nach einer adjuvanten Therapie kontrovers diskutiert. Gelänge es, prognostische Faktoren zu finden, die bei gleicher Therapie den individuellen Krankheitsverlauf vorhersagen könnten, so wäre es möglich, die Patienten nach diesen Kriterien zu stratifizieren. Mit dem Nachweis des c-kit Rezepors und des Tumorsuppressorgens FHIT beim SCLC gelang es, zwei Gene mit prognostischer Bedeutung zu beschreiben. Der Verlust der Expression von FHIT oder c-kit war mit einem signifikant schlechteren Überleben der Patienten mit SCLC vergesellschaftet. Diese Untersuchungen könnten Grundlage für klinische Studien sein bei denen Patienten mit ungünstiger Markergenkonstellation mit Verlust des c-kit-Rezeptors und des FHIT-Gens eine intensivere Chemo- bzw. Radiotherapie erhalten um so deren Prognose zu verbessern.

Nachdem wir die prognostische Bedeutung von c-kit und FHIT gezeigt hatten, wollten wir im dritten Teil dieser Arbeit einen umfassenderen Einblick in die molekulare Pathogenese von Lungenkarzinomen gewinnen. Erst die Entwicklung neuer Methoden eröffnete uns die Möglichkeit, eine Genexpressionsanalyse von primären Lungenkarzinomen durchzuführen. Hierzu gehörte zum einen die selektive Isolierung von Tumorzellen aus einer heterogenen Gewebeprobe mit der Laser-Capture Mikrodissektion sowie die Bestimmung des Transkriptoms der Tumorzellen durch die Oligonukleotid-Arraytechnologie mit Hilfe einer biomedizinischen Datenverarbeitung. Mit diesen Methoden erstellten wir eine molekulare Datenbank von Lungenkarzinomen unterschiedlicher Histologie, deren Genexpressionsprofile sich einerseits untereinander und andererseits von gesundem Lungengewebe signifikant unterschieden. In Abhängigkeit des Subtyps erhielten wir dabei Einblick in die unterschiedliche Pathophysiologie der Lungenkarzinome. Beim Plattenephithelkarzinom

fanden wir drei zentrale Gene, deren Überexpression den Zellzyklus in Richtung Proliferation und Zellteilung lenken. Diese Gene gehören zu den Cyklinen und den cyklinabhängigen Kinasen (CDK). Die Bedeutung dieses Signalweges liegt darin, dass in den letzten Jahren eine neue Substanzgruppe, die „small molecule inhibitors“, entwickelt wurde, die spezifisch an verschiedenen Stellen der intrazellulären Signalkaskade eingreifen können. Diese CDK-Modulatoren blockieren die ATP-Bindungsstelle der CDKs. Einer dieser Modulatoren ist Flavopiridol, ein Pan-CDK-Inhibitor, der in einer klinischen Phase II Studie bei 20 Patienten mit fortgeschrittenem NCSLC verwendet wurde. Das mediane Überleben dieser Patienten lag bei 7,5 Monaten, was dem Zeitraum entspricht den ein Patient üblicherweise mit einer chemotherapeutischen Behandlung erreichen würde (Senderowicz, 2003). Auf der Grundlage dieser Ergebnisse kam es zu einer randomisierten Phase III-Studie, in der eine chemotherapeutische Standardbehandlung mit einer Kombinationstherapie aus Flavopiridol und Chemotherapie verglichen wird. Da Flavopiridol jedoch ein Pan-CDK-Inhibitor ist und somit auch CDKs inhibiert, die in der Pathophysiologie der NSCLCs wahrscheinlich keine Rolle spielen, könnten unsere Ergebnisse einer spezifischeren Inhibition relevanter Zellzyklusgene dienen.

Die Identifizierung neuer therapeutisch relevanter Gene für eine Therapie bei Patienten mit NSCLC ist notwendig, da sich die Prognose der Patienten quoad vitam kaum verbessert hat. Seit Entdeckung der Überexpression des epidermalen Wachstumsfaktor-Rezeptors-1 (EGFR-1) beim NSCLC wurden eine Reihe von „small molecule inhibitors“ entwickelt, welche die EGFR-1-Tyrosinkinase selektiv inhibieren. EGFR-1 und die nachgeschaltete Signalkaskade sind für das Zellwachstum, Expression proangiogenetischer Faktoren sowie eine verminderte Empfindlichkeit der Tumorzelle gegenüber einer Strahlen- oder Chemotherapie von Bedeutung. In klinischen Phase III-Studien führte die Hemmung von EGFR-1 bei 10 % bis 20 % der stark vorbehandelten Patienten mit NSCLC zu einem Tumorrückgang um mehr als 50 % (Perez-Soler, 2004). Da nur ca. 10 % der Patienten auf die molekulare Therapie ansprechen, haben wir zur Identifizierung dieser Patientengruppe eine klinische Studie initiiert. Ziel ist die Therapieoptimierung durch die Identifikation solcher Gene, die als Indikator für ein Ansprechen auf den EGFR-1-gerichteten Tyrosinkinaseinhibitor dienen könnten. Vor Therapiebeginn mit dem EGFR-1-Tyrosinkinase-Inhibitor Erlotinib wird den Patienten daher bronchoskopisch eine Tumorprobe entnommen,

von der unter Einsatz der Laser Capture Microdissektion und Array-Technologie ein Genexpressionsprofil erstellt wird. Das analysierte Transkriptom des Tumors wird unter besonderer Berücksichtigung der EGF-Rezeptorfamilie und nachgeschalteter Signaltransduktionmoleküle mit dem Therapieansprechen des Patienten korreliert, um auf diesem Weg pädiktive Gene zu ermitteln. Damit könnte es gelingen, auf molekularer Ebene die Gruppe von Patienten zu identifizieren, die von einer tumorgerichteten Therapie mit Erlotinib einen besonderen Nutzen haben.

## 6. Literatur


Berns KI.
Parvovirus replication.
Microbiol Rev. 1990 Sep;54(3):316-29.

Buning H, Ried MU, Perabo L, Gerner FM, Huttner NA, Enssle J, Hallek M.
Receptor targeting of adeno-associated virus vectors.
Gene Ther. 2003 Jul;10(14):1142-51

Check E.
Harmful potential of viral vectors fuels doubts over gene therapy.
Nature. 2003 Jun 5;423(6940):573-4.

Duverger V, Sartorius U, Klein-Bauernschmitt P, Krammer PH, Schlehofer JR.
Enhancement of cisplatin-induced apoptosis by infection with adeno-associated virus type 2.
Int J Cancer. 2002 Feb 10;97(5):706-12.

Forgacs E, Zochbauer-Muller S, Olah E, Minna JD.
Molecular genetic abnormalities in the pathogenesis of human lung cancer.
Pathol Oncol Res. 2001;7(1):6-13.

Girard L, Zochbauer-Muller S, Virmani AK, Gazdar AF, Minna JD.
Genome-wide allelotyping of lung cancer identifies new regions of allelic loss, differences between small cell lung cancer and non-small cell lung cancer, and loci clustering.
Cancer Res. 2000 Sep 1;60(17):4894-906.

Girod A, Ried M, Wobus C, Lahm H, Leike K, Kleinschmidt J, Deleage G, Hallek M.
Genetic capsid modifications allow efficient re-targeting of adeno-associated virus type 2.
Nat Med. 1999 Sep;5(9):1052-6. Erratum in: Nat Med 1999 Dec;5(12):1438.

Gogali A, Charalabopoulos K, Constantopoulos S.
Integrin receptors in primary lung cancer.
Exp Oncol. 2004 Jun;26(2):106-10.

Grimm D, Kern A, Rittner K, Kleinschmidt JA.
Novel tools for production and purification of recombinant adenoassociated virus vectors.
Hum Gene Ther. 1998 Dec 10;9(18):2745-60.

Hanna E, Shrieve DC, Ratanatharathorn V, Xia X, Breau R, Suen J, Li S.
A novel alternative approach for prediction of radiation response of squamous cell carcinoma of head and neck.
Cancer Res. 2001 Mar 15;61(6):2376-80.

Heinrich MC, Rubin BP, Longley BJ, Fletcher JA.
Biology and genetic aspects of gastrointestinal stromal tumors: KIT activation and cytogenetic alterations.
Hum Pathol. 2002 May;33(5):484-95.

Hibi K, Takahashi T, Sekido Y, Ueda R, Hida T, Ariyoshi Y, Takagi H, Takahashi T.
Coexpression of the stem cell factor and the c-kit genes in small-cell lung cancer.
Oncogene. 1991 Dec;6(12):2291-6.

Hollon T.
Researchers and regulators reflect on first gene therapy death.
Nat Med. 2000 Jan;6(1):6.

Horster A, Teichmann B, Hormes R, Grimm D, Kleinschmidt J, Sczakiel G.
Recombinant AAV-2 harboring gfp-antisense/ribozyme fusion sequences monitor transduction, gene expression, and show anti-HIV-1 efficacy.
Gene Ther. 1999 Jul;6(7):1231-8.

Ji L, Fang B, Yen N, Fong K, Minna JD, Roth JA.
Induction of apoptosis and inhibition of tumorigenicity and tumor growth by adenovirus vector-mediated fragile histidine triad (FHIT) gene overexpression.
Cancer Res. 1999 Jul 15;59(14):3333-9

Kase S, Sugio K, Yamazaki K, Okamoto T, Yano T, Sugimachi K.
Expression of E-cadherin and beta-catenin in human non-small cell lung cancer and the clinical significance.
Clin Cancer Res. 2000 Dec;6(12):4789-96.

Krug LM, Crapanzano JP, Azzoli CG, Miller VA, Rizvi N, Gomez J, Kris MG, Pizzo B, Tyson L, Dunne M, Heelan RT.
Imatinib mesylate lacks activity in small cell lung carcinoma expressing c-kit protein: a phase II clinical trial.
Cancer. 2005 May 15;103(10):2128-31.

Levine AJ.
p53, the cellular gatekeeper for growth and division.
Cell. 1997 Feb 7;88(3):323-31.

Monahan PE, Jooss K, Sands MS.
Safety of adeno-associated virus gene therapy vectors: a current evaluation.
Expert Opin Drug Saf. 2002 May;1(1):79-91.

Moss RB, Rodman D, Spencer LT, Aitken ML, Zeitlin PL, Waltz D, Milla C, Brody AS, Clancy JP, Ramsey B, Hamblett N, Heald AE.
Repeated adeno-associated virus serotype 2 aerosol-mediated cystic fibrosis transmembrane regulator gene transfer to the lungs of patients with cystic fibrosis: a multicenter, double-blind, placebo-controlled trial.
Chest. 2004 Feb;125(2):509-21

Perez-Soler R.
The role of erlotinib (Tarceva, OSI 774) in the treatment of non-small cell lung cancer.
Clin Cancer Res. 2004 Jun 15;10(12 Pt 2):4238s-4240s.

Roz L, Gramegna M, Ishii H, Croce CM, Sozzi G.
Restoration of fragile histidine triad (FHIT) expression induces apoptosis and suppresses tumorigenicity in lung and cervical cancer cell lines.
Proc Natl Acad Sci U S A. 2002 Mar 19;99(6):3615-20.

Rygaard K, Nakamura T, Spang-Thomsen M.
Expression of the proto-oncogenes c-met and c-kit and their ligands, hepatocyte growth factor/scatter factor and stem cell factor, in SCLC cell lines and xenografts.
Br J Cancer. 1993 Jan;67(1):37-46.

Samulski RJ, Chang LS, Shenk T.
Helper-free stocks of recombinant adeno-associated viruses: normal integration does not require viral gene expression.
J Virol. 1989 Sep;63(9):3822-8

Schiller JH, Adak S, Cella D, DeVore RF 3rd, Johnson DH. Topotecan versus observation after cisplatin plus etoposide in extensive-stage small-cell lung cancer: E7593--a phase III trial of the Eastern Cooperative Oncology Group.
J Clin Oncol. 2001 Apr 15;19(8):2114-22.

Schiller JH, Harrington D, Belani CP, Langer C, Sandler A, Krook J, Zhu J, Johnson DH; Eastern Cooperative Oncology Group. Comparison of four chemotherapy regimens for advanced non-small-cell lung cancer.
N Engl J Med. 2002 Jan 10;346(2):92-8.

Schwarzbach MH, Eisold S, Burguete T, Willeke F, Klein-Bauernschmitt P, Schlehofer JR, Herfarth C, Ridder R, von Knebel Doeberitz M.
Sensitization of sarcoma cells to doxorubicin treatment by concomitant wild-type adeno-associated virus type 2 (AAV-2) infection.
Int J Oncol. 2002 Jun;20(6):1211-8.

Senderowicz AM.
Small-molecule cyclin-dependent kinase modulators.
Oncogene. 2003 Sep 29;22(42):6609-20.

Smith J, Herrero R, Erles K, Grimm D, Munoz N, Bosch FX, Tafur L, Shah KV, Schlehofer JR.
Adeno-associated virus seropositivity and HPV-induced cervical cancer in Spain and Colombia.
Int J Cancer. 2001 Nov;94(4):520-6.

Toledo G, Sola JJ, Lozano MD, Soria E, Pardo J.
Loss of FHIT protein expression is related to high proliferation, low apoptosis and worse prognosis in non-small-cell lung cancer.
Mod Pathol. 2004 Apr;17(4):440-8.

Wang L, Herzog RW.
AAV-mediated gene transfer for treatment of hemophilia.
Curr Gene Ther. 2005 Jun;5(3):349-60

Wistuba II, Gazdar AF, Minna JD.
Molecular genetics of small cell lung carcinoma.
Semin Oncol. 2001 Apr;28(2 Suppl 4):3-13.

Vihinen-Ranta M, Suikkanen S, Parrish CR.
Pathways of cell infection by parvoviruses and adeno-associated viruses.
J Virol. 2004 Jul;78(13):6709-14.

## 7. Abkürzungsverzeichnis

| | |
|---|---|
| **AAV-2** | **: adeno-assoziiertes Virus Typ-2** |
| **CDK** | **: cyklin dependent kinase** |
| **CLL** | **: chronische lymphatische Leukämie** |
| **c-kit** | **: cellular homologue of kit, the Hardy-Zuckerman 4 feline sarcoma virus oncogene** |
| **EGFP** | **: enhanced green fluorescence protein** |
| **EGFR-1** | **: epidermal growth factor receptor-1** |
| **FACS** | **: fluorescence activated cell sorting** |
| **FGFR-1** | **: fibroblast growth factor receptor-1** |
| **FHIT** | **: fragile histidine triad** |
| **GFP** | **: green fluorescence protein** |
| **HeLa** | **: Zervixkarzinomzelllinie der Patientin Helen Lang** |
| **ICA** | **: infectious center assay** |
| **ICAM-1** | **: intercellular adhesion molecule-1** |
| **kd** | **: Kilodalton** |
| **LCM** | **: laser capture microdissection** |
| **NSCLC** | **: non-small lung cell carcinoma** |
| **p16** | **: Protein der Größe 16 kd** |
| **p53** | **: Protein der Größe 53 kd** |
| **rAAV-2** | **: rekombinant hergestelltes adeno-assoziiertes Virus Typ-2** |
| **r-AAV-2-EGFP** | **: rAAV-2, Vekor für EGFP** |
| **r-AAV-2-p53** | **: rAAV-2, Vekor für p53** |
| **Rb** | **: Retinoblastoma** |
| **qPCR** | **: quantitative polymerase chain reaction** |
| **SAM** | **: significance analysis of microarrays** |
| **SCID** | **: severe combined immundeficiency** |
| **SCLC** | **: small cell lung cancer** |
| **SIRS** | **: systemic inflammatory response syndrome** |

| | |
|---|---|
| **SCF** | **: stem cell factor** |
| **TKI** | **: Tyrosinkinaseinhibitor** |
| **TSG** | **: Tumorsuppressorgen** |
| **VST** | **: variance stabilizing transformation** |
| **wt-AAV-2** | **: Wild-Typ des adeno-assoziiertes Virus Typ-2** |

## 8. Danksagung

An erster Stelle danke ich meinem Mentor Herrn Professor Dr. Rainer Haas für sein Vertrauen, welches er stets in mich setzte. Dieses begann, seit er mich als Arzt im Praktikum am Universitätsklinikum Heidelberg einstellte. Durch die von ihm angeregte Tätigkeit am Deutschen Krebsforschungszentrum in Heidelberg 1997, verbunden mit meiner klinischen Tätigkeit auf der Station Plügge, die zur Kooperationseinheit Molekulare Hämatologie/Onkologie gehörte, eröffnete er mir die einzigartige Möglichkeit molekulare Medizin und klinische Tätigkeit zu verbinden, was mein Tun und meine Ziele bis heute prägt. Die dauerhafte Unterstützung und Förderung, mit der er maßgeblich zum Erfolg meiner wissenschaftlichen Arbeit beigetragen hat, führte dazu, dass ich ihm nach Düsseldorf folgte, als er Direktor der Klinik für Hämatologie, Onkologie und klinische Immunologie an die Heinrich-Heine Universität wurde.

Während meiner Zeit am Deutschen Krebsforschungszentrum lernte ich Herrn Priv. Doz. Dr. Ralf Kronenwett kennen, der dort mein betreuender Mentor war. Die offene, freundliche Aufnahme in seine Arbeitsgruppe, die stetige Diskussionsbereitschaft und Unterstützung eröffnete mir die Welt der molekularen Medizin. Der Erfolg jeder meiner Publikationen ist eng mit ihm verknüpft und unser gemeinsamer Wechsel von Heidelberg nach Düsseldorf führte über eine berufliche Zusammenarbeit weit hinaus.

Mein besonderer Dank gilt meinen beiden Doktoranden, Herrn Mark-Andre Wulf und Frau Judith Neukirchen für ihren steten Einsatz und der hervorragenden Zusammenarbeit, woraus ein freundschaftliches Verhältnis entstand.

Weiterhin möchte ich mich bei Herrn Dr. Ulrich Steidl und Herrn Dr. Roland Fenk für den Optimismus, die Kollegialität und ihre Freundschaft bedanken.

Abschließend danke ich meinen Eltern und meiner Frau Christine sowie meinen beiden Kindern Jan und Greta, die mich stets unterstützten und deren Kraft mich immer wieder antrieb und antreiben wird.

## 10. Zusammengefasste Publikationen

**A)** **Rohr UP**, Kronenwett R, Grimm D, Kleinschmidt J, Haas R.
Primary human cells differ in their susceptibility to rAAV-2-mediated gene transfer and duration of reporter gene expression.
J Virol Methods. 2002;105:265-75.

**B)** **Rohr UP**, Wulf MA, Stahn S, Steidl U, Haas R, Kronenwett R.
Fast and reliable titration of recombinant adeno-associated virus type-2 using quantitative real-time PCR. J Virol Methods. 2002;106:81-8.

**C)** **Rohr UP**, Heyd F, Neukirchen J, Wulf MA, Queitsch I, Kroener-Lux G, Steidl U, Fenk R, Haas R, Kronenwett R. Quantitative real-time PCR for titration of infectious recombinant AAV-2 particles. J Virol Methods; 2005, 127:40-45

**D)** **Rohr UP**, Wulf MA, Stahn S, Heyd F, Steidl U, Fenk R, Opalka B, Pitschke G, Prisack HB, Bojar H, Haas R, Kronenwett R.
Non-small lung cancer cells are prime targets for p53 gene transfer mediated by a recombinant adeno-associated virus type-2 vector. Cancer Gene Ther. 2003;10:898-906.

**E)** **Rohr UP**, Rehfeld N, Pflugfelder L, Geddert H, Muller W, Steidl U, Fenk R, Graf T, Schott M, Thiele KP, Gabbert HE, Germing U, Kronenwett R, Haas R.
Expression of the tyrosine kinase c-kit is an independent prognostic factor in patients with small cell lung cancer. Int J Cancer. 2004;111:259-63.

**F)** **Rohr UP**, Rehfeld N, Geddert H, Pflugfelder L, Bruns I, Neukirch J, Rohrbeck A, Grote HJ, Steidl U, Fenk R, Opalka B, Gabbert HE, Kronenwett R, Haas R.
Prognostic relevance of fragile histidine triad protein expression in patients with small cell lung cancer. Clin Cancer Res. 2005;11:180-5

ELSEVIER

Journal of Virological Methods 105 (2002) 265–275

Journal of Virological Methods

www.elsevier.com/locate/jviromet

# Primary human cells differ in their susceptibility to rAAV-2-mediated gene transfer and duration of reporter gene expression

Ulrich-Peter Rohr [a,*], Ralf Kronenwett [a], Dirk Grimm [b], Jürgen Kleinschmidt [b], Rainer Haas [a]

[a] *Klinik für Hämatologie, Onkologie und klinische Immunologie, Heinrich-Heine-Universität Düsseldorf, Moorenstraße 5, D-40225 Düsseldorf, Germany*

[b] *Deutsches Krebsforschungszentrum, Forschungsschwerpunkt Angewandte Tumorvirologie, Im Neuenheimer Feld 242, D-69120 Heidelberg, Germany*

Received 14 March 2002; received in revised form 21 May 2002; accepted 23 May 2002

**Abstract**

The susceptibility of a variety of different primary tissues was examined to long-term transduction with recombinant adeno-associated virus type 2 (rAAV-2) and factors influencing the transduction efficiency. In contrast to others using cell lines and animal models, emphasis was placed on the use of primary human cells. Enhanced green fluorescent protein (EGFP) marker gene expression was examined using fluorescence-activated cell sorting analysis. The most effective target cells for rAAV-2-mediated gene transfer were bronchial epithelial, artery endothelial as well as smooth and skeletal muscle cells with mean transduction rates ranging from 34.3 to 81.6%. Lower transduction rates between 4.3 and 19.5% were found in chondrocytes, dermal papilla follicle epithelial cells and fibroblasts. No transduction was observed in melanocytes, granulocyte colony-stimulating factor (G-CSF)-mobilized $CD34^+$ cells or malignant $CD19^+$ cells from patients with chronic lymphocytic leukemia. A proportion of EGFP-expressing skeletal muscle and smooth muscle cells was maintained over a period of 6 weeks after transduction ($42.7 \pm 5.4$ and $67.1 \pm 0.9\%$, respectively). Interestingly, among hair follicle epithelial cells the proportion of transduced cells increased from $8 \pm 0.5$ to $36 \pm 7.7\%$ in the course of 6 weeks. In contrast, for endothelial cells, bronchial epithelial cells and fibroblasts, a rapid decline in the number of EGFP expressing cells were noted. An inverse relationship between the proportion of cells in G2/M phase of cell cycle and long-term gene expression was observed. All rAAV-2 susceptible primary cells expressed FGFR-1 and the αV integrin consistent with their role as co-receptors for AAV-2. In conclusion, AAV-2 is a suitable vector system for transduction and evaluation of functional effects of long-term gene expression in primary human muscle and hair follicle cells. 

*Keywords:* AAV-2; Tropism; Transduction efficiency; αV integrin; FGFR-1; Cell cycle

* Corresponding author. Tel.: +49-211-8117720; fax: +49-211-8118853
*E-mail address:* urohr-uni-duesseldorf@gmx.de (U.-P. Rohr).

0166-0934/02/$ - see front matter 
PII: S0166-0934(02)00117-9

## 1. Introduction

Recombinant adeno-associated virus type 2 (rAAV-2) vectors are useful for transfer of therapeutic genes into human cells particularly since wild-type AAV-2 (wt-AAV-2), a replication-deficient single stranded human DNA virus, is not pathogenic in humans (Berns and Bohenzky, 1987; Berns, 1990; Muzyczka, 1992). Infection is initiated by binding of AAV-2 to a low-affinity membrane-associated heparan sulfate (HS) proteoglycan (Summerford and Samulski, 1998; Qiu et al., 2000), while entry of AAV-2 is mediated by at least one of two high-affinity co-receptors described recently. These are the human fibroblast growth factor receptor (Qing et al., 1999) and the αVβ5 integrin (Summerford et al., 1999). The host range in animals and cell types affected by wt-AAV-2 or rAAV-2 is relatively broad (Kaplitt et al., 1994; Fisher et al., 1997; Snyder et al., 1997; Halbert et al., 1997; Rolling et al., 1997; Monahan et al., 1998). While the safe administration of rAAV-2 in a clinical study has been shown for patients with haemophilia B (Kay et al., 2000), tropism of AAV-2 was examined using mainly animal models or cell lines. Comparisons of the results between different animal systems are inconsistent and adaptation to the human system seems difficult. A systematic analysis of duration of rAAV-2-mediated transgene expression for human cells has not been carried out so far. In the current study, a variety of primary human cells were examined including tissues of mesenchymal, endodermal and neuroektodermal origin. Long-term marker gene expression and variables related to transduction efficiency such as receptor status and cell cycle state were of particular interest.

## 2. Material and methods

### 2.1. Cells

The human embryonic kidney cell line 293T (Pear et al., 1993) was cultured in Dulbecco's modified Eagle's medium (DMEM Sigma, Deissenhofen, Germany) supplemented with 10% heat-inactivated foetal calf serum, 2 mM glutamate, 100 IU/ml penicillin and 100 μg/ml streptomycin. For the culturing of HeLa cells (Gey et al., 1952) RPMI-1640 medium (Sigma, Deissenhofen, Germany) was used instead of DMEM medium containing the same additives listed above. Both cell lines were cultured at 37 °C in 5% $CO_2$ and were passaged twice a week after trypsinization. Primary non-hematopoietic human cells were obtained from PromoCell (Heidelberg, Germany) and cultured in the respective growth medium (PromoCell) according to the manufacturer's instructions. Cells were passaged when confluence of 75–80% was reached. Primary human non-hematopoietic cells were skeletal muscle cells derived from M. rectus abdominis, fibroblasts isolated from foreskin, smooth muscle cells isolated from umbilical cord artery, bronchial epithelial cells, hyaline chondrocytes, melanocytes, umbilical artery endothelial cells, and dermal papilla follicle epithelial cells. All primary cells were isolated from normal human tissue and stored in liquid nitrogen. After recovery from cryopreservation, type-specificity was confirmed by indirect immunofluorescence. The following antibodies were used: mouse anti human CD31 (DAKO, Hamburg, Germany), mouse anti-human smooth muscle alpha actin (DAKO), mouse anti-human cartilage proteoglycan (Chemicon, Hofheim, Germany), rabbit anti-human skeletal myosin (Sigma, Taufkirchen, Germany), mouse anti-human fibroblast (Dianova, Hamburg, Germany), mouse anti-human pan-cytokeratin (DAKO), mouse anti-human melanom (DAKO), and mouse anti-human alkaline phosphatase (Sigma). The following secondary antibodies were used: goat anti-mouse IgG fluorescein isothiocyanate (FITC) (Dianova), and goat anti-rabbit IgG FITC (Sigma). Using PCR, HIV, hepatitis B, hepatitis C or Mycoplasma were not detected. For all experiments, $1 \times 10^3$–$1 \times 10^4$ cells per well were grown in 24-well plates with media being replaced every second day.

Hematopoietic $CD34^+$ cells were obtained from leukapheresis products of patients with breast carcinoma in complete remission after informed consent ($n = 5$). After cytotoxic chemotherapy supported with 300 μg/d of recombinant human granulocyte colony-stimulating factor (G-CSF; R-

metHuG-CSF, Amgen, Thousand Oaks, CA), cells were collected using a Fenwal CS3000 (Baxter, Munich, Germany) and $CD34^+$ cells were selected using the Baxter Isolex 300SA Magnetic Cell Separation System (Baxter, Munich, Germany) as described (Hohaus et al., 1997). $CD34^+$ cells were cultured in RPMI-1640 medium supplemented with 10% heat-inactivated foetal calf serum, 2 mM glutamate, 100 U/ml penicillin-streptomycin, 100 ng/ml interleukin-3 (IL-3), 10 ng/ml stem cell factor (SCF) and 100 ng/ml IL-6. Cells from four patients with chronic lymphocytic leukemia with a proportion of lymphocytes ranging between 91 and 98% were cultured in RPMI-1640 medium supplemented with 10% heat-inactivated foetal calf serum, 2 mM glutamate, 100 U/ml penicillin-streptomycin and 10 ng/ml IL-2. All cytokines were obtained from PromoCell (Heidelberg, Germany). Primary hematopoietic cells were cultured in 24-well plates with $1 \times 10^5$ cells per well after examination of viability using trypan blue.

### 2.2. Adenovirus-free production and purification of recombinant AAV-2 vector stocks and "pseudo"-stocks

For preparation of rAAV-2 vector stocks, $1 \times 10^7$ 293T cells were co-transfected with 20 μg vector plasmid pAAV-gfp-AR6- and 20 μg helper plasmid pDG (Grimm et al., 1998) by calcium phosphate precipitation. The vector plasmid pAAV-gfp-AR6- (Hörster et al., 1999) contains the gene for enhanced green fluorescent protein (EGFP) and the HIV-1-directed antisense sequence AR6 under the control of the immediate early HCMV promoter, an SV40 splice and a polyadenylation signal flanked by the inverted terminal repeats (ITRs) of the AAV-2 clone psub201 (Samulski et al., 1989). The helper plasmid pDG contains all packaging and helper functions of AAV-2 (rep, cap) and adenovirus (E2A, E4, VA) for rAAV-2 particle production. 293T cells were harvested 72 h after transfection and were subjected to three cycles of freezing and thawing to release virus. The cell lysate was sonicated 10 times with pulsed 50% duty cycles at 200 W using a Branson Sonifier cell disrupter B-15 (Branson, Schwäbisch Gmuend, Germany) and spun down at 5000 g for 30 min. After adding CsCl to the viral supernatant to a final density of 1.38 g/ml, the solution was underlayed with 1.5 ml of 1.45 g/ml CsCl and spun in a Beckman L5-50B Ultracentrifuge (Beckman Coulter, Munich, Germany) at 36 000 rpm at 10 °C for 24 h. Fractions of 500–600 μl were collected starting from the bottom of the tube and the refractive index of each fraction was determined. rAAV-2 particles were enriched in those fractions with a refractive index of 1.3717, corresponding to a density of 1.4 $g/cm^3$. The fractions containing between $4 \times 10^8$ and $2 \times 10^9$ infectious particles (IP) per ml were pooled resulting in a large vector stock with a final titer of $6 \times 10^8$ IP per ml. All fractions were dialysed twice against phosphate-buffered saline (PBS) for 6 h and RPMI for 24 h at 4 °C. Pseudo-stocks were prepared as described above but lacking the helper plasmid necessary for generation of viral particles. Pseudo-stocks were used as a negative control in order to avoid false positive results related to biologically active vector-encoded proteins which can contaminate virus preparations (Alexander et al., 1997). HeLa cells, which were incubated with the pseudo-stock-preparation containing no rAAV-2 particles, did not show EGFP fluorescence.

### 2.3. Titration of infectious viral particles using fluorescence-activated cell sorting

A flow cytometric method was used for titration of infectious rAAV-2 particles as previously described (Hörster et al., 1999). Briefly, $1 \times 10^5$ HeLa cells were seeded in 500 μl medium in 24-well plates. After 1 h, 1–500-fold serial dilution of virus suspension was performed and 5 μl of each dilution step was added to the cells. Cells were incubated at 37 °C for 48 h and harvested after removing the medium. 50 μl 0.02% Trypsin/EDTA (Bio-Whittacker, Verviers, Belgium) was used for washing and detachment. Trypsin was inactivated by adding 500 μl of 10% foetal calf serum (FCS)/PBS. Following two washing steps with 1 ml PBS, cells were resuspended in 500 μl PBS. After determination of the total cell numbers, fluorescence-activated cell sorting (FACS)

analysis was carried out using a Becton Dickinson FACSCalibur (Heidelberg, Germany) with a 2 W argon ion laser and EGFP fluorescence measured using a 530/15 nm (FITC) band pass filter. The percentage of green fluorescent cells was determined by FACS and was multiplied by the total cell numbers. Assuming that each EGFP-positive HeLa cell was infected by one rAAV-2 particle, viral titers were deduced from the percentage of transduced cells and the quantity of virus used.

### 2.4. Transduction experiments and FACS analysis

Primary human cells were cultured in 24-well plates as described above and transduced with a multiplicity of infection per cell (MOI) of 50. The fraction of the pseudo-stock with a similar refractive index as the viral fraction was used as a negative control. Following transduction, the medium of the cells was replaced by fresh medium every second day. For examination of immediate and long-term EGFP expression, primary cells were harvested by incubation with trypsin/EDTA, washed twice with PBS as described above and resuspended in 500 μl of PBS 2, 7, 14, 21, 28, 35 and 42 days after transduction. Cells were then subjected to FACS analysis using a FACSCalibur. After gating on viable cells, data were analysed using the Becton Dickinson CELL QUEST software. Primary hematopoietic cells were incubated with viral particles (MOI of 50) or pseudo-preparation for 24 h. Following centrifugation, the medium was removed and replaced by fresh RPMI medium. After further 24 h, cells were washed twice with PBS and subjected to FACS analysis. For identification of $CD34^+$ hematopoietic stem cells and B cells from patients with chronic lymphocytic leukemia, the antibodies (Ab) CD34-PE (Becton-Dickinson, Heidelberg, Germany) and CD19-PE (Coulter-Immunotech, Hamburg, Germany) were used, respectively. PE-conjugated $IgG_1$ isotype-identical antibody (Coulter-Immunotech, Hamburg, Germany) was used to evaluate non-specific binding. Cells were incubated with the mAbs in 500 μl PBS containing 1% bovine serum albumin (BSA) at 4 °C for 30 min. Then virus- and pseudo-stock-treated cells were subjected to FACS analysis. $CD34^+$ cells or malignant $CD19^+$ B-cells were gated and the number of cells showing apparent EGFP fluorescence was calculated as described above.

### 2.5. Cell cycle analysis

$5 \times 10^4$ cells were harvested using trypsin/EDTA and washed twice with PBS as described above, centrifuged at 1000 g and resuspended in 500 μl RPMI 1640 and 500 μl PBS. 3 ml of ice cold ethanol was added to the cell suspension. After a 30 min period of incubation on ice, cells were washed with PBS, centrifuged at 1000 g and resuspended in 450 μl propidium iodide (PI)(50 μg/ml) and 50 μl RNase (5 mg/ml)(Sigma, Deisenhofen, Germany) for 30 min. Cells were then subjected to FACS analysis. PI-fluorescence intensity was detected at 630 nm using a FACSCalibur. Integrational fractions of G0/G1, S, G2/M-phases of cell cycle were calculated in percent using the MODFITLT v2.0 software (Becton Dickinson).

### 2.6. Analysis of fibroblast growth factor receptor-1 (FGFR-1) and αV integrin expression on the surface of primary cells

For analysis of FGFR-1 and αV integrin expression, $5 \times 10^3$ cells per well in 24-well plates were incubated with 500 μl of 2% formalin for 15 min at room temperature. Cells were washed three times with PBS and incubated with ice-cold methanol at −20 °C for 5 min. After three times of washing with PBS, cells were incubated with FITC-conjugated anti-CD51 (αV) antibody (Clone AMF7, Immunotech, Marseille, France) or the non-conjugated Ab Anti-FGFR-1 antibody (Sigma). For indirect immunofluorescence detection, monoclonal FITC-conjugated anti-rabbit (Sigma) were used as secondary Ab. Expression of FGFR and αV integrin on the cell surface was detected via fluorescence microscopy. The level of receptor expression was classified into four categories no expression (−), low (+), moderate (++) and high (+++) expression as described (Press et al., 1993; Hepburn et al., 1995). This semi-quantitative approach was chosen instead of Western blot since a large number of

experiments were undertaken at the same time with a limited number of primary cells.

## 3. Results

### 3.1. Transduction efficiencies in primary human cells

Human cells of different tissue origin were used to examine their susceptibility for transduction of rAAV-2. For each cell type at least three or more experiments were performed on freshly isolated primary cells which had been cultivated over a period between 2 and 7 days. This corresponds to a cultivation period of less than three cell passages. FACS analysis was carried out 48 h after transduction to determine the proportion of cells expressing the reporter gene EGFP (Fig. 1). Using an MOI of 50 per cell the rate of transduction observed among the different cell types varied considerably (Fig. 2). Skeletal and smooth muscle cells were the most suitable target cells for rAAV-2 with mean transduction efficiencies of 81.6% (SD, ±1.9%) and 51.0% (SD, ±0.1%), respectively (Fig. 3). The susceptibility of artery endothelial cells and bronchial epithelium was intermediate as reflected by mean transduction rates of 44.3% (SD, ±8.7%) and 34.3% (SD, ±23.7%), respectively (Fig. 2). Dermal fibrob-

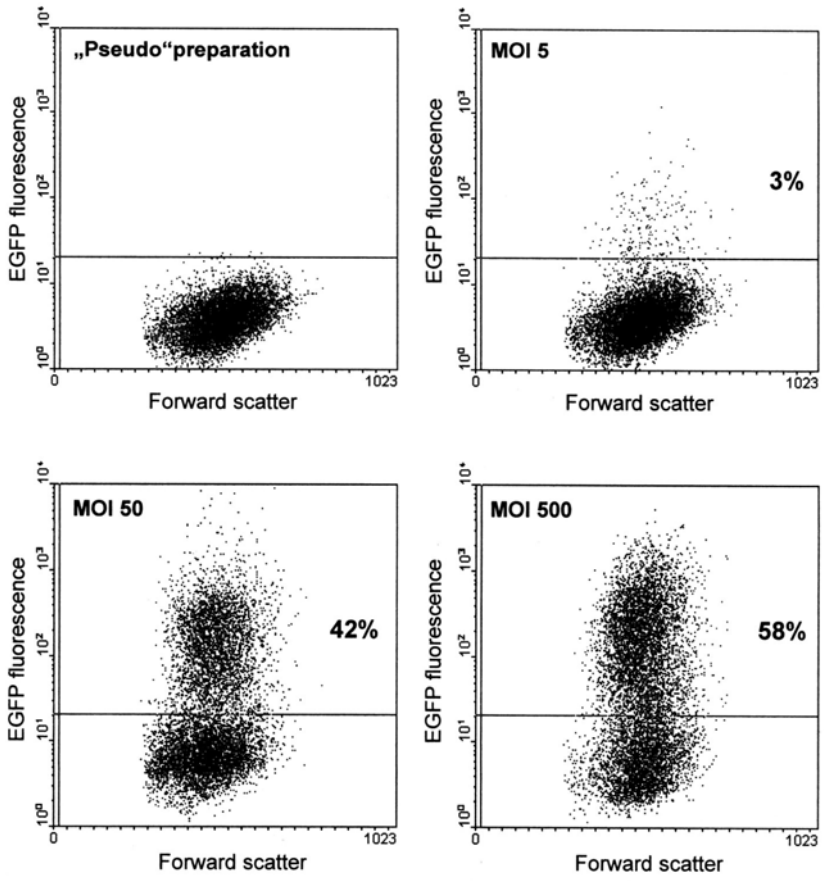


Fig. 1. Representative FACS analysis of arterial endothelial cells at different MOIs per cell 48 h after transduction.

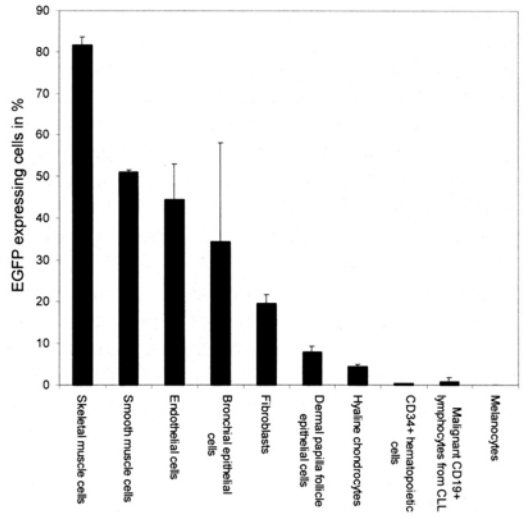


Fig. 2. Transduction rates of rAAV-2 in different human cell types after 48 h. An MOI of 50 was used. The mean transduction rates and standard deviations of three independent experiments are indicated.

lasts, dermal papilla follicle epithelial cells and hyaline chondrocytes were less transducable with mean transduction efficiencies of 19.5% (SD, ± 2.2%), 7.9% (SD, ± 0.14%) and 4.3% (SD, ± 0.7%), respectively.

With a mean transduction rate of 0.3% (range, 0–1.3%) which was along the baseline, we had no evidence that normal G-CSF-mobilized $CD34^+$ hematopoietic progenitor cells enriched from leukapheresis products of five different donors were susceptible for rAAV-2. Similar results were observed with malignant $CD19^+$ hematopoietic cells from four different patients with chronic lymphocytic leukemia showing a mean transduction rate of only 0.9% (range, 0–1.7%). In the same line, no significant transduction of rAAV-2 was observed in melanocytes.

### *3.2. Long-term gene expression in primary human cells*

Transduced cells were cultivated over a time period of 42 days in order to examine the duration of gene expression. For this assessment, between one and four experiments were performed for each cell type. In general, a rapid decline of EGFP expression was observed for bronchus-derived human epithelial cells, artery endothelial cells, smooth muscle and skeletal muscle cells with a mean proportion of EGFP-expressing cells between 0.3 and 13.6% after 42 days (Fig. 4). The finding for dermal fibroblasts was somewhat different with a transient increase on day 7 followed by a decrease similar to that observed for the four above mentioned cell types. In contrast, human dermal papilla follicle epithelial cells showed a significant increase in the proportion of transduced cells between 14 and 28 days of cultivation resulting in a plateau of 36% (SD, ± 7.7%) EGFP-expressing cells on day 42.

The transduction rates reported above were observed with cells which were passaged three times after they were obtained from the provider. With respect to short cultivation period of the cells, this series of experiments is termed as early transduction. In a second set of experiments, late transduction experiments were carried out following cultivation of the primary cells for 28 days in order to examine the transduction efficiencies in relation to cell differentiation and aging.

Similar to the observations made with respect to the early transduction experiments, a rapid decrease in the proportion of EGFP-expressing cells was observed for endothelial cells, bronchial epithelial cells and dermal fibroblasts. Again, dermal papilla follicle epithelial cells behaved differently. For this cell type, an increase in the proportion of transduced cells was observed between day 7 and 14 reaching a plateau of 38.7% EGFP-positive cells on day 42. Different from the early transduction experiments, a significant increase in the proportion of EGFP-expressing smooth and skeletal muscle cells was found with a mean value of 59.8% (SD, ± 12.8%) and 61.4% (SD, ± 19%) on day 14, respectively. The proportion of EGFP-expressing smooth and skeletal muscle cells remained relatively stable with a plateau of 67.1% (SD, ± 0.9%) and 42.7% (SD, ± 5.4%) on day 42, respectively (Fig. 4).

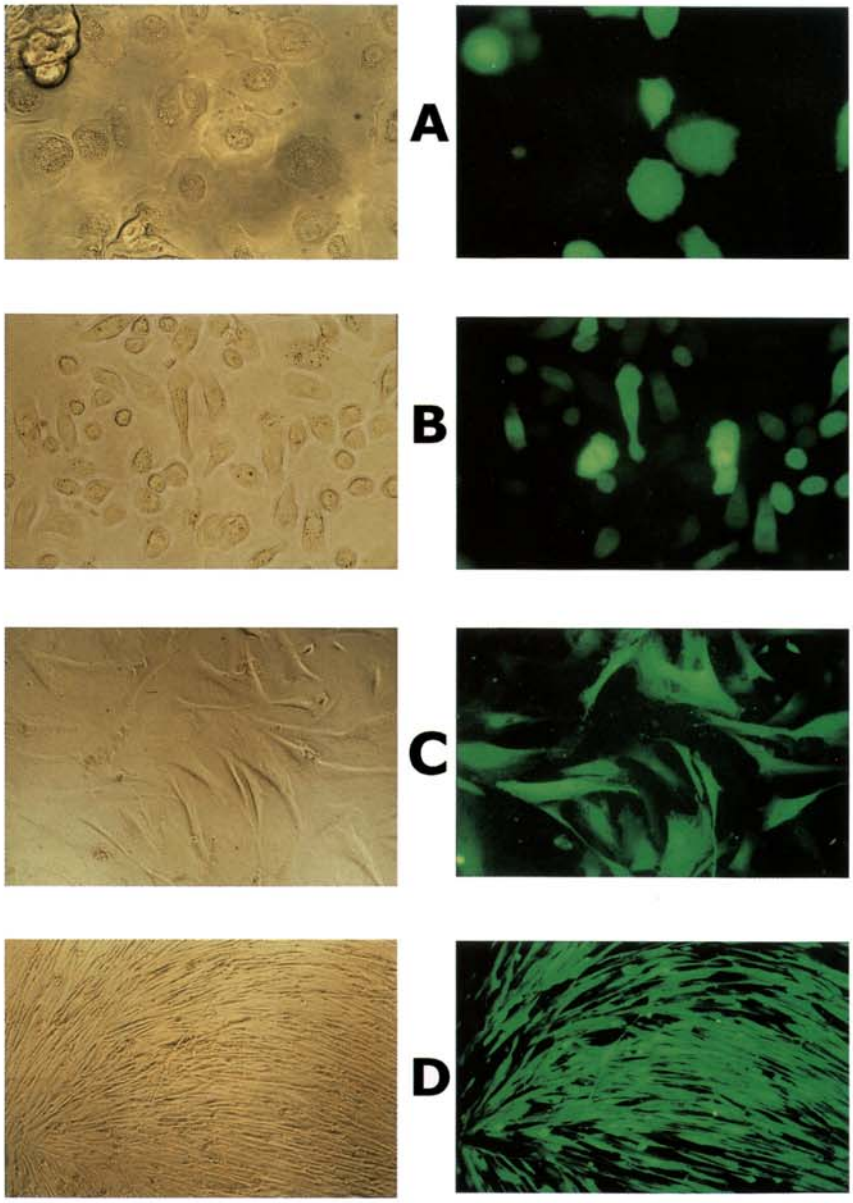


Fig. 3. EGFP expression of rAAV-2-transduced human cells. Left side: phase contrast microscopy; right side: corresponding fluorescence microscopy. (A) Endothelial cells 7 days after transduction (magnification 400 ×). (B) Bronchial epithelial cells 2 days after transduction (magnification 400 ×). (C) Smooth muscle cells 28 days after transduction (magnification 400 ×). (D) Skeletal muscle cells 2 days after transduction (magnification 100 ×).

Table 1
FGFR-1 and αV-integrin receptor status on different human tissues

| | FGFR-1 | | αV-integrin | |
|---|---|---|---|---|
| | Early experimental setting | Late experimental setting | Early experimental setting | Late experimental setting |
| Endothelial cells | ++ | ++ | ++ | ++ |
| Bronchial epithelial cells | +++ | +++ | + | + |
| Skeletal muscle cells | +++ | +++ | ++ | + |
| Smooth muscle cells | ++ | ++ | + | + |
| Follicle papilla epithelial cells | + | + | ++ | ++ |
| Fibroblasts | +++ | +++ | ++ | ++ |
| Hematopoietic stem cell | –[a] | Not performed | –[a] | Not performed |
| Malignant lymphocytes | –[a] | Not performed | –[a] | Not performed |

The level of receptor expression was classified into four categories: no expression (–), low (+), moderate (++) and high (+++) expression.
[a] Additionally, FACS-analysed for FGFR-1 and αV-integrin receptor status.

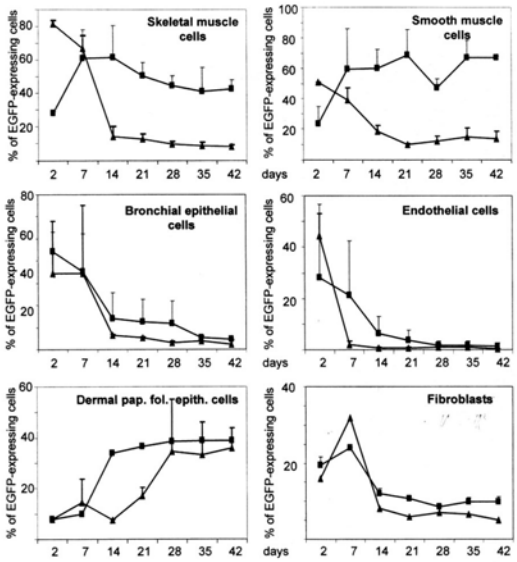


Fig. 4. rAAV-2-mediated long-term gene expression into human cells. Two experimental series were performed using an MOI of 50. In the first set of experiments, human cells were transduced which were passaged less than four times after obtaining the cells from the provider. A second set of transduction experiments were performed 28 days after cultivation using cells of the same lot. The results of the early (▲) and late transduction (■) experiments are indicated.

### *3.3. Expression of FGFR-1 and αV integrin on the surface of primary cells and cell cycle analysis*

With the exception of the normal CD34$^+$ and leukemic CD19$^+$ hematopoietic cells, all cell types examined expressed both FGFR-1 and αV integrin (Table 1). Time-dependent changes were not observed except for a decline of αV integrin expression in skeletal muscle cells. Therefore, cell types susceptible for rAAV-2-mediated gene transfer expressed FGFR-1 and αV integrin. On the other hand, cells not transducable by rAAV-2 such as hematopoietic cells did not express αV integrin or FGFR-1 on their surface.

In order to examine whether the cell cycle state was related to the transduction rates, cell cycle analyses were performed before the early and late transduction experiments. A significant decrease in the proportion of cells in G2/M was observed for dermal papilla follicle epithelial cells, dermal fibroblasts, skeletal as well as smooth muscle cells (Fig. 5). In contrast, for human endothelial cells and bronchial epithelial cells an increase in the proportion of cells in G2/M was found. Initially, the proportion of cells in G2/M was 16.16 and 26.42% in comparison to 32.16 and 29.77% at the time when late transduction experiments were performed. When cell cycle was viewed in the context

of rAAV-2-mediated duration of gene expression, only cell types with a proportion of cells in G2/M phase of less than 3%, such as smooth and skeletal muscle cells, contained a constant or increasing number of EGFP-positive cells over a period of 42 days. Cell types with a proportion of cells in G2/M phase of more than 15%, such as arterial endothelium or bronchial epithelium, showed a decline in EGFP expression following transduction.

## 4. Discussion

Somatic gene therapy provides a potentially curative treatment for patients with inherited diseases of monogenetic origin. This has been shown in a clinical phase-1-trial with patients suffering from hemophilia B (Kay et al., 2000). The encouraging results of this clinical study led us to look for other human cell types that could serve as target cells for an rAAV-2-mediated gene transfer. The ex-vivo study was also undertaken since the majority of results published on the tropism of rAAV-2 is derived from experiments performed with cell lines or cells from animal models. The shortcoming of these models is best exemplified if one considers that the number of copies found in muscle cells of mice and dogs was approximately 100-fold smaller in comparison to results observed in humans (Herzog et al., 1997; Snyder et al., 1997; Kay et al., 2000).

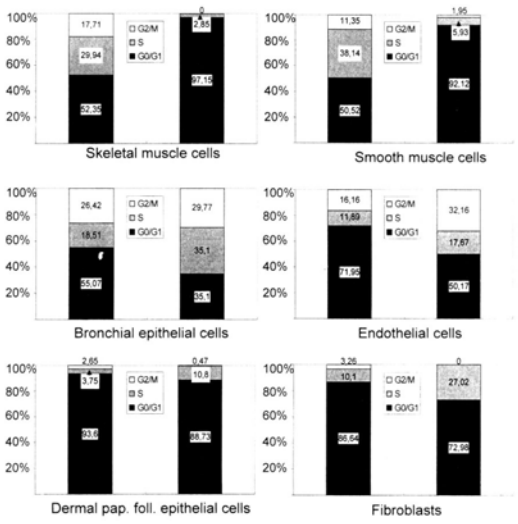


Fig. 5. Cell cycle analysis of human cells. Left bars reflect the cell cycle state of the tissue within three cell passages after obtaining the cells from the provider. Right bars show the cell cycle state after a cultivation time of 28 days.

In the present study, a broad array of different tissue types of neuroectodermal, endodermal and cells of mesenchymal origin was included. Addressing the question of tropism, it was found that the two previously described co-receptors required for rAAV-2 uptake were present on the membrane of all cell types examined except for $CD34^+$ normal hematopoietic progenitor cells and $CD19^+$ leukemic cells. At that point, low-affinity membrane-associated HS proteoglycan were not sought as the data from the literature suggest an almost ubiquitous presence on cells of different tissues and species (Summerford and Samulski, 1998; Qiu et al., 2000). The lack of co-receptors on the hematopoietic cells is the most likely explanation that no expression of the marker gene was observed. Other researchers have reported transduction efficiencies of $CD34^+$ cells between 5 and 100% (Fisher-Adams et al., 1996; Ponnazhagan et al., 1997; Schimmenti et al., 1998; Chatterjee et al., 1999; Nathwani et al., 2000). The discrepancy is most likely explained by the source of $CD34^+$ cells, as these investigators used $CD34^+$ cells from bone marrow and cord blood rather than G-CSF-mobilized $CD34^+$ cells from peripheral blood (PB) as we did.

We now turn to the cells which are potential target cells for rAAV-2 as the co-receptors are expressed in the cell membrane. The transduction rates noted varied between a minimum of 4.3% for hyaline chondrocytes and 81.6% for skeletal muscle cells. The heterogeneity observed and the relative differences found for the respective cell types were similar when the cells were used following a cultivation time period of 28 days. This finding clearly indicates that further propagation of the primary cells in culture did not influence the immediate uptake and processing of the recombinant vector. The picture is different when the duration of transgene expression was exam-

ined. This parameter is of relevance since it reflects the suitability of a given tissue for long-term expression of the gene to be delivered. It was shown that maintenance of transgene expression over a period of 42 days was inversely related to the proportion of cells in G2/M phase of the cell cycle. This relationship is best illustrated for skeletal and smooth muscle cells. When skeletal muscle cells were transduced following a cultivation period of 28 days the proportion of cells in G2/M phase decreased from 18 to 0%, while the proportion of EGFP-positive cells following an observation period of 42 days after transduction increased from a mean of 29 to 43%. Obviously, irrespective of the cell cycle state, a sufficient transduction of the muscle cells took place, while the final intracellular fate of the vector appeared to probably be related to particular conditions associated with the cell cycle. Our findings are in line with results of other investigators showing that quiescent cells can be efficiently transduced by AAV-2 (Flotte et al., 1994; Podsakoff et al., 1994). From previous studies of other investigators it seems that head-to-tail concatamers of the vector can develop (Fisher et al., 1997; Miao et al., 1998; Duan et al., 1998) which might favour transgene expression in quiescent cells.

In particular, our results are consistent with the findings of the phase-1-trial in patients with haemophilia B proving that human skeletal muscle is indeed a highly suitable target cell for AAV-2 with respect to susceptibility *and* duration of transgene expression. Under in-vitro culture conditions we were able to detect transgene expression in skeletal muscle cells over a time period of 1 year using fluorescence microscopy. The same is true for smooth muscle cells and to some extent for follicle endothelial cells which are susceptible to the viral vector and sustain prolonged gene expression. These human tissues are therefore prime candidates for gene delivery and prolonged gene expression in the setting of in-vitro or in-vivo studies. In contrast, other rAAV-2 susceptible target cells such as endothelial or bronchial epithelial cells, used currently for gene transfer protocols, lack the capability of sustained marker gene expression under in-vitro conditions. These findings might be of relevance for the rAAV-2-mediated delivery of genes to elucidate functional aspects of long-term transgene expression in the human system.

## Acknowledgements

We thank Michael Kirsch, Anke Boeckmann and Claudia Rieth for excellent technical assistance and Georg Sczakiel, Wolfgang Nedbal, Andrea Hörster and Birgit Teichmann for fruitful discussions.

## References

Alexander, I.E., Russell, D.W., Miller, A.D., 1997. Transfer of contaminants in adeno-associated virus vector stocks can mimic transduction and lead to artifactual results. Hum. Gene Ther. 8, 1911–1920.

Berns, K.I., 1990. Parvovirus replication. Microbiol. Rev. 54, 316–329.

Berns, K.I., Bohenzky, R.A., 1987. Adeno-associated viruses: an update. Adv. Virus Res. 32, 243–306.

Chatterjee, S., Li, W., Wong, C.A., Fisher-Adams, G., Lu, D., Guha, M., Macer, J.A., Forman, S.J., Wong, K.K. Jr., 1999. Transduction of primitive human marrow and cord blood-derived hematopoietic progenitor cells with adeno-associated virus vectors. Blood 93, 1882–1894.

Duan, D., Sharma, P., Yang, J., Yue, Y., Dudus, L., Zhang, Y., Fisher, K.J., Engelhardt, J.F., 1998. Circular intermediates of recombinant adeno-associated virus have defined structural characteristics responsible for long-term episomal persistence in muscle tissue. J. Virol. 72, 8568–8577.

Fisher-Adams, G., Wong, K.K. Jr., Podsakoff, G., Forman, S.J., Chatterjee, S., 1996. Integration of adeno-associated virus vectors in $CD34^+$ human hematopoietic progenitor cells after transduction. Blood 88, 492–504.

Fisher, K.J., Jooss, K., Alston, J., Yang, Y., Haecker, S.E., High, K., Pathak, R., Raper, S.E., Wilson, J.M., 1997. Recombinant adeno-associated virus for muscle directed gene therapy. Nat. Med. 3, 306–312.

Flotte, T.R., Afione, S.A., Zeitlin, P.L., 1994. Adeno-associated virus vector gene expression occurs in nondividing cells in the absence of vector DNA integration. Am. J. Respir. Cell Mol. Biol. 11, 517–521.

Gey, G.O., Coffman, W.D., Kubicek, M.T., 1952. Tissue culture studies of the proliferative capacity of cervical carcinoma and normal epithelium. Cancer Res. 12, 264–265.

Grimm, D., Kern, A., Rittner, K., Kleinschmidt, J.A., 1998. Novel tools for production and purification of recombinant adenoassociated virus vectors. Hum. Gene Ther. 9, 2745–2760.

Halbert, C.L., Standaert, T.A., Aitken, M.L., Alexander, I.E., Russell, D.W., Miller, A.D., 1997. Transduction by adeno-associated virus vectors in the rabbit airway: efficiency, persistence, and readministration. J. Virol. 71, 5932–5941.

Hepburn, P.J., Glynne-Jones, E., Goddard, L., Gee, J.M., Harper, M.E., 1995. Cell proliferation in prostatic carcinoma: comparative analysis of Ki-67, MIB-1 and PCNA. Histochem. J. 27, 196–203.

Herzog, R.W., Hagstrom, J.N., Kung, S.H., Tai, S.J., Wilson, J.M., Fisher, K.J., High, K.A., 1997. Stable gene transfer and expression of human blood coagulation factor IX after intramuscular injection of recombinant adeno-associated virus. Proc. Natl. Acad. Sci. USA 94, 5804–5809.

Hörster, A., Teichmann, B., Hormes, R., Grimm, D., Kleinschmidt, J., Sczakiel, G., 1999. Recombinant AAV-2 harboring gfp-antisense/ribozyme fusion sequences monitor transduction, gene expression, and show anti-HIV-1 efficacy. Gene Ther. 6, 1231–1238.

Hohaus, S., Pförsich, M., Murea, S., Abdallah, A., Lin, Y.S., Funk, L., Voso, M.T., Kaul, S., Schmid, H., Wallwiener, D., Haas, R., 1997. Immunomagnetic selection of CD34$^+$ peripheral blood stem cells for autografting in patients with breast cancer. Br. J. Haematol. 97, 881–888.

Kaplitt, M.G., Leone, P., Samulski, R.J., Xiao, X., Pfaff, D.W., O'malley, K.L., During, M.J., 1994. Long-term gene expression and phenotypic correction using adeno-associated virus vectors in the mammalian brain. Nat. Genet. 8, 148–154.

Kay, M.A., Manno, C.S., Ragni, M.V., Larson, P.J., Couto, L.B., Mcclelland, A., Glader, B., Chew, A.J., Tai, S.J., Herzog, R.W., Arruda, V., Johnson, F., Scallan, C., Skarsgard, E., Flake, A.W., High, K.A., 2000. Evidence for gene transfer and expression of factor IX in haemophilia B patients treated with an AAV vector. Nat. Genet. 24, 257–261.

Miao, C.H., Snyder, R.O., Schowalter, D.B., Patijn, G.A., Donahue, B., Winther, B., Kay, M.A., 1998. The kinetics of rAAV integration in the liver. Nat. Genet. 19, 13–15.

Monahan, P.E., Samulski, R.J., Tazelaar, J., Xiao, X., Nichols, T.C., Bellinger, D.A., Read, M.S., Walsh, C.E., 1998. Direct intramuscular injection with recombinant AAV vectors results in sustained expression in a dog model of hemophilia. Gene Ther. 5, 40–49.

Muzyczka, N., 1992. Use of adeno-associated virus as a general transduction vector for mammalian cells. Curr. Top. Microbiol. Immunol. 158, 97–129.

Nathwani, A.C., Hanawa, H., Vandergriff, J., Kelly, P., Vanin, E.F., Nienhuis, A.W., 2000. Efficient gene transfer into human cord blood CD34$^+$ cells and the CD34$^+$ CD38$^-$ subset using highly purified recombinant adeno-associated viral vector preparations that are free of helper virus and wild-type AAV. Gene Ther. 7, 183–195.

Pear, W.S., Nolan, G.P., Scott, M.L., Baltimore, D., 1993. Production of high-titer helper-free retroviruses by transient transfection. Proc. Natl. Acad. Sci. USA 90, 8392–8396.

Ponnazhagan, S., Mukherjee, P., Wang, X.S., Qing, K., Kube, D.M., Mah, C., Kurpad, C., Yoder, M.C., Srour, E.F., Srivastava, A., 1997. Adeno-associated virus type 2-mediated transduction in primary human bone donor variation and correlation of transgene expression with cellular differentiation. J. Virol. 71, 8262–8267.

Podsakoff, G., Wong, K.K. Jr., Chatterjee, S., 1994. Efficient gene transfer into nondividing cells by adeno-associated virus-based vectors. J. Virol. 68, 5656–5666.

Press, M.F., Pike, M.C., Chazin, V.R., Hung, G., Udove, J.A., Markowicz, M., Danyluk, J., Godolphin, W., Sliwkowski, M., Akita, R., et al., 1993. Her-2/neu expression in node-negative breast cancer: direct tissue quantitation by computerized image analysis and association of overexpression with increased risk of recurrent disease. Cancer Res. 53, 4960–4970.

Qing, K., Mah, C., Hansen, J., Zhou, S., Dwarki, V., Srivastava, A., 1999. Human fibroblast growth factor receptor 1 is a co-receptor for infection by adeno-associated virus 2. Nat. Med. 5, 71–77.

Qiu, J., Handa, A., Kirby, M., Brown, K.E., 2000. The interaction of heparin sulfate and adeno-associated virus 2. Virology 269, 137–147.

Rolling, F., Nong, Z., Pisvin, S., Collen, D., 1997. Adeno-associated virus-mediated gene transfer into rat carotid arteries. Gene Ther. 4, 757–761.

Samulski, R.J., Chang, L.S., Shenk, T., 1989. Helper-free stocks of recombinant adeno-associated viruses: normal integration does not require viral gene expression. J. Virol. 63, 3822–3828.

Schimmenti, S., Boesen, J., Claassen, E.A., Valerio, D., Einerhand, M.P., 1998. Long-term genetic modification of rhesus monkey hematopoietic cells following transplantation of adenoassociated vector-transduced CD34 + cells. Hum. Gene Ther. 9, 2727–2734.

Snyder, R.O., Miao, C.H., Patijn, G.A., Spratt, S.K., Danos, O., Nagy, D., Gown, A.M., Winther, B., Meuse, L., Cohen, L.K., Thompson, A.R., Kay, M.A., 1997. Persistent and therapeutic concentrations of human factor IX in mice after hepatic gene transfer of recombinant AAV vectors. Nat. Genet. 16, 270–276.

Summerford, C., Samulski, R.J., 1998. Membrane-associated heparan sulfate proteoglycan is a receptor for adeno-associated virus type 2 virions. J. Virol. 72, 1438–1445.

Summerford, C., Bartlett, J.S., Samulski, R.J., 1999. AlphaV-beta5 integrin: a co-receptor for adeno-associated virus type 2 infection. Nat. Med. 5, 78–82.

ELSEVIER

Journal of Virological Methods 106 (2002) 81–88

Journal of Virological Methods

www.elsevier.com/locate/jviromet

# Fast and reliable titration of recombinant adeno-associated virus type-2 using quantitative real-time PCR

Ulrich-Peter Rohr *, Marc-Andre Wulf, Susanne Stahn, Ulrich Steidl, Rainer Haas, Ralf Kronenwett

*Klinik für Hämatologie, Onkologie und klinische Immunologie, Heinrich-Heine-Universität Düsseldorf, Moorenstraße 5, D-40225 Düsseldorf, Germany*

Received 13 February 2002; received in revised form 19 June 2002; accepted 20 June 2002

**Abstract**

In this study, a quantitative real-time PCR (qPCR) was developed to determine genomic rAAV-2 titers using the Light-Cycler technology. Since the CMV promoter is the most commonly used promoter in gene therapeutic approaches, primers were designed which hybridize with the human CMV promoter sequence. PCR products were detected by the addition of SYBR green. qPCR of a 5 log spanning serial dilution of the vector plasmid containing one CMV promoter per plasmid molecule yielded a high amplification efficiency of 1.99 per cycle. To quantify the copy number of viral genomes, the qPCR curves of adeno-associated virus type 2 (AAV-2) samples were related to a standard curve assessed by the 5 log spanning serial vector plasmid dilution (0.01–100 pg DNA). For validation of the method, rAAV-2 preparations were analyzed by a standard method and qPCR in parallel. As standard method, flow cytometry was used for titration of infectious viral particles on HeLa cells using the Enhanced Green Fluorescent Protein as a marker. A significant correlation was found between the results obtained by flow cytometry and the results from the qPCR over a 5 log range ($r = 0.85$, $P < 0.0001$). The mean ratio between infectious rAAV-2 particles titrated via flow cytometry and genomic copies of rAAV-2 measured by qPCR of the same sample was 1:253. The higher titers found by qPCR might be due to multiple transduction of a single cell or to non-infectious particles generated during rAAV-2 preparation. In conclusion, qPCR is a fast and reliable method for determination of rAAV-2 titers and might be a powerful tool for standardization of rAAV-2 preparations particularly in the context of clinical studies. 

*Keywords:* rAAV-2; Titration; Real-time PCR

## 1. Introduction

The adeno-associated virus type 2 (AAV-2) is one of the most promising candidates for gene therapeutic applications (High, 2001). The non-pathogenic nature of the virus, infection of dividing and non-dividing cells, the potential for site-

* Corresponding author. Tel.: +49-211-8117720; fax: +49-211-8118853

*E-mail address:* urohr-uni-duesseldorf@gmx.de (U.-P. Rohr).

0166-0934/02/$ - see front matter 
PII: S0166-0934(02)00138-6

specific integration as well as the low immunogenicity are advantages in favor of AAV-2. To date, AAV-2 vectors have been evaluated in preclinical studies for Parkinson's disease (Shen et al., 2000) as well as in clinical studies for cystic fibrosis (Wagner et al., 1998) and haemophilia B (Kay et al., 2000). An essential precondition in planning and testing of rAAV-2 vectors in clinical studies is the quantitation of recombinant virus particles. An optimal titration assay must be fast, reliable and easy to perform. At present, most assays are based on the capability of the virus to transduce cultured cells. Following transduction, either the intracellular replication of the recombinant virus genomes or the expression of an easily detectable transgene is measured (Salvetti et al., 1998; Malik et al., 1997; Atkinson et al., 1998; Horster et al., 1999). Other assays are independent from the infectivity of the virus. They depend on lysis of the core unit and release of the single-stranded DNA. Serial dilutions of dot blotted DNA is compared to a plasmid probe and the number of particles is calculated (Flotte et al., 1992). In addition to the possibility that assays can be influenced by various parameters (Kube and Srivastava, 1997; Salvetti et al., 1998; Clark et al., 1996) all assays are time-consuming procedures. In this report, a new real-time PCR method is presented for a fast and reliable quantitation of recombinant AAV-2 particles. The method is independent from marker gene expression and might be a powerful tool for standardization of rAAV-2 preparations in the context of clinical studies.

## 2. Material and methods

### 2.1. Cells

The human embryonic kidney cell line 293T (Pear et al., 1993) was cultured in Dulbecco's modified Eagle's medium (DMEM Sigma, Deissenhofen, Germany) supplemented with 10% heat-inactivated fetal calf serum, 2 mM glutamate, 100 IU/ml penicillin and 100 μg/ml streptomycin. Cells were cultured at 37 °C in 5% $CO_2$ and were passaged twice a week. For culturing of HeLa cells RPMI-1640 medium (Sigma, Deissenhofen, Germany) was used instead of DMEM medium containing the same additives listed above.

### 2.2. Production and purification of recombinant AAV-2 vector stocks

For preparation of rAAV-2 vector stocks, $1 \times 10^7$ 293T cells were co-transfected with 20 μg vector plasmid pAAV-gfp-AR6- and 20 μg helper plasmid pDG (Grimm et al., 1998) by calcium phosphate precipitation. The vector plasmid pAAV-gfp-AR6- (Horster et al., 1999) contained the gene for Enhanced Green Fluorescent Protein (EGFP) and the HIV-1-directed antisense sequence AR6 under the control of the immediate early HCMV promoter, a SV40 splice and a polyadenylation signal flanked by the inverted terminal repeats (ITRs) of the AAV-2 clone psub201 (Samulski et al., 1989). The helper plasmid pDG contains all packaging and helper functions of AAV-2 (rep, cap) and adenovirus (E2A, E4, VA) for rAAV-2 particle production. 293T cells were harvested 72 h after transfection and were subjected to three cycles of freezing and thawing to release virus. The cell lysate was sonicated 10 times with pulsed 50% duty cycles at 200 W using a Branson Sonifier cell disrupter B-15 (Branson, Schwäbisch Gmuend, Germany) and spun down at $5000 \times g$ for 30 min. rAAV-2 preparations were purified and concentrated using the Iodixanol method as described (Zolotukhin et al., 1999). Using a Quick-Seal tube (Beckmann, Munich, Germany), 5 ml of viral suspension was underlayed by the following solutions: 3 ml of 15% iodixanol and 1 M NaCl in PBS–MK buffer (1 × phosphate-buffered saline (PBS), 1 mM $MgCl_2$ and 2.5 mM KCl), 2 ml of 25% iodixanol in PBS–MK buffer containing Phenol Red (2.5 μl of a 0.5% stock solution per ml of the iodixanol solution), 2 ml of 40% iodixanol in PBS–MK buffer; and finally 2 ml of 60% iodixanol in PBS–MK buffer containing Phenol Red (0.01 μg/ml). Tubes were sealed and centrifuged in a Ti 75 rotor (Beckmann) at 60,000 rpm for 5 h at 18 °C. Twenty-four fractions of 500–600 μl were collected starting from the bottom of the tube. All 24 collected fractions were dialyzed twice against PBS

for 6 h and RPMI for 24 h at 4 °C. Fractions were analyzed for rAAV-2 particles using FACS analysis as stated below. Viral particles were concentrated in the 40% iodixanol/PBS buffer solution prior to dialyzation.

### 2.3. Titration of infectious viral particles using fluorescence-activated cell sorting

Flow cytometry for titration of infectious rAAV-2 particles was performed as previously described (Horster et al., 1999). Virus suspension was one to 500-fold serially diluted. $1 \times 10^5$ HeLa cells were seeded in 500 μl medium in 24-well plates and 5 μl of each viral dilution was added to the cells. Cells were incubated at 37 °C for 48 h and harvested after removing the medium. Fifty microliters 0.02% trypsin/EDTA (Bio-Whittacker, Verviers, Belgium) was used for washing and detachment. Trypsin was inactivated by adding 500 μl of 10% FCS/PBS. Following two washing steps with 1 ml PBS, cells were resuspended in 500 μl PBS. After determination of the total cell numbers, FACS analysis was performed using a Becton Dickinson FACSCalibur (Heidelberg, Germany) with a 2 W argon ion laser and EGFP fluorescence was measured using a 530/15 nm (FITC) band pass filter. The percentage of green fluorescent cells was determined by FACS and was multiplied by the total cell numbers. Assuming that each EGFP-positive HeLa cell was infected by one rAAV-2 particle, viral titers were deduced from the percentage of transduced cells and diluted suspension.

### 2.4. CMV promoter-specific quantitative real-time PCR (qPCR)

PCR was performed using the LightCycler-FastStart DNA Master SYBR Green system (Roche Molecular Biochemicals, Mannheim, Germany). PCR was carried out in a final volume of 20 μl using 0.8 μl of each primer (0.4 μM), 3.2 μl MgCl (25 mM), 2 μl of the supplied enzyme mix, 11.2 μl $H_2O$ and finally 2 μl of the template. The enzyme mix contained the reaction buffer, FastStart *Taq* DNA polymerase and DNA double strand-specific SYBR Green I dye for detection of PCR products. PCR was performed in a LightCycler (Roche) with a 10 min pre-incubation at 95 °C followed by 50 cycles of 15 s at 95 °C (denaturation), 5 s at 67 °C (annealing) and 10 s at 72 °C (amplification). PCR products were subjected to melting curve analysis using the light cycler system to exclude the amplification of unspecific products. Finally, the PCR products were analyzed by conventional agarose gel electrophoresis. Primers were synthesized by Thermo Hybaid GmbH, Interactiva Division Ulm, Germany. The following primers were used:

CMV forward: 5′GGC-GGA-GTT-GTT-ACG-ACA-T-3′CMV reverse: 5′GGG-ACT-TTC-CCT-ACT-TGG-CA-3′.

A fragment length of 201 base pairs of the qPCR product is expected using the primers.

### 2.5. Quantitative analysis of the rAAV-2 preparations

In each qPCR run a standard curve was generated using a 5 log spanning serial dilution of the vector plasmid pAAV-gfp-AR6- containing one CMV promoter per plasmid molecule. Serial dilution ranged from 0.01 to 100 pg of the vector plasmid. Each dilution step was measured in triplicate per Light Cycler run. The standard curve was calculated by the Light Cycler 5.32 software (LC-Run Version 5.32, Roche) by regression of the crossing points of the PCR curves from the dilution series of the vector plasmid. The amplification efficiency (AE) of each PCR cycle was calculated from the slope $s$ of the standard curve using the following formula:

$$AE = 10^{1/(-s)}.$$

Recombinant AAV-2 containing fractions were either directly applied to PCR reaction using 2 μl of the viral sample or were pre-treated with DNase. For DNase digestion, 5 μl of the viral sample were incubated with 1 μl of DNase I (7500 U/ml; Amersham Pharmacia Biotec., Hamburg,

Germany) in a final volume of 50 µl at 37 °C for 30 min. DNase I was inactivated by incubation at 65 °C for 10 min. Additional experiments were performed using Proteinase K treatment after DNase I incubation as described (Clark et al., 1999). For Proteinase K (Boeringer Mannheim, Germany) digestion, 10 µg of Proteinase K were added to the viral sample at 50 °C for 60 min. Proteinase K was inactivated at 95 °C for 20 min. Two microliters of the sample were then applied to PCR using the PCR conditions as described above. Specificity of the PCR products was analyzed by melting curve analysis. For quantitation of the template number in unknown rAAV-2 samples, the LC software referred the PCR result of the unknown sample to the standard curve derived from the plasmid dilution series. The single-stranded nature of the AAV-2 genome as well as the double-stranded plasmid standard curve values were taken into consideration. The value from each sample was multiplied by the dilution factor (1:10) and by 500 to obtain the titer per milliliter (2 µl × 500 = 1 ml). Assuming that one rAAV-2 particle contained one single DNA copy and that 1 pg DNA of the 6889 bp vector plasmid corresponded to $1.3 \times 10^5$ plasmid molecules the viral rAAV-2 titer was calculated. For reliability of the qPCR, the coefficient of variation (CV) was calculated by dividing the standard deviation by the mean particle titer.

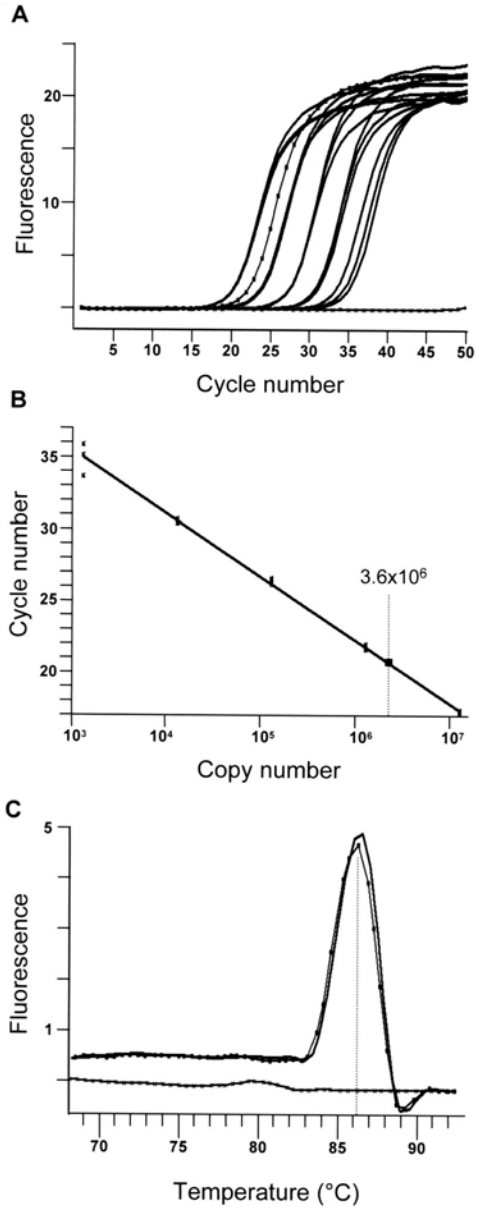


Fig. 1

## 3. Results

### 3.1. rAAV-2 standard curve

Using the Light Cycler real time PCR technology, a standard curve of the vector plasmid

Fig. 1. Quantitation of rAAV-2 samples by real-time PCR. (A) PCR curves of a representative Light Cycler run for titration of a rAAV-2 sample. PCR curves of the sample with unknown rAAV-2 titer (+), of serially diluted vector plasmid (−) and negative control (x) are presented. (B) Standard curve calculated from the PCR curves of the 5 log spanning dilution between 0.01 and 100 pg of vector plasmid DNA. Each dilution was assessed in triplicates. Standard curve was obtained by regression of the values from the diluted plasmid. The viral copy number in the rAAV-2 sample with unknown titer is indicated by the dotted line. (C) Melting curve analysis of qPCR products of viral sample (+), vector plasmid (−) and negative control (x). qPCR product of the viral sample and the vector plasmid had identical melting points at 86.2 °C.

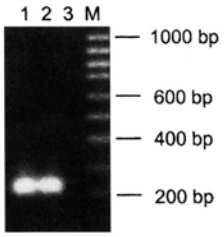


Fig. 2. Analysis of qPCR products using agarose gel electrophoresis. Lane M: 1 kb DNA ladder; lane 1: qPCR product from vector plasmid; lane 2: qPCR product from rAAV-2 sample; lane 3: negative control.

pAAV-gfp-AR6- was generated using a 5 log spanning serial dilution between 100 and 0.01 pg DNA (Fig. 1a and b). The mean regression coefficient of 12 performed regression curves was $0.993 \pm 0.01$. The mean slope of the 12 regression curves was $-3.34 \pm 0.3$ indicating an amplification efficiency of 1.99 per cycle.

qPCR analysis of further dilutions of the vector plasmid down to 0.1 fg, DNA vector plasmid copies could be detected indicating a high sensitivity of the assay. Melting curve analysis (Fig. 1c) and agarose gel electrophoresis (Fig. 2) were performed demonstrating specificity of the qPCR products.

### *3.2. Quantitation of rAAV-2 particles in a complete iodixanol gradient using FACS analysis and qPCR*

A complete gradient of a rAAV-2 preparation consisting of 24 fractions (AR-1, AR-2, ..., AR-24) was analyzed using qPCR and FACS in parallel. As assessed by FACS analysis, viral rAAV-2 particles were concentrated in fractions 2–7 with titers ranging from $2.1 \times 10^5$ to $2.5 \times 10^7$ viral particles per ml with a peak in fraction 5 (Fig. 3). In contrast to FACS analysis, two peak fractions were detected by qPCR when all fractions were analyzed without prior DNase treatment. One peak with $1.45 \times 10^9$ particles per ml was detected in fraction 5, the second peak with $8.1 \times 10^9$ copies per ml was found in fraction 13 (Fig. 3). Assuming that vector plasmids used during rAAV-2 production can contaminate fractions of the iodixanol gradient after purification and concentration, all fractions were treated with

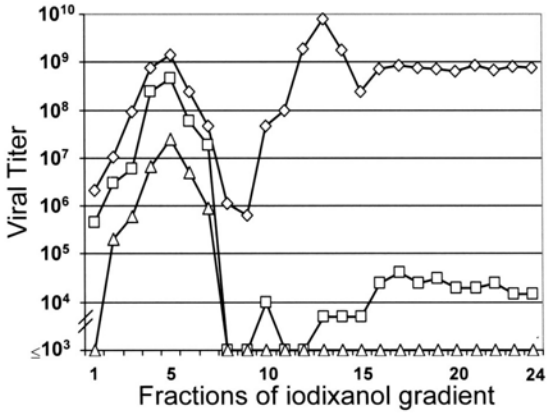


Fig. 3. Comparison of viral titers of a complete iodixanol gradient of purified rAAV-2 using FACS analysis (△), qPCR of samples without DNase pre-treatment (◇) or qPCR with DNase pre-treatment (□).

DNase and were analyzed by qPCR again. As a result, the second peak of the gradient was erased. The remaining peak of fraction 5 contained $4.5 \times 10^8$ rAAV-2 particles per ml. With respect to the peak fraction, titers of DNase treated and untreated fractions did not significantly differ indicating that qPCR reaction was not influenced by DNase pre-treatment. The influence of Proteinase K treatment was analyzed after DNase I treatment, which is an absolute requirement as a pre-analytical step of qPCR-based rAAV-2 titration. Using the rAAV-2 containing fractions AR-3–AR-7 as titrated by FACS, viral titers of Proteinase K treated and untreated fractions were assessed by qPCR. Interestingly, the viral titers of Proteinase K treated and untreated fractions were similar (Fig. 4). Since the differences in titer of Proteinase K treated and untreated fractions were not statistically different, further quantitative analysis of rAAV-2 samples were carried out without Proteinase K digestion.

### *3.3. Reliability of real-time PCR and FACS*

For reliability of the new method compared to the standard method, an intra-assay and inter-assay analysis was carried out for qPCR and FACS. The coefficient of variation (CV) was

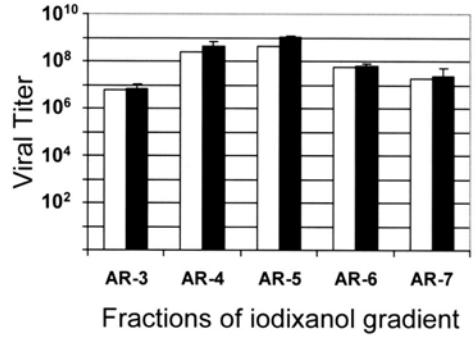


Fig. 4. Comparison of viral titers with or without Proteinase K treatment. White bars represent the viral titers obtained using DNase I treatment alone. Black bars represent the viral titers obtained using DNase I and additional Proteinase K digestion.

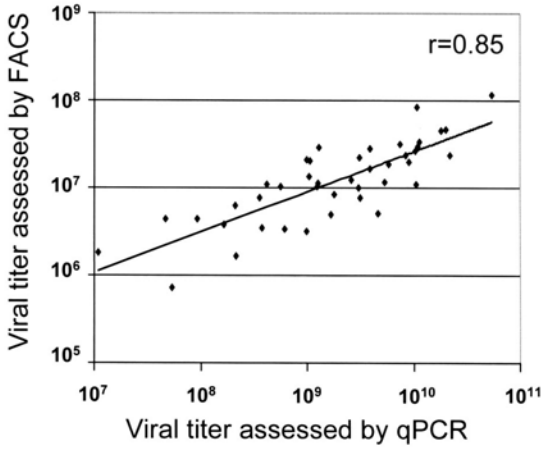


Fig. 5. Comparison of viral titers using qPCR and FACS analysis in 42 different rAAV-2 samples.

calculated as described in Section 2. Using qPCR and FACS, viral titer was calculated three times for each of five fractions in one experiment (intra-assay comparison). Quantitative analysis of the 15 samples using qPCR or FACS-based titration method resulted in a mean CV of 0.04 (range: 0.02–0.07) and 0.06 (range: 0.3–0.11), respectively. For qPCR and FACS inter-assay comparison, day-to-day variation (with new mixtures of the reagents) resulted in a mean CV of 0.48 (range 0.31–0.56) and 0.10 (range 0.08–0.13), respectively.

### *3.4. Comparison of viral titers assessed by FACS analysis and qPCR*

To compare the new titration method with an established one, 42 samples from 17 different viral preparations were analyzed by conventional FACS analysis and qPCR. As demonstrated in Fig. 5, a significant correlation over a 5 log spanning range of ε rAAV-2 titers was found comparing the two methods. The Pearson correlation coefficient of 0.85 was statistically significant ($P < 0.0001$). The titers assessed by qPCR were in mean 253-fold higher (SD ±241) than those from FACS analysis.

## 4. Discussion

Recombinant adeno-associated virus has been shown to be a powerful vector for delivery of therapeutic genes into human target cells referring to the results of first clinical trials (Kay et al., 2000). For large-scale use of a vector in clinical trials the development and availability of high throughput production, efficient concentration and purification of the vector as well as reliable titration methods of viral particles are essential prerequisites. While progress has been achieved in production and purification of recombinant AAV-2 particles there is still space for improvement of quantitation procedures. A variety of assays based on biological functionality of the virus or assays measuring DNA containing particles are commonly used. Examples for these assays are fluorescence cell assays based on FACS analysis (Malik et al., 1997) or fluorescence microscopy (Veldwijk et al., 1999), dot-blot hybridization assays (Flotte et al., 1992) or serial dilution replication assays (Salvetti et al., 1998; Drittanti et al., 2000). Although all methods are of proven value for the quantitation of viral titers, they can be influenced by parameters such as the helper virus used (Fisher et al., 1996), the choice of promoter and the cell type used for infection

(Salvetti et al., 1998; Clark et al., 1996) or the concentration of magnesium (Kube and Srivastava, 1997) leading to significant differences in resulting rAAV-2 titers (Clark et al., 1996; Ferrari et al., 1996; Fisher et al., 1996).

Other groups have used real-time PCR technology to quantify viral particles (Gao et al., 2000; Drittanti et al., 2000; Cao et al., 2000). The qPCR titration assays used so far as well as the conventional fluorescence cell assays are based on the detection of a marker gene or the therapeutic gene. For clinical application of rAAV-2, the reporter genes must be removed from the vector plasmid and can therefore not be used for titration. In this study, a standardized, unique real-time method independent from marker or therapeutic genes is presented. The primers were targeted against the commonly used and widely accepted CMV promoter resulting in a possibility to transfer this method to the majority of recombinant rAAV-2 constructs. Using this technique, which is fast, reliable and easy to perform, the time necessary for titration of an unknown viral suspension was shortened from 2 to 3 days to less than 3 h.

To compare qPCR with FACS titration method, titers of different rAAV-2 preparations were analyzed in parallel. The FACS based method was used as reference since this was a reliable standard method in our laboratory as well as in other groups (Malik et al., 1997; Horster et al., 1999). A significant correlation of 0.85 was found between both methods. Interestingly, the mean particle ratio assessed by FACS and qPCR was 1:256. The reason for the difference in viral titers comparing both methods might be that in qPCR viral genomes and not infectious particles were assessed. Using qPCR, all DNA containing particles are included for calculation of the viral titer but not all of the particles are infective resulting in a higher titer of rAAV-2 particles when compared to a method measuring infectious particles. This is supported by findings that viral preparations have particle-to-infectivity ratios between 56 and 1000 (Zolotukhin et al., 1999; Ruffing et al. 1992; Flotte et al., 1992). Another explanation for the difference of titers assessed by FACS and qPCR is the assumption that for the FACS-based assay at least one infectious rAAV-2 particle has entered the target cell. In case that more than one infectious viral particle entered the target cell, the true rAAV-2 titer might be underestimated by FACS analysis.

In conclusion, qPCR is presented as a powerful tool for rapid quantitation of viral rAAV-2 titers independently from the transgene and without the presence of a marker gene and might contribute to the use of rAAV-2 vectors in clinical trials. Next to simplification of titration and standardization of rAAV-2 preparations for clinical large-scale use it might be possible to extend this technique for a quantitative monitoring of rAAV-2 genomes present in human tissues which have been treated with rAAV-2 vectors.

## References

Atkinson, E.M., Debelak, D.J., Hart, L.A., Reynolds, T.C., 1998. A high-throughput hybridization method for titer determination of viruses and gene therapy vectors. Nucl. Acids Res. 26, 2821–2823.

Cao, L., Liu, Y., During, M.J., Xiao, W., 2000. High-titer, wild-type free recombinant adeno-associated virus vector production using intron-containing helper plasmids. J. Virol. 74, 11 456–11 463.

Clark, K.R., Liu, X., McGrath, J.P., Johnson, P.R., 1999. Highly purified recombinant adeno-associated virus vectors are biologically active and free of detectable helper and wild-type viruses. Hum. Gene Ther. 10, 1031–1039.

Clark, K.R., Voulgaropoulou, F., Johnson, P.R., 1996. A stable cell line carrying adenovirus-inducible rep and cap genes allows for infectivity titration of adeno-associated virus vectors. Gene Ther. 3, 1124–1132.

Drittanti, L., Rivet, C., Manceau, P., Danos, O., Vega, M., 2000. High throughput production, screening and analysis of adeno-associated viral vectors. Gene Ther. 7, 924–929.

Ferrari, F.K., Samulski, T., Shenk, T., Samulski, R.J., 1996. Second-strand synthesis is a rate-limiting step for efficient transduction by recombinant adeno-associated virus vectors. J. Virol. 70, 3227–3234.

Fisher, K.J., Gao, G.P., Weitzman, M.D., DeMatteo, R., Burda, J.F., Wilson, J.M., 1996. Transduction with recombinant adeno-associated virus for gene therapy is limited by leading-strand synthesis. J. Virol. 70, 520–532.

Flotte, T.R., Solow, R., Owens, R.A., Afione, S., Zeitlin, P.L., Carter, B.J., 1992. Gene expression from adeno-associated virus vectors in airway epithelial cells. Am. J. Respir. Cell Mol. Biol. 7, 349–356.

Gao, G., Qu, G., Burnham, M.S., Huang, J., Chirmule, N., Joshi, B., Yu, Q.C., Marsh, J.A., Conceicao, C.M., Wilson, J.M., 2000. Purification of recombinant adeno-associated

virus vectors by column chromatography and its performance in vivo. Hum. Gene Ther. 11, 2079–2091.

Grimm, D., Kern, A., Rittner, K., Kleinschmidt, J.A., 1998. Novel tools for production and purification of recombinant adenoassociated virus vectors. Hum. Gene Ther. 9, 2745–2760.

High, K.A., 2001. Gene therapy: a 2001 perspective. Haemophilia 7 (Suppl. 1), 23–27.

Horster, A., Teichmann, B., Hormes, R., Grimm, D., Kleinschmidt, J., Sczakiel, G., 1999. Recombinant AAV-2 harboring gfp-antisense/ribozyme fusion sequences monitor transduction, gene expression, and show anti-HIV-1 efficacy. Gene Ther. 6, 1231–1238.

Kay, M.A., Manno, C.S., Ragni, M.V., Larson, P.J., Couto, L.B., McClelland, A., Glader, B., Chew, A.J., Tai, S.J., Herzog, R.W., Arruda, V., Johnson, F., Scallan, C., Skarsgard, E., Flake, A.W., High, K.A., 2000. Evidence for gene transfer and expression of factor IX in haemophilia B patients treated with an AAV vector. Nat. Genet. 24, 257–261.

Kube, D.M., Srivastava, A., 1997. Quantitative DNA slot blot analysis: inhibition of DNA binding to membranes by magnesium ions. Nucl. Acids Res. 25, 3375–3376.

Malik, P., McQuiston, S.A., Yu, X.J., Pepper, K.A., Krall, W.J., Podsakoff, G.M., Kurtzman, G.J., Kohn, D.B., 1997. Recombinant adeno-associated virus mediates a high level of gene transfer but less efficient integration in the K562 human hematopoietic cell line. J. Virol. 71, 1776–1783.

Pear, W.S., Nolan, G.P., Scott, M.L., Baltimore, D., 1993. Production of high-titer helper-free retroviruses by transient transfection. Proc. Natl. Acad. Sci. USA 90, 8392–8396.

Ruffing, M., Zentgraf, H., Kleinschmidt, J.A., 1992. Assembly of viruslike particles by recombinant structural proteins of adeno-associated virus type 2 in insect cells. J. Virol. 66, 6922–6930.

Salvetti, A., Oreve, S., Chadeuf, G., Favre, D., Cherel, Y., Champion-Arnaud, P., David-Ameline, J., Moullier, P., 1998. Factors influencing recombinant adeno-associated virus production. Hum. Gene Ther. 9, 695–706.

Samulski, R.J., Chang, L.S., Shenk, T., 1989. Helper-free stocks of recombinant adeno-associated viruses: normal integration does not require viral gene expression. J. Virol. 63, 3822–3828.

Shen, Y., Muramatsu, S.I., Ikeguchi, K., Fujimoto, K.I., Fan, D.S., Ogawa, M., Mizukami, H., Urabe, M., Kume, A., Nagatsu, I., Urano, F., Suzuki, T., Ichinose, H., Nagatsu, T., Monahan, J., Nakano, I., Ozawa, K., 2000. Triple transduction with adeno-associated virus vectors expressing tyrosine hydroxylase, aromatic-L-amino-acid decarboxylase, and GTP cyclohydrolase I for gene therapy of Parkinson's disease. Hum. Gene Ther. 11, 1509–1519.

Veldwijk, M.R., Schiedlmeier, B., Kleinschmidt, J.A., Zeller, W.J., Fruehauf, S., 1999. Superior gene transfer into solid tumour cells than into human mobilised peripheral blood progenitor cells using helpervirus-free adeno-associated viral vector stocks. Eur. J. Cancer 35, 1136–1142.

Wagner, J.A., Reynolds, T., Moran, M.L., Moss, R.B., Wine, J.J., Flotte, T.R., Gardner, P., 1998. Efficient and persistent gene transfer of AAV-CFTR in maxillary sinus. Lancet 351, 1702–1703.

Zolotukhin, S., Byrne, B.J., Mason, E., Zolotukhin, I., Potter, M., Chesnut, K., Summerford, C., Samulski, R.J., Muzyczka, N., 1999. Recombinant adeno-associated virus purification using novel methods improves infectious titer and yield. Gene Ther. 6, 973–985.

Available online at www.sciencedirect.com
SCIENCE DIRECT
ELSEVIER
Journal of Virological Methods 127 (2005) 40–45
Journal of Virological Methods
www.elsevier.com/locate/jviromet

# Quantitative real-time PCR for titration of infectious recombinant AAV-2 particles

Ulrich-Peter Rohr[a,*,1], Florian Heyd[a,1], Judith Neukirchen[a,1], Marc-Andre Wulf[a], Iris Queitsch[b], Gabriele Kroener-Lux[b], Ulrich Steidl[a], Roland Fenk[a], Rainer Haas[a], Ralf Kronenwett[a]

[a] *Klinik für Haematologie, Onkologie und klinische Immunologie, Heinrich-Heine-Universitaet Duesseldorf, Moorenstraße 5, D-40225 Duesseldorf, Germany*
[b] *Progen Biotechnik GmbH, Maaßstraße 30, 69123 Heidelberg, Germany*

Received 30 December 2004; received in revised form 3 March 2005; accepted 8 March 2005
Available online 12 April 2005

**Abstract**

In this report, we present a fast, reliable and easy to perform method to quantify infectious titers of recombinant AAV-2 (rAAV-2) particles using the LightCycler technology, which is independent from the therapeutic transgene and without the presence of a marker gene. The method is based on the life cycle of AAV-2: after infection of the host cell, the single stranded (ss) AAV-2 genome is converted into a double stranded (ds) form. Following infection with rAAV-2, HeLa cells were lysed and ssDNA of transcriptionally inactive particles were efficiently removed by ssDNA-specific S1 nuclease digestion. The remaining viral dsDNA can be quantified by quantitative real-time PCR (qPCR). For validation of the new method, rAAV-2 preparations were analyzed by two other standard methods for titration of infectious particles in parallel, i.e. the infectious center assay (ICA) as well as flow cytometry using GFP as a marker. Comparing the infectious titers of 40 different AAV-2 fractions assessed by qPCR with the titers determined by FACS analysis a significant correlation ($r=0.87$, $p<0.001$) with a mean ratio of the titers assessed by qPCR and FACS of 1.92 (S.D. $\pm$ 1.59) was found. Further, the titers of seven rAAV-2 fractions using qPCR and ICA covering 5 log ranges were compared and a significant correlation was found between the results ($r=0.80$, $p<0.001$) with a mean ratio of 3.38 (S.D. $\pm$ 1.79), respectively.


*Keywords:* rAAV-2; Infectious assay; qPCR

## 1. Introduction

Clinical trials using rAAV-2 as gene delivery system for the treatment of cystic fibrosis (Wagner et al., 1998) and haemophilia B (Kay et al., 2000) have shown the potential of this vector system in human gene therapy (Moss et al., 2004). Several methods for titration of genomic rAAV-2 particles have been described, such as dot-blot analysis, capsid ELISA for the titration of assembled particles or qPCR (Flotte et al., 1992; Grimm et al., 1999; Rohr et al., 2002a; Veldvijk et al., 2002). However, measuring only the genomic titer of vector preparations is perfidious since the infectious titer can greatly vary showing particle-to-infectivity ratios between 56 and 1000 (Flotte et al., 1992; Ruffing et al., 1992; Zolotukhin et al., 1999). This fact limits the use of genomic particle calculations for clinical trials. Quantification of infectious viral particles containing recombinant genes is based on the serial dilution replication assays involving superinfection with Adenovirus or wild-type AAV-2 or using stable-transfected helper cell lines followed by dot-blot or PCR analysis (Salvetti et al., 1998; Cao et al., 2000; Drittanti et al., 2000). Although all the methods are of proven value for the quantification of infectious rAAV-2 titers, they are time-

* Corresponding author. Tel.: +49 211 8117760; fax: +49 211 8118853.
*E-mail addresses:* urohr-uni-duesseldorf@gmx.de (U.-P. Rohr), judith.neukirchen@uni-duesseldorf.de (J. Neukirchen).
[1] These authors contributed equally to this work.

0166-0934/$ – see front matter © 2005 Elsevier B.V. All rights reserved.
doi:10.1016/j.jviromet.2005.03.006

consuming procedures and can be influenced by different factors such as the helper virus or the cell type used for infection leading to differences in rAAV-2 titers. Fluorescence-based assays have also been used to determine the infectious particles (Hörster et al., 1999; Veldvijk et al., 2002), but this approach is limited to those AAV-2 preparations carrying the coding sequence for a fluorescent marker protein.

The presented assay for quantification of viral particles is based on the life cycle of AAV-2 following the infection of a host cell. After binding of AAV-2 particles to their receptor, heparan sulfate proteoglycan and a co-receptor, e.g. αVβ5 integrin (Summerford and Samulski, 1998; Summerford et al., 1999), endocytosis of AAV-2 particles and endosomal processing leads to nuclear translocation of the virions (Sanlioglu et al., 2000; Seisenberger et al., 2001). In the nucleus, viral ssDNA is converted by de-novo synthesis of the second strand (Ferrari et al., 1996; Fisher et al., 1996) into dsDNA (Nakai et al., 2000), which is transcriptionally active. Non-infectious viral particles either do not enter the cell or they are not further processed after endocytosis. The viral DNA is preserved in its single stranded form, which can be efficiently removed by digestion with ssDNA-specific S1 nuclease. The remaining viral dsDNA can be considered as the DNA of transcriptionally active viral particles that can be quantified by qPCR. In this report, a S1 nuclease digestion followed by qPCR was used to quantify 47 different AAV-2-GFP preparations. The results from the new method were compared with the results from two standard methods using FACS analysis or infectious center assay.

## 2. Materials and methods

### 2.1. Cell culture

293T cells and HeLa RC32 were cultured in Dulbecco's modified Eagle's medium (DMEM, Sigma, Deissenhofen, Germany) supplemented with 10% heat inactivated fetal calf serum (PAA Laboratories, Linz, Austria), 2 mM L-glutamine, 100 U/ml penicillin and 0.1 mg/ml streptomycin (all Sigma) in a humidified atmosphere with 5% $CO_2$ at 37 °C. HeLa cells were cultured under the same conditions using RPMI-1640 medium (Sigma) instead of DMEM.

### 2.2. Production of recombinant AAV-2 vector stocks

Recombinant AAV-2 vector stocks containing the egfp-gene (*AAV-2-gfp*) were produced as previously described (Rohr et al., 2002b). Briefly, 293T cells were cotransfected with 20 μg vector plasmid (pAAV-gfp-AR6-) and 20 μg helper plasmid (pDG) using calcium phosphate precipitation. Three days later, 293T cells were harvested and lysed by three freeze–thaw cycles following the sonication. The lysate was centrifuged and the supernatant was subjected to an Iodixanol gradient to purify viral particles (Zolotukhin et al., 1999). After centrifugation, fractions of 500 μl were collected and dialysed against RPMI-1640 for 24 h at 4 °C. AAV-2-gfp fractions were quantified using FACS analysis for infectious titration (Hörster et al., 1999; Rohr et al., 2002a) and qPCR for genomic titration (Rohr et al., 2002a), as described previously.

### 2.3. Titration of genomic and infectious particles using qPCR

Genomic rAAV-2 particles were titrated as described previously by Rohr et al. (2002a). For titration of the infectious particles, $5 \times 10^4$ HeLa cells per well were seeded in 24-well plates and infected with 20 μl viral suspension 1 h later. For all experiments, uninfected HeLa cells served as negative control. After 24 h, cells were trypsinised, cell pellets were washed once with PBS and resuspended in 50 μl PBS without $Ca^{2+}$ and $Mg^{2+}$ (Biochrom, Berlin, Germany). Ten micrograms of proteinase K (Sigma) was added, and the mixture was incubated at 50 °C for 1 h vortexing occasionally. The enzyme was inactivated by heating the samples to 97 °C for 15 min, the lysate was centrifuged for 10 min at 13,000 × *g* and the supernatant was transferred into a fresh tube. Ten microlitres of the whole cell lysate were supplemented with S1 nuclease reaction buffer and 10 U S1 nuclease (Promega, Madison, WI, USA), and incubated for 30 min at 37 °C. Following an inactivation step (97 °C, 15 min), the mixture was diluted 1:100 in order to prevent inhibition of the PCR by S1 nuclease reaction buffer. All qPCRs were carried out in a LightCycler using the LightCycler-FastStart DNA Master SYBR Green I kit and the LightCycler 5.32 software (Roche Molecular Biochemicals, Mannheim, Germany). CMV promoter-specific qPCR was performed, as described recently (Rohr et al., 2002a). Final concentrations in the PCR mixture were 0.4 μM of each primer, 5 mM $MgCl_2$ and 2 μl template in a final volume of 20 μl. The PCR protocol used was: 10 min 95 °C followed by 50 cycles of 15 s 95 °C, 5 s 67 °C, 10 s 72 °C and melting curve analysis. The following primers yielding no 100% match in the human genome were used (Thermo Hybaid GmbH, Interactiva Division Ulm, Germany): forward: 5′-GGC-GGA-GTT-GTT-ACG-ACA-T-3′ and reverse: 5′-GGG-ACT-TTC-CTA-CTT-GGC-A-3′. In order to determine the copy number of CMV promoter-containing viral DNA in whole cell lysates of AAV-2-gfp-infected HeLa cells, a standard curve was generated using the plasmid pAAV-gfp-AR6- (Rohr et al., 2002a), ranging from $1.3 \times 10^1$ to $1.3 \times 10^7$ copies. The amplification efficiency (AE) of each PCR cycle was calculated from the slope *s* of the standard curve using the following formula: $AE = 10^{1/(-s)}$. PCR products were analyzed by agarose gel electrophoresis (1.5%), the expected product length was 200 bp. The following calculation yielded infectious particles per ml:

$$\text{Infectious particles per ml} = \frac{(\text{copy number in qPCR}) \times a \times b \times c}{d}$$

*a*, dilution of whole cell lysate = 100; *b*, final volume of whole cell lysate = 55 μl; *c*, factor to yield infectious particle per ml = 50/ml because 20 μl viral suspension were used to infect HeLa cells; *d*, template volume in qPCR = 2 μl.

### 2.4. Titration of infectious particles using ICA

Infectious rAAV-2 particles were titrated as described by Salvetti et al. (1998). Briefly, HeLa RC32 cells (Chadeuf et al., 2000) and HeLa control cells were seeded in 48-well plates at a density of $6 \times 10^4$ cells/well in DMEM/10% FCS. The following day, HeLa RC32 cells were infected with different serial dilutions of rAAV with Adenovirus (MOI of 500) in DMEM/5% FCS. As control, HeLa RC32 cells were infected with Adenovirus only to control for AAV contamination in the adenoviral preparation or rAAV only to control for Adenovirus contamination in the rAAV preparation. In addition, HeLa cells were infected with rAAV plus Adenovirus in different dilutions to control for wild-type AAV contamination. The next day cells were trypsinised, washed with 0.9% NaCl and filtered on a Zeta blotting membrane (Bio-Rad Laboratories). The filters were collected and incubated for 5 min at RT on Whatman paper wetted with denaturation buffer (0.5 M NaOH, 1.5 M NaCl), and then for 5 min at RT on Whatman paper wetted with neutralization buffer (1 M Tris–HCl, 2× SSC, pH 7.5). Filters were dried and hybridized with a Fluorescein labelled DNA probe over night at 65 °C (Gene Images Random Prime Labelling Module, Amersham). After wash of the filters (first wash 1× SSC/0.1% SDS, 65 °C; second wash 0.5× SSC/0.1% SDS, 65 °C) the signal was detected using the Gene Images CDP-Star Detection Module (Amersham) and Hyperfilm ECL (Amersham).

## 3. Results

### 3.1. S1 nuclease digestion

To remove the ssDNA of non-infectious viral particles, the lysates were digested with ssDNA-specific S1 nuclease. The digestion time and the amount of S1 nuclease units were varied to optimise the reaction conditions. A whole cell lysate of AAV-2-gfp-infected HeLa cells was treated with 1 U S1 nuclease for 10 or 60 min, or 10 U S1 nuclease for 30 min, and the remaining CMV promoter-containing DNA was quantified by qPCR ($n = 2$). The copy number was reduced by the factors 19.8 (S.D. ± 1.2), 18.0 (S.D. ± 0.1) and 18.2 (S.D. ± 1.2), respectively, compared to the sample without nuclease treatment. This result indicates a similar degradation of viral ssDNA in all the three conditions.

For all further experiments, the whole cell lysates were treated with 10 U S1 nuclease for 30 min (Fig. 1A). In order to assess the optimal time point for the assay following infec-

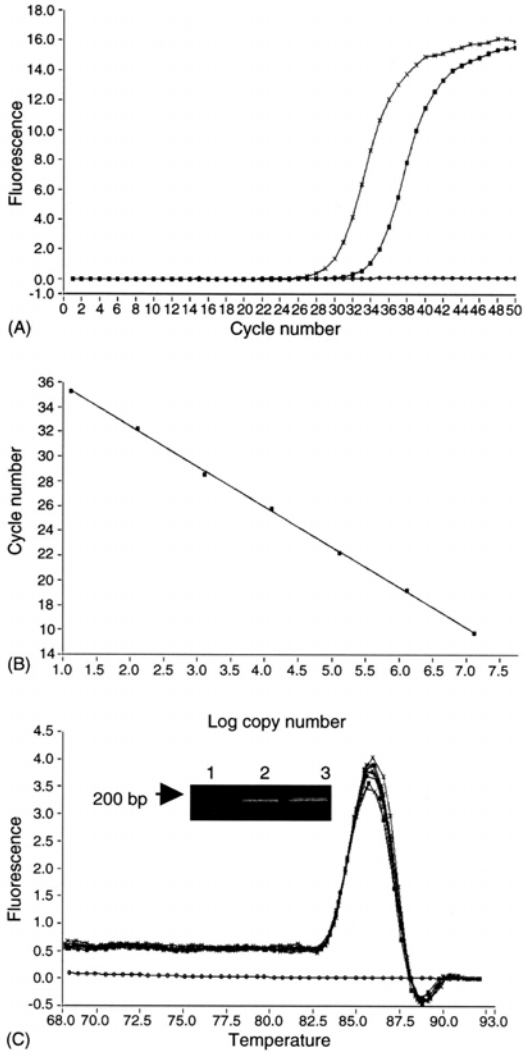


Fig. 1. Quantification of infectious AAV-2-gfp particles using qPCR. (A) The qPCR curves show quantifications of whole cell lysate of uninfected HeLa cells (open circles), whole cell lysate of AAV-2-gfp-infected cells without S1 nuclease treatment (crosses) and the same lysate with S1 nuclease treatment (filled squares). (B) A representative standard curve for the quantification of viral samples. Seven 10-fold-dilution steps ranging from $1.3 \times 10^1$ to $1.3 \times 10^7$ copies of the plasmid pAAV-gfp-AR6- were used to generate the standard curve. (C) Melting curve analysis of the samples shown in A and B. The products obtained from the vector plasmid (crosses) and from the viral sample (filled squares) had identical melting points of 86.2 °C (open circles: negative control). Agarose gel electrophoresis (1.5%) of the PCR products shows that the vector plasmid (lane 2) and a whole cell lysate of infected cells (lane 3) yielded products with the same length. The lysate of uninfected cells yielded no PCR product (lane 1). The expected product length was 200 bp.

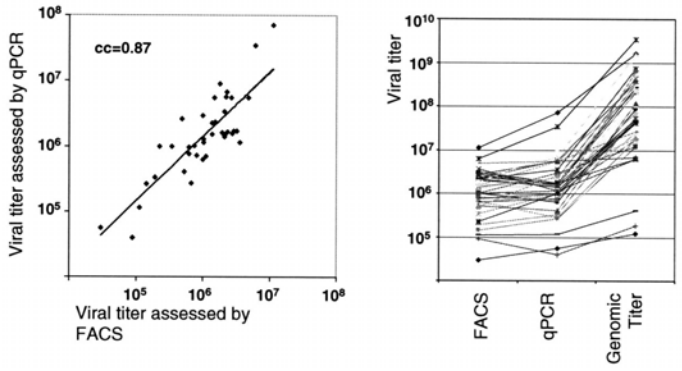


Fig. 2. Comparison of infectious titers. (A) The infectious titers of 40 AAV-2-gfp fractions were assessed by FACS analysis and qPCR. (B) In addition, the genomic titers were shown in comparison to the titration results of 40 AAV-2-gfp fractions with FACS analysis and qPCR.

tion, cells were treated with the same AAV-2-GFP preparations for 24 or 48 h. Comparing the infectious titers obtained from both time points, the values differed only marginally by the factor 1.32 (S.D. $\pm$ 0.72, $n = 6$). As a result, a 24-h period between the infection and harvesting of cells was chosen for further experiments.

### 3.2. Sensitivity, efficiency and specificity of the qPCR

For the quantification of viral DNA, a standard curve was generated using the vector plasmid pAAV-gfp-AR6- (Rohr et al.,2002a). Seven 10-fold serial dilutions were used ranging from $1.3 \times 10^1$ to $1.3 \times 10^7$ copies (Fig. 1B). Lowest copy number of 13 copies could reproducibly be detected in all the reactions ($n = 9$). The mean regression coefficient was 1, the mean slope was $-3.32 \pm 0.09$, indicating an amplification efficiency of 2 per cycle ($n = 9$). Melting curve analysis and agarose gel electrophoresis demonstrated the specificity of PCR (Fig. 1C). No PCR product was obtained using the lysate from uninfected HeLa cells.

### 3.3. Reproducibility of the assay

In order to determine the reliability of the new method, the inter-experimental differences of the qPCR, the inter-experimental differences of the S1 nuclease digestion followed by qPCR and the inter-experimental differences of the whole experimental procedure (including infection of HeLa cells, S1 nuclease digestion and qPCR) was assessed. To obtain the inter-experimental differences of only the qPCR, the viral DNA in AAV-2-gfp-infected HeLa cells (after nuclease digestion) was quantified. The copy numbers of 19 samples obtained in two independent qPCRs differed in mean by the factor 1.22 (S.D. $\pm$ 0.15). To assess the reproducibility of the S1 nuclease digestion and qPCR, AAV-2-gfp-infected HeLa cells of nine samples were digested with S1 nuclease and quantified by qPCR in two independent experiments. A variability of the factor 1.19 (S.D. $\pm$ 0.17) was obtained. In order to determine the inter-experimental difference of the whole experimental procedure, including the infection of HeLa cells, S1 nuclease digestion and quantification of viral DNA by qPCR was repeated twice and the results were compared. The values differed on average by the factor 2.10 (S.D. $\pm$ 1.22) ($n = 8$).

### 3.4. Comparison of viral titers assessed by qPCR and FACS analysis

To compare the new infectious titration method with an established one, the infectious titers of 40 different AAV-2-gfp samples were assessed using qPCR and FACS analysis in parallel. A statistically significant ($p < 0.0001$) correlation over a 5 log spanning range was seen between the results obtained by FACS and qPCR with a Pearson correlation coefficient of $r = 0.87$ (Fig. 2A). The quotient of infectious particles assessed by qPCR and infectious particles assessed by FACS was 1.92 (S.D. $\pm$ 1.59), respectively. The mean particle-to-infectivity ratio of qPCR and FACS was 163 (range: 2–818) and 108 (range: 1.2–913) (Fig. 2B).

### 3.5. Comparison of viral titers assessed by qPCR and the infectious center assay

Next to FACS analysis, the ICA is also commonly used for titration of infectious rAAV-2 particles. Therefore, the ICA as a second method for titration of infectious particles of seven different rAAV-2 samples was performed in parallel, and the results were compared with those from qPCR and the corresponding genomic particle titer (Fig. 3A). Comparing the infectious titer results of ICA and qPCR, a significant correlation of 0.8 ($p < 0.001$) was found over a 5 log range (Fig. 3B). The mean ratio between infectious particles assessed by qPCR and ICA was 3.38 (S.D. $\pm$ 1.79), and the mean particle-to-infectivity ra-

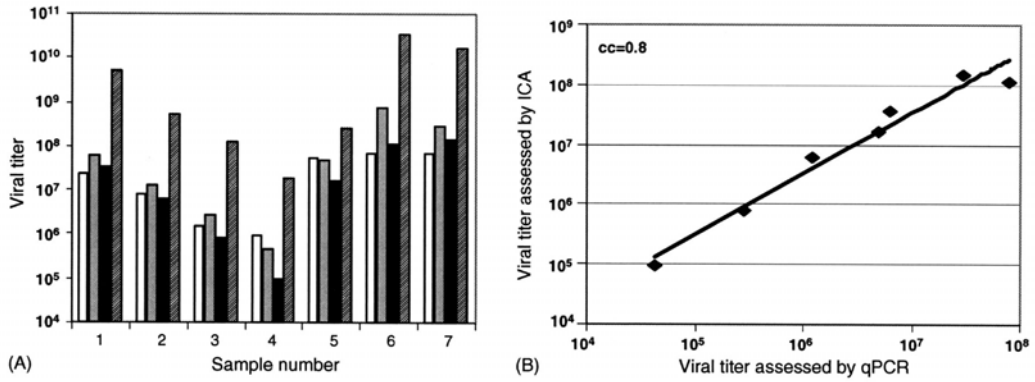


Fig. 3. Comparison of infectious titers using ICA and qPCR. (A) Infectious titers of seven AAV-2-gfp fractions were assessed by FACS-analysis (white bars), qPCR (grey bars) and ICA analysis (black bars) in parallel. Genomic titers are represented by lined bars for all 7 fractions. (B) Correlation of the results of seven infectious titers using ICA analysis and qPCR.

tio of qPCR and ICA was 46 (range: 5.5–82.5) and 145 (range: 16–301).

## 4. Discussion

Following the production and purification of a rAAV-2 vector stock, the genomic titer of a viral preparation includes infectious, biologically active particles as well as uninfectious DNA-containing particles showing great variations in particle-to-infectivity ratios between 56 and 1000 (Flotte et al., 1992; Ruffing et al., 1992; Zolotukhin et al., 1999). Consequently, only the minority of endocytosed viral particles is infectious while the majority of the particles represent intracellular virions, which are not further processed in one of the following steps: endosomal processing, nuclear transport, uncoating and gene conversion. Viral trafficking to the nucleus and nuclear processing are the major obstacles for AAV-2 infection rather than endocytosis of the viral particles (Duan et al., 2000). Such viral particles have been shown to enter the cell but to stay in a single stranded, transcriptionally inactive state.

In this study, a novel method was established for the titration of infectious, transcriptionally active rAAV-2 particles, which circumvents serial dilution, the use of radioactivity and superinfection with Adenovirus or wild-type AAV-2. The qPCR-based method is shorter to perform than the methods currently in use, and more than 20 unknown virus-containing suspensions can be quantified within 5 h after a 24 h incubation period. This incubation period was chosen since we demonstrated only a marginal difference between the infectious titers obtained from different time points. Our results are in line with others showing that 93% of all the AAV-2 particles are nucleus-associated after 3 h incubation with HeLa cells (Sanlioglu et al., 2000), and the conversion of viral ssDNA into dsDNA is accomplished 24 h after infection (Vincent-Lacaze et al., 1999), with a maximal presence of transcriptionally active dsAAV-2 circular intermediates 24 h post infection (Duan et al., 1999; Vincent-Lacaze et al., 1999). In order to test the reliability of the assay, the inter-experimental difference of the method including infection of the HeLa cells, ssDNAse digestion and qPCR was determined, and the results of viral preparation on day-to-day variation differed, on average, by the factor 2.1 (S.D. $\pm$ 1.22). Comparing the standard deviation of the presented assay with the standard deviation of infectious dot-blot endpoint dilution analysis sample, which might differ up to the factor 100 (Atkinson et al., 1998).

To compare the infectious titers of 40 rAAV-2 samples, assessed with qPCR method with FACS titration analysis, a significant correlation of the results between the methods was seen with a correlation coefficient 0.87. The FACS based titration method was used as a reference since it was a reliable standard method for us and others (Hörster et al., 1999; Rohr et al., 2002b). Next to FACS analysis, the ICA was chosen as a second sensitive method for the titration of infectious rAAV-2 particles. Again, a significant correlation could be demonstrated between the results of the assays showing a correlation coefficient of 0.8 with a mean difference of the obtained values of 3.38. The reason for the difference between the qPCR and the ICA results might be explained by the post-infectious conversion of viral ssDNA into transcriptionally active dsDNA. Nakai et al. (2000) presented evidence that after AAV-2 infection the viral ssDNA is converted by the recruitment of an infectious plus and minus ssDNA to form the dsDNA independently of de-novo DNA synthesis. This might explain a factor 2 difference between the qPCR and ICA results since the qPCR detects both the plus and minus ssDNA from two infectious viral particles. In conclusion, qPCR is a fast and easy to perform tool for the determination of infectious rAAV-2 titers, independent from marker gene expression and applicable to any therapeutic gene such as *p53* (Rohr et al., 2003), which is an essential prerequisite for gene therapeutic clinical trials.

## Acknowledgements

This work was supported by the Leukämie Liga e. V. Duesseldorf and Lions Club, Neuss.

## References

Atkinson, E.M., Debelak, D.J., Hart, L.A., Reynolds, T.C., 1998. A high-throughput hybridization method for titer determination of viruses and gene therapy vectors. Nucl. Acids Res. 26, 2821–2823.

Cao, L., Liu, Y., During, M.J., Xiao, W., 2000. High-titer, wild-type free recombinant adeno-associated virus vector production using intron-containing helper plasmids. J. Virol. 74, 11456–11463.

Chadeuf, G., Favre, D., Tessier, J., Provost, N., Nony, P., Kleinschmidt, J., Moullier, P., Salvetti, A., 2000. Efficient recombinant adeno-associated virus production by a stable rep-cap HeLa cell line correlates with adenovirus-induced amplification of the integrated rep-cap genome. J. Gene Med. 2, 260–268.

Drittanti, L., Rivet, C., Manceau, P., Danos, O., Vega, M., 2000. High throughput production, screening and analysis of adeno-associated viral vectors. Gene Ther. 7, 924–929.

Duan, D., Sharma, P., Dudus, L., Zhang, Y., Sanlioglu, S., Yan, Z., Yue, Y., Ye, Y., Lester, R., Yang, J., Fisher, K.J., Engelhardt, J.F., 1999. Formation of adeno-associated virus circular genomes is differentially regulated by adenovirus E4 ORF6 and *E2a* gene expression. J. Virol. 73, 161–166.

Duan, D., Yue, Y., Yan, Z., Yang, J., Engelhardt, J.F., 2000. Endosomal processing limits gene transfer to polarized airway epithelia by adeno-associated virus. J. Clin. Invest. 105, 1573–1587.

Ferrari, F.K., Samulski, T., Shenk, T., Samulski, R.J., 1996. Second-strand synthesis is a rate-limiting step for efficient transduction by recombinant adeno-associated virus vectors. J. Virol. 70, 3227–3234.

Fisher, K.J., Gao, G.P., Weitzman, M.D., DeMatteo, R., Burda, J.F., Wilson, J.M., 1996. Transduction with recombinant adeno-associated virus for gene therapy is limited by leading-strand synthesis. J. Virol. 70, 520–532.

Flotte, T.R., Solow, R., Owens, R.A., Afione, S., Zeitlin, P.L., Carter, B.J., 1992. Gene expression from adeno-associated virus vectors in airway epithelial cells. Am. J. Respir. Cell. Mol. Biol. 7, 349–356.

Grimm, D., Kern, A., Pawlita, M., Ferrari, F.K., Samulski, R.J., Kleinschmidt, J.A., 1999. Titration of AAV-2 particles via a novel capsid ELISA: packaging of genomes can limit production of recombinant AAV-2. Gene Ther. 6, 1322–1330.

Hörster, A., Teichmann, B., Hormes, R., Grimm, D., Kleinschmidt, J., Sczakiel, G., 1999. Recombinant AAV-2 harboring gfp-antisense/ribozyme fusion sequences monitor transduction, gene expression, and show anti-HIV-1 efficacy. Gene Ther. 6, 1231–1238.

Kay, M.A., Manno, C.S., Ragni, M.V., Larson, P.J., Couto, L.B., McClelland, A., Glader, B., Chew, A.J., Tai, S.J., Herzog, R.W., Arruda, V., Johnson, F., Scallan, C., Skarsgard, E., Flake, A.W., High, K.A., 2000. Evidence for gene transfer and expression of factor IX in haemophilia B patients treated with an AAV vector. Nat. Genet. 24, 257–261.

Moss, R.B., Rodman, D., Spencer, L.T., Aitken, M.L., Zeitlin, P.L., Waltz, D., Milla, C., Brody, A.S., Clancy, J.P., Ramsey, B., Hamblett, N., Heald, A.E., 2004. Repeated adeno-associated virus serotype 2 aerosol-mediated cystic fibrosis transmembrane regulator gene transfer to the lungs of patients with cystic fibrosis: a multicenter, double-blind, placebo-controlled trial. Chest 125, 509–521.

Nakai, H., Storm, T.A., Kay, M.A., 2000. Recruitment of single-stranded recombinant adeno-associated virus vector genomes and intermolecular recombination are responsible for stable transduction of liver in vivo. J. Virol. 74, 9451–9463.

Rohr, U., Wulf, M., Stahn, S., Steidl, U., Haas, R., Kronenwett, R., 2002a. Fast and reliable titration of recombinant adeno-associated virus type-2 using quantitative real-time PCR. J. Virol. Methods 106, 81–89.

Rohr, U., Kronenwett, R., Grimm, D., Kleinschmidt, J., Haas, R., 2002b. Primary human cells differ in their susceptibility to rAAV-2-mediated gene transfer and duration of reporter gene expression. J. Virol. Methods 105, 265–275.

Rohr, U., Wulf, M., Stahn, S., Heyd, F., Steidl, U., Fenk, R., Opalka, B., Pitschke, G., Prisack, H., Bojar, H., Haas, R., Kronenwett, R., 2003. Non-small lung cancer cells are prime targets for *p53* gene transfer mediated by a recombinant adeno-associated virus type-2 vector. Cancer Gene Ther. 10, 898–906.

Ruffing, M., Zentgraf, H., Kleinschmidt, J.A., 1992. Assembly of viruslike particles by recombinant structural proteins of adeno-associated virus type 2 in insect cells. J. Virol. 66, 6922–6930.

Salvetti, A., Orève, S., Chadeuf, G., Favre, D., Cherel, Y., Champion-Arnaud, P., David-Ameline, J., Moullier, P., 1998. Factors influencing recombinant adeno-associated virus production. Hum. Gene Ther. 9, 695–706.

Sanlioglu, S., Benson, P.K., Yang, J., Atkinson, E.M., Reynolds, T., Engelhardt, J.F., 2000. Endocytosis and nuclear trafficking of adeno-associated virus type 2 are controlled by Rac1 and Phosphatidylinositol-3 kinase activation. J. Virol. 74, 9184–9196.

Seisenberger, G., Ried, M.U., Endreß, T., Büning, H., Hallek, M., Bräuchle, C., 2001. Real-time single-molecule imaging of the infection pathway of an adeno-associated virus. Science 294, 1929–1932.

Summerford, C., Bartlett, J.S., Samulski, R.J., 1999. αVβ5 integrin: a co-receptor for adeno-associated virus type 2 infection. Nat. Med. 5, 78–82.

Summerford, C., Samulski, R.J., 1998. Membrane-associated heparan sulfate proteoglycan is a receptor for adeno-associated virus type 2 virions. J. Virol. 72, 1438–1445.

Veldvijk, M.R., Topaly, J., Laufs, S., Hengge, U.R., Wenz, F., Zeller, W.J., Fruehauf, S., 2002. Development and optimization of a real-time quantitative PCR-based method for the titration of AAV-2 vector stocks. Mol. Ther. 6, 272–278.

Vincent-Lacaze, N., Snyder, R.O., Gluzman, R., Bohl, D., Lagarde, C., Danos, O., 1999. Structure of adeno-associated virus vector DNA following transduction of skeletal muscle. J. Virol. 73, 1949–1955.

Wagner, J.A., Reynolds, T., Moran, M.L., Moss, R.B., Wine, J.J., Flotte, T.R., Gardner, P., 1998. Efficient and persistent gene transfer of AAV-CFTR in maxillary sinus. Lancet 351, 1702–1703.

Zolotukhin, S., Byrne, B.J., Mason, E., Zolotukhin, I., Potter, M., Chesnut, K., Summerford, C., Samulski, R.J., Muzyczka, N., 1999. Recombinant adeno-associated virus purification using novel methods improves infectious titer and yield. Gene Ther. 6, 973–985.

Cancer Gene Therapy (2003) 10, 898–906

www.nature.com/cgt

# Non-small lung cancer cells are prime targets for *p53* gene transfer mediated by a recombinant adeno-associated virus type-2 vector

**Ulrich-Peter Rohr,[1] Marc-Andre Wulf,[1] Susanne Stahn,[1] Florian Heyd,[1] Ulrich Steidl,[1] Roland Fenk,[1] Bertram Opalka,[2] Gerald Pitschke,[3] Hans-Bernd Prisack,[3] Hans Bojar,[3] Rainer Haas,[1] and Ralf Kronenwett[1]**

*[1]Klinik für Hämatologie, Onkologie und klinische Immunologie, Heinrich-Heine-Universität Düsseldorf, Moorenstraße 5, D-40225 Düsseldorf, Germany; [2]Innere Klinik und Poliklinik (Tumorforschung), Universitätsklinikum Essen, Hufelandstraße 55, D-45122, Germany; and [3]Institut für Onkologische Chemie, Heinrich-Heine-Universität Düsseldorf, Düsseldorf, Germany.*

In this study, we elucidated the potential of recombinant adeno-associated virus type-2 (rAAV-2) vectors for lung cancer gene therapy. Cell lines of the three major histological subtypes of non-small cell lung cancer (NSCLC) were highly susceptible for rAAV-2 showing transduction rates between 63.4 and 98.9%. In contrast, cell lines of small cell carcinomas were resistant to rAAV-2 infection. For restoration of p53 function in p53 deficient NSCLC, a rAAV-2 vector was constructed containing wt p53 cDNA. Following transduction with rAAV-p53, cell growth of all NSCLC cell lines was significantly reduced in a dose-dependent manner between 44 and 71.7% in comparison with rAAV-GFP transduced cells. The reduction of tumor cell growth was associated with increased apoptosis. Adding cisplatin to rAAV-p53-infected cells led to a significant growth inhibition between 81 and 91% indicating a synergistic effect between cisplatin and rAAV-p53. Interestingly, the tumor cells surviving cisplatin and rAAV-p53 treatment were inhibited in their ability to form colonies as reflected by a reduction of colony growth between 57 and 90.4%. In conclusion, rAAV-2 vectors exhibit a strong tropism for NSCLC. Successful inhibition of tumor cell growth following transduction with a rAAV-p53 vector underlines the potential role of rAAV-2 in cancer gene therapy.
*Cancer Gene Therapy* (2003) **10,** 898–906. doi:10.1038/sj.cgt.7700643

***Keywords: AAV-2; tropism; P53; apoptosis; lung cancer***

Lung cancer is the leading cause of cancer-related deaths with an increasing incidence worldwide.[1] One of the most frequently used agents in the treatment of lung cancer is cisplatin. Although cisplatin is able to induce apoptosis via p53 independent mechanisms,[2] cisplatin-mediated induction of p53 expression mainly triggers the apoptotic pathway. A loss of p53 function which can be found in more than 50% of tumors of lung cancer patients is responsible for the failure of cisplatin-based chemotherapy[3,4] and is associated with a poor prognosis.[5] To overcome the treatment failure of cisplatin in lung cancer with altered p53 it seems to be useful to restore p53 in lung cancer cells. For introduction of a therapeutic gene such as p53, a vector is necessary with unique properties. One promising vehicle with great potential for gene delivery is the adeno-associated virus type-2. The nonpathogenic nature of the virus, infection of dividing and nondividing cells as well as the low immunogenicity are advantages in favor of adeno-associated virus type-2 (AAV-2). In this report, we examined the tropism of recombinant adeno-associated virus type-2 (rAAV-2) for a variety of lung cancer cell lines and identified all major histological NSCLC subtypes as promising targets for a AAV-2-mediated gene transfer. The potential of rAAV-2 vectors in cancer gene therapy was exemplified for the p53 gene, as a significant reduction of tumor cells was observed after transduction with rAAV-p53. In addition, we describe overadditive antitumor effects of a p53 encoding rAAV-2 vector in combination with cisplatin in lung cancer cells.

*Received March 8, 2003.*
*Address correspondence and reprint requests to: Dr U-P Rohr. E-mail: urohr-uni-duesseldorf@gmx.de*

## Material and methods

### *Cell lines and plasmids*

Lung cancer cell lines H23, H322 (adenocarcinoma), H157 (squamous cell carcinoma), H1299, H460 (large-cell carcinoma) and H69, H82, H187, H526, H889 (small-cell carcinoma) were cultured in RPMI-1640 medium (Sigma, Deissenhofen, Germany) supplemented with

10% heat-inactivated fetal calf serum, 2 mM glutamine, 100 IU/ml penicillin and 100 $\mu$g/ml streptomycin. All cell lines were cultured at 37°C in 5% $CO_2$. The lung cancer cell lines were obtained from the American Tissue Culture Collection. The human 293T cell line was cultured in DMEM containing the same supplements as stated above at 37°C in 5% $CO_2$. Vector plasmid pAAV-gfp-AR6- and helper plasmid pDG have been previously described.[6]

### *Analysis of FGFR and αV integrin expression*

For analysis of FGFR and αV integrin expression on SCLC cell line H69 and NSCLC cell line H157, $1 \times 10^5$ cells were incubated with FITC-conjugated anti-CD51 (αV) antibody (Ab)(Clone AMF7; Immunotech, Marseille, France) or the nonconjugated Ab anti-FGFR-1 Ab (Sigma). Monoclonal PE-conjugated anti-rabbit (Sigma) was used as secondary Ab. Cells were subjected to FACS analysis using a FACSCalibur. After gating on viable cells, data were analyzed using the Becton Dickinson CELL QUEST software.

### *Construction of vector plasmid pAAV-p53*

Plasmids were constructed using standard molecular biology techniques. The pAAV-gfp-AR6 plasmid kindly provided by Andrea Hörster[6] was used as the backbone. pAAV-gfp-AR6 contains the gene for the enhanced green fluorescent protein (EGFP) and the HIV-1-directed antisense sequence AR6 under the control of the immediate-early HCMV promoter, a SV40 splice and a polyadenylation signal flanked by the inverted terminal repeats (ITRs) of the AAV-2 clone psub201.[7] pAAV-gfp-AR6 was digested with *Nhe*I (BioLabs, UK) and *Xba*I (BioLabs) excising the AR6 and EGFP transgene insert to yield the 5545 bp backbone of the plasmid. The pVP22-p53 plasmid containing the wild-type human p53 cDNA (kindly donated by Bernd Prisack, Onkologische Chemie, Düsseldorf, Germany) was digested with *Hin*dIII (BioLabs). The *Hin*dIII site was transformed into a *Nhe*I site using Klenow polymerase. After blunt-end religation the human wild-type p53 cDNA was excised from pVP22-p53 by digestion with *Nhe*I and *Xba*I yielding a 1188 bp fragment which was ligated with the pAAV-gfp-AR6 backbone. The new vector plasmid pAAV-p53 contained the gene for wt-p53 under the control of the immediate-early HCMV promoter, a SV40 splice and a polyadenylation signal flanked by the ITRs.

### *Production and purification of recombinant AAV-2 vector stocks*

For preparation of rAAV-2 vector stocks, $1 \times 10^7$ 293T cells were cotransfected with 20 $\mu$g vector plasmid (pAAV-gfp-AR6- or pAAV-p53) and 20 $\mu$g helper plasmid pDG[8] by calcium phosphate precipitation. The helper plasmid pDG contained all AAV-2 (rep, cap) and adenoviral genes (E2A, E4, VA) necessary for rAAV-2 particle production. 293T cells were harvested 72 hours after transfection and were subjected to three cycles of freezing and thawing to release virus. The cell lysate was sonicated 10 times with pulsed 50% duty cycles at 200 W using a Branson Sonifier cell disrupter B-15 (Branson, Schwäbisch Gmuend, Germany) and spun down at 5000 *g* for 30 minutes. rAAV-2 preparations were purified and concentrated using the Iodixanol method as described.[9] Fractions were analyzed for rAAV-2 particles using FACS analysis as stated below.

### *Titration of infectious viral particles using fluorescence-activated cell sorting*

Flow cytometry for titration of infectious rAAV-GFP particles was performed as previously described.[10] Briefly, $1 \times 10^5$ HeLa cells were seeded in 500 µl medium in 24-well plates and 1, 2 or 5 $\mu$l of viral suspension was added to the cells. Cells were incubated at 37°C for 48 hours. For detachment, 50 $\mu$l of 0.02% Trypsin/EDTA (Bio-Whittaker, Verviers, Belgium) was used. Trypsin was inactivated by adding 500 $\mu$l of 10% FCS/PBS. Following two washing steps with 1 ml PBS, cells were resuspended in 500 $\mu$l PBS. After determination of the total cell numbers, FACS analysis was performed using a Becton Dickinson FACSCalibur (Heidelberg, Germany) with a 2 W argon ion laser and EGFP fluorescence was measured using a 530/15 nm (FITC) band-pass filter. The percentage of green fluorescent cells was determined by FACS and was multiplied by the total cell number. Assuming that each EGFP-positive HeLa cell was infected by one rAAV-2 particle, viral titers were deduced from the percentage of transduced cells and diluted suspension.

### *Titration of genomic rAAV-2 titers using CMV promoter-specific quantitative real-time PCR (qPCR)*

Viral preparations were titrated by CMV promoter-specific qPCR as recently described.[11] qPCR was performed in a LightCycler using the FastStart DNA Master SYBR Green kit (Roche Molecular Biochemicals, Mannheim, Germany). Final concentrations in the PCR were: primers: 0.4 $\mu$M each, $MgCl_2$: 5 mM, template: 2 $\mu$l in a final volume of 20 $\mu$l. PCR was performed with a 10 minute preincubation at 95°C followed by 50 cycles of 15 seconds at 95°C (denaturation), 5 seconds at 67°C (annealing) and 10 seconds at 72°C (amplification). PCR products were subjected to melting-curve analysis using the light-cycler system to exclude the amplification of unspecific products. Finally, the PCR products were analyzed by conventional agarose gel electrophoresis (1.5%) and the product length was 201 bp. Primers were synthesized by Thermo Hybaid GmbH, Interactiva Division Ulm, Germany. The following primers were used:

CMV forward :
5′GGC-GGA-GTT-GTT-ACG-ACA-T-3′

CMV reverse :
5′GGG-ACT-TTC-CTA-CTT-GGC-A-3′

### *Western blot analysis*

Western Blot was performed as described.[12] Briefly, H1299 cells were plated in 12-well plates and incubated with rAAV-p53 particles ranging between 250 and 1000 genomic copies per cell for 24 h. Cells were washed twice with ice-cold PBS, scraped off the plate and lysed in ice-cold cell lysis buffer (20 mM Tris-HCl, 1 mM CDTA, 1 mM EGTA, 1% Triton X-100, 0.1 M DTT, 0.5 M leupeptin, 0.1M PMSF). Protein samples were electrophoretically separated on 15% SDS-polyacrylamide gels and transferred to polyvinylidene difluoride membranes (Milipore, Schwalbach, Germany) for 1 hour. After blocking, membranes were incubated overnight at 4°C with mouse anti-human p53 monoclonal antibody (Zymed, San Francisco; dilution 1:1000). A peroxidase-coupled rabbit anti-mouse secondary antibody was used for detection of primary antibodies (Amersham Biosciences, Freiburg, Germany; dilution 1:1000) for 1 hour. Immunocomplexes formed on the membrane were visualized with an enhanced chemiluminescence (ECL) kit (Amersham) according to the manufacturer's instructions.

### *Transduction experiments*

Lung cancer cell lines (H1299, H157 and H23) were cultured in 24-well plates as described above and transduced with rAAV-GFP or rAAV-p53 at different concentrations. At 3 days after transduction, tumor cells were detached with trypsin/EDTA and resuspended with RPMI medium in a final volume of 1000 $\mu$l.

For cisplatin experiments, dose–response curves for cisplatin were determined by dilutions of cisplatin ranging from 1 to 0.1 $\mu$g/ml. A cisplatin concentration of 0.25 $\mu$g/ml led to a mean cell growth inhibition of 53.3% (SD + 22.5) in all three NSCLC cell lines (H199, H23, H157). This concentration was considered as suitable to evaluate subadditive, additive or overadditive growth inhibitory effects of rAAV-p53 and cisplatin on NSCLC cells. Performing transduction experiments using rAAV-2 and cisplatin, NSCLC cell lines were cultured in 24-well plates containing cisplatin in a concentration of 0.25 $\mu$g/ml. Transduction was performed as described above. After 3 days of virus and cisplatin coincubation, cells were detached using trypsin/EDTA and resuspended with RPMI medium in a final volume of 1000 $\mu$l. Growth inhibition was assessed as stated below.

### *Assessment of viable cells*

Cells were counted using a Neubauer counting chamber. The survival rate in percent was calculated by dividing the number of viable treated cells by the number of viable untreated control cells multiplied by 100. The viability of cells was assessed by trypane blue exclusion. Inhibition in percent was calculated by the following formula: inhibition in % = 100%−survival rate in %. All experiments were performed at least in triplicate.

### *Clonogenic assay*

Clonogenic assays were performed seeding $5 \times 10^2$ viable cells treated with rAAV-GFP alone, rAAV-p53 alone, cisplatin alone, rAAV-GFP in combination with cisplatin or rAAV-p53 in combination with cisplatin into 25 $cm^2$ flasks for 3 days. After 7 days, colonies were counted using a light microscope. Only colonies containing more than 50 cells were counted. The percentage of colonies was calculated by division of colony numbers derived from treated cells by those from untreated cells and multiplied by 100.

### *Apoptosis assay*

The apoptosis rate was determined using an Annexin V binding assay as described.[13] Briefly, 48 hours after treatment of H1299 cells with rAAV-p53, rAAV-GFP and/or cisplatin, cells were suspended in 200 $\mu$l of Annexin V binding buffer (Pharmingen, Heidelberg, Germany). A volume of 100 $\mu$l was added to 10 $\mu$l of PE-conjugated control antibody (Pharmingen). The remaining 100 $\mu$l cell suspension was added to 10 $\mu$l of Annexin V–PE (Pharmingen). A volume of 10 $\mu$l of 7-amino-actinomycin D (7-AAD) (BD PharMingen, Germany) was added to PE-control and AnnexinV–PE sample in order to detect and exclude necrotic cells. After an incubation time of 15 minutes at room temperature, cells were washed and analyzed using a Becton Dickinson FACSCalibur (Heidelberg, Germany) with a 2 W argon ion laser. The proportion of apoptotic and necrotic cells, that is, Annexin V binding cells and 7-AAD binding cells, was assessed using the Cell Quest software (Becton Dickinson). Annexin positive cells showing no 7-AAD staining were regarded as apoptotic.

### *Statistical analysis*

For statistical analysis, the Student's *t*-test was used. Statistical significance was defined as $P < 0.05$.

## Results

### *Tropism of rAAV-2 for lung cancer cells*

In order to evaluate the tropism of rAAV-2 for lung cancer cells of different histological subtypes, 10 different lung cancer cell lines were transduced with a recombinant AAV-GFP vector with a MOI of 50 viral particles per cell. All cell lines of NSCLC such as adenocarcinoma (H23, H322), squamous cell carcinoma (H157) and large-cell carcinoma (H1299, H460) were highly susceptible for rAAV-2 showing transduction rates between 63.4 and 98.9% with a mean transduction rate of 84.1% (SD ± 19.9) 5 days after infection (Fig 1a, b). In contrast, cell lines of SCLC (H69, H82, H187, H526, H889) were resistant to rAAV-2 infection showing a range of mean transduction rates between 1.1% (SD ± 1.1) and 5.9% (SD ± 3.0) 5 days after transduction. In order to explain the differences of tropism, the expression of the AAV-2 co-receptors FGFR-1 and αV integrin necessary for viral

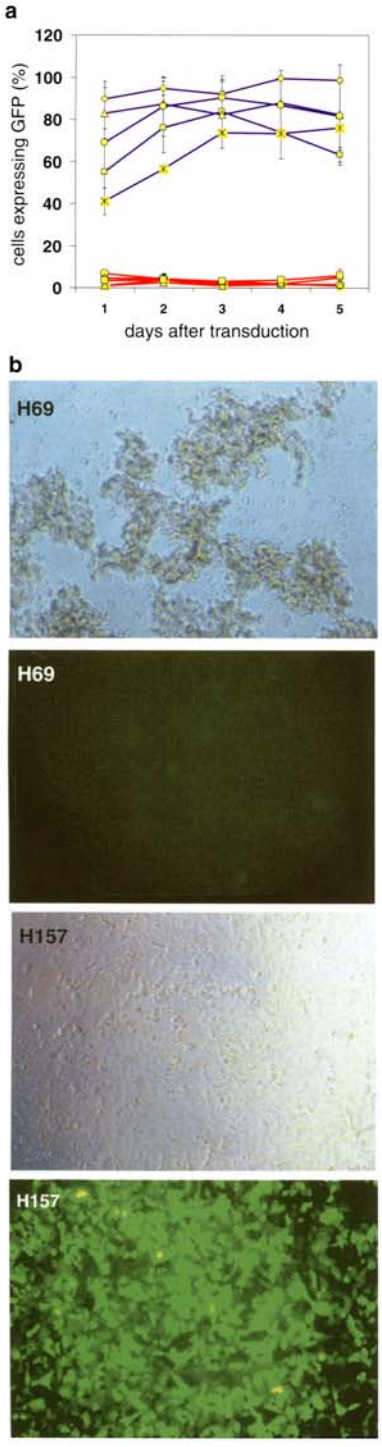


**Figure 1** Differences in rAAV-2 tropism between small-cell lung cancer (SCLC) and NSCLC cell lines **(a)** Differences in transduction rates between SCLC and NSCLC. Blue lines represent NSCLC (◇ H157, □ H460, △ H1299, * H322, ○ H23), red lines SCLC cell lines (+ H69, ○ H82, △ H187, ◇ H526, □ H889). **(b)** Phase-contrast microscopy and corresponding fluorescence microscopy from a representative experiment following rAAV-GFP transduction of SCLC cell line H69 (upper pictures) or NSCLC cell line H157 (lower pictures) using a MOI of 50 per cell. **(c)** Immunofluorescence analysis of alpha V integrin and fibroblast growth factor receptor-1 expression on SCLC cell line H69 and NSCLC cell line H157. Control antibody stainings are indicated by black curves, specific staining by colored curves.

cell entry was examined on the rAAV-2 resistant SCLC cell line H69 as well as on the NSCLC cell line H157 showing the highest transduction rate of 98.9%. As assessed by flow cytometry, the SCLC cell line H69 showed no rAAV-2 coreceptor expression, whereas FGFR-1 and αV integrin expression was present on all H157 cells (Fig 1c).

### *Successful rAAV-2-mediated transfer of the p53 gene*

A high susceptibility of rAAV-2 was observed for NSCLC cells using a rAAV-GFP vector. In order to generate a *therapeutic* rAAV-2 vector, we constructed an adeno-associated vector carrying the p53 gene. After infection of the p53-negative cell line H1299 with rAAV-p53 using MOIs between 250 and 1000 genomic particles per cell, restoration of p53 expression was detected by immunoblotting (Fig 2).

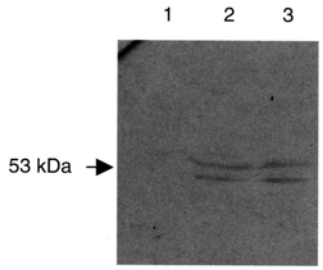


**Figure 2** Detection of p53 expression after rAAV-2-mediated p53 gene transfer by immunoblotting. Lane 1: rAAV-GFP transduced H1299 cells. Lane 2: p53 positive control. Lane 3: rAAV-p53-transduced H1299 cells using a MOI of 600 genomic particles per cell.

### *Cytotoxic effect of rAAV-p53 on NSCLC*

Since rAAV-p53 infection of the p53-negative cell line H1299 resulted in expression of p53 protein, we next asked if transduction with the therapeutic vectors would lead to decreased tumor cell growth. To this end, the three NSCLC cell lines H1299, H23 and H157 of the histological subtypes large cell, squamous and adenocarcinoma were infected with rAAV-p53. All three cell lines had no functional p53 due to deletion or mutation of the p53 gene. A low, intermediate and high concentration of rAAV-p53 with $3 \times 10^1$ ($1\times$), $1.5 \times 10^2$ ($5\times$), $6 \times 10^2$ ($20\times$) genomic particles per cell was chosen for all experiments. As a result, growth of all three cell lines H23, H157 and H1299 was reduced by rAAV-p53 in a dose-dependent manner showing an inhibition of 1.2–44%, 4.5–71.7% and 14.8–70.3%, respectively, compared to untreated control cells (Fig 3a, b). Proliferation was not impaired in tumor cells infected with a rAAV-GFP control.

### *Induction of apoptosis by rAAV-p53*

Expression of p53 can induce cell-cycle arrest and apoptosis. Therefore, induction of apoptosis in NSCLC tumor cells was examined using the new vector rAAV-p53. H1299 cells were incubated with $6 \times 10^2$ rAAV-p53 or rAAV-GFP particles per cell for 2 days and analyzed for apoptotic cells using an annexin V-binding assay with exclusion of necrotic cells using the 7-AAD nucleic acid dye. Cisplatin was used as a positive control with a concentration of 0.25 $\mu$g/ml. Untreated cells showed a

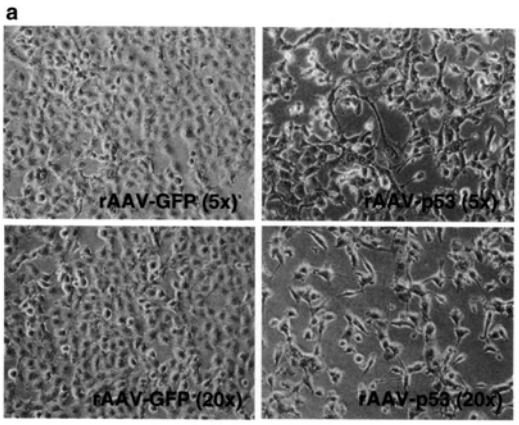


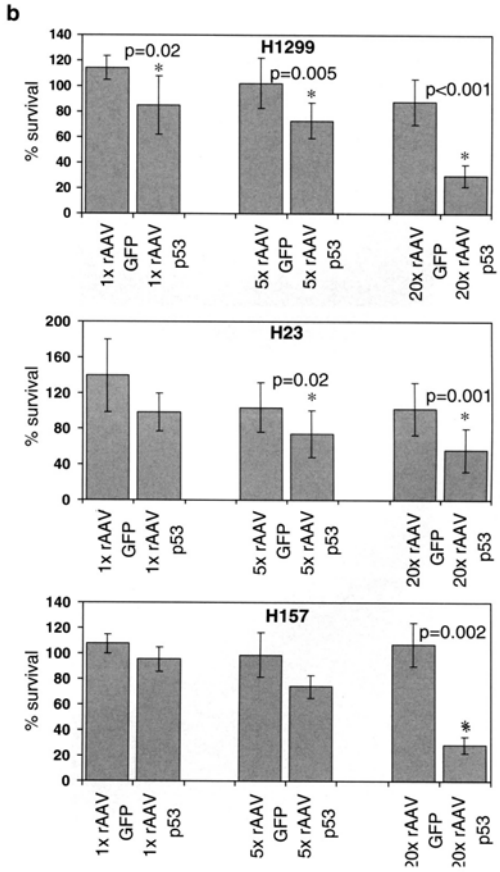


**Figure 3** Cytotoxic effect of rAAV-p53 on NSCLC cell lines. **(a)** Transduction of cell line H23 using rAAV-GFP and rAAV-p53 at a concentration of $1.5 \times 10^2$ ($5\times$) or $6 \times 10^2$ ($20\times$) particles per cell. **(b)** Cytotoxic effects of rAAV-GFP in comparison with the control vector rAAV-GFP of all three cell lines H1299, H23 and H157 as assessed by trypane blue exclusion 3 days following transduction. The survival rate in percent was calculated by dividing the number of viable treated cells by the number of viable untreated control cells multiplied by 100. The viability of cells was assessed by trypane blue exclusion. A low, intermediate and high concentration of rAAV-2 with $3 \times 10^1$ ($1\times$), $1.5 \times 10^2$ ($5\times$), $6 \times 10^2$ ($20\times$) particles per cell was used. Standard deviations as well as statistical significances (*) and respective *P*-values are indicated.

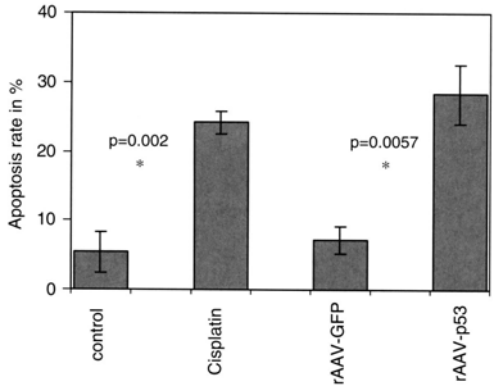


**Figure 4** Induction of apoptosis by rAAV-p53. H1299 cells were transduced with $6 \times 10^2$ rAAV-p53 or rAAV-GFP particles per cell and analyzed for apoptotic cells using an Annexin V-binding assay 2 days following transduction. Cisplatin was used as a positive, untreated cells as a negative control. 7-AAD was used for the detection of necrotic cells in flow cytometric assays. Annexin V positive/ 7-AAD negative cells were regarded as apoptotic. Standard deviations and statistical differences are indicated.

spontaneous apoptosis rate of 5.4% (SD +2.9%) while cisplatin increased the rate of apoptotic cells to 24.2% (SD +1.7%). Cells that had been infected with the control vector rAAV-GFP had an apoptosis rate of 7.7% (SD +1.9%). Cells treated with the therapeutic vector rAAV-p53 showed the highest apoptosis rate of 28.3% (SD+4.3%) (Fig 4).

### *Cytotoxic effect of rAAV-p53 in combination with cisplatin*

In order to enhance the chemosensitivity of NSCLCs by introduction of p53, we tested the combination of rAAV-p53 with the DNA-damaging agent cisplatin. The growth of H1299, H23 and H157 was reduced by 64.5% (SD±16.9), 62.7% (SD±18.2) and 32.6% (SD±13.5), respectively, using cisplatin alone (Fig 5a, b). Combination of rAAV-p53 and cisplatin led to a further inhibition of growth in a dose-dependent manner. The mean growth inhibition of H1299, H23 and H157 cells treated with a combination of cisplatin and increasing doses of rAAV-p53 were between 66.3–90.7%, 70.1–91% and 41.9–81%,

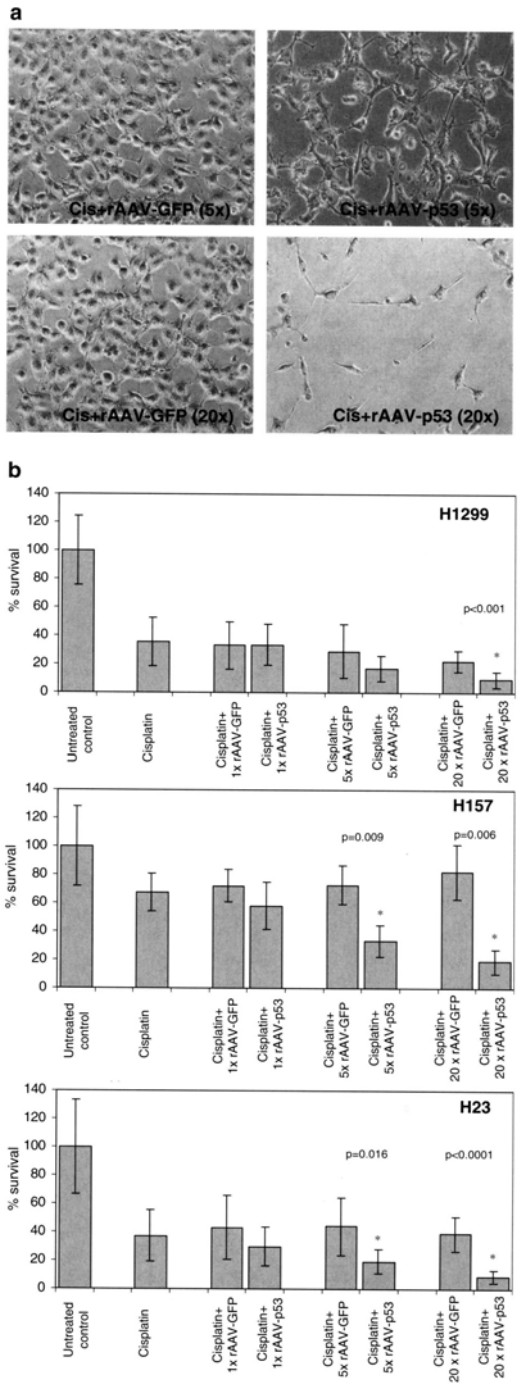


**Figure 5** Cytotoxic effect of rAAV-p53 in combination with cisplatin. **(a)** Differences in the inhibition of cell growth on H23 using rAAV-GFP or rAAV-p53 at a concentration of $1.5 \times 10^2$ (5×) or $6 \times 10^2$ (20×) particles per cell in combination with the DNA-damaging agent cisplatin. **(b)** Growth reduction of H1299, H23 and H157 using cisplatin alone or either a combination of rAAV-GFP or rAAV-p53 (at a concentration of $3 \times 10^1$ (1×), $1.5 \times 10^2$ (5×), $6 \times 10^2$ (20×) particles per cell) with cisplatin. An overadditive inhibition of cell growth was found for H23. Standard deviations as well as statistical significances (*) and respective *P*-values are indicated.

respectively. The reduction of the tumor cell number following combined vector and cisplatin treatment was statistically significant for intermediate and high vector concentrations compared to the control rAAV-GFP. In an attempt to evaluate subadditive, additive or over-additive growth inhibitory effects of rAAV-p53 and cisplatin on NSCLC cells, we first performed experiments using the single agents. Based on these results we calculated hypothetical combined survival rates by adding the effects of cisplatin and rAAV-p53 given as single agents. The calculated survival rates were compared with the measured survival rates of the combined treatment. In H1299 and H157 additive effects were found with survival rates almost identical to the calculated results. In contrast, the inhibition was overadditive in cell line H23. This was reflected by a growth inhibition of 91% which was higher than the expected growth inhibition of 79% when simply adding the effects of cisplatin or rAAV-p53 given as single agents.

### *Effects of rAAV-p53 and cisplatin on clonogenic growth*

Following combined rAAV-p53 and cisplatin treatment of NSCLC between 9 and 19% of the tumor cells still survived. Therefore, we were interested in the ability of those surviving tumor cells for clonogenic growth. As assessed by trypane blue exclusion, an equivalent number of cells that had survived the treatment of cisplatin (with or without rAAV-GFP or rAAV-p53) was washed and placed in a cell culture plate with regular cell culture medium. After 7 days, the colonies were counted. Generally, cells surviving combined cisplatin and rAAV-p53 treatment had a significantly inhibited ability to form colonies in comparison with cells without pretreatment. The inhibitory effects were overadditive which is best exemplified for cell line H157. Neither a treatment of cells with cisplatin or rAAV-p53 as single agents had a significant inhibitory effect on the development of colonies compared to the untreated cells. In contrast, the combined treatment led to a 57% (SD$\pm$9.5%) inhibition of clonogenic colony growth (Fig 6). The overadditive inhibitory effect on colony growth was also seen for cell line H1299 with a colony reduction of 90.4% (SD$\pm$3.41%).

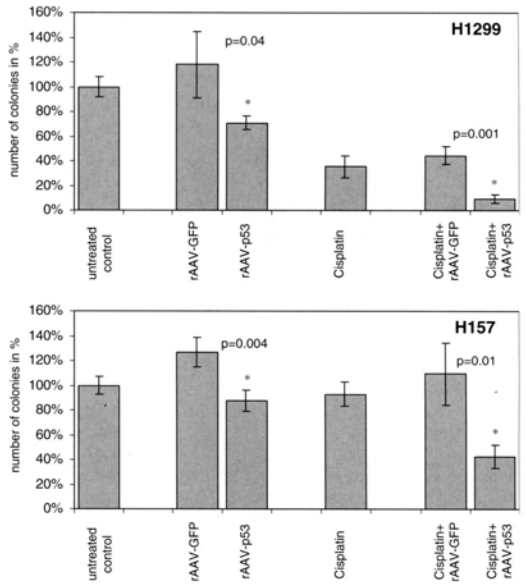


**Figure 6** Effects of rAAV-p53 and cisplatin on clonogenic growth of NSCLC cell lines H1299 and H157. Following cisplatin or either combined rAAV-GFP or rAAV-p53 (at a concentration of $6 \times 10^2$ particles per cell) and cisplatin treatment of NSCLC, surviving tumor cells were assessed for clonogenic growth. Colonies were counted 7 days after removement of the cytotoxic drugs. Standard deviations as well as statistical significances (*) and respective *P*-values are indicated.

## Discussion

In this study, we show that rAAV-2 vectors have a strong tropism for NSCLCs. All NSCLCs were highly susceptible for rAAV-2 with transduction rates between 60 and 98.9%. In contrast, SCLCs were resistant to rAAV-2 infection. Those differences of lung cancer susceptibility to rAAV are most likely explained by receptor status of the cells. rAAV-2 susceptible NSCLC cells expressed the essential coreceptors for viral internalization FGFR-1 and alphaV-integrin[14,15] while SCLC cells did not.

Most common viral vectors in gene therapy have been recombinant retroviruses and adenoviruses. However, the vectors can be associated with serious adverse events due to the biologic behavior of the vector system. Early-generation adenoviral vectors were highly immunogenic possibly causing a systemic inflammatory response syndrome (SIRS) leading to multiple organ failure.[16] Genes carried by retroviral vectors are randomly integrated into the genome of the cell. This potentially leads to insertional mutagenesis which is currently under investigation in a French trial of gene therapy for X-linked severe combined immune deficiency in which one out of 11 patients developed a monoclonal gamma-delta T-cell lymphoproliferative disorder 30 months after retroviral vector treatment (Press release of the European Society of Gene Therapy, November 2002).

In comparison to *wild-type* AAV-2, *recombinant* AAV-2 vectors have lost the ability for site-specific integration into chromosome 19 due to the removal of the rep-coding sequences. Extra-chromosomal, not integrated, genomes are the major intracellular form of *recombinant* AAV, which greatly decreases the potential risk of vector-related mutagenesis. Further, AAV-2 is not associated with any human disease and the weak immunogenicity of AAV-2 enables a safe vector administration into a target-tissue for several times as shown in a clinical study for patients with haemophilia B.[17] Finally, AAV-2 has a high transduction capacity in primary *human* cells.[10] Although rAAV vectors play an important role in the substitutional

therapy of genetic disorders, the potential of rAAV-2 for cancer gene therapy was disregarded so far. For a cancer therapy, *wild-type* AAV-2 offers some unique properties. Next to a direct antioncogenic effect of wt-AAV,[18,19] infection with wt-AAV-2-prevented chemotherapy-related toxic side effects[20] and mediated sensitivity to chemotherapy.[21,22] Moreover, infection and gene expression occur in both nondividing and dividing cells. As a result, we were interested if *recombinant* AAV-2 vectors can play a role in the treatment of lung cancer. Therefore, a rAAV-2 vector was constructed containing the wt-p53 gene. This tumor suppressor gene was chosen since p53 functions are well documented[23] and growth inhibitory effects were already shown for lung,[24] colorectal[25] or pancreatic[26] cancer cell lines using an adenovirus-mediated gene transfer. After transduction of lung cancer cell lines using our rAAV-p53, p53 was successfully restored and a significant growth inhibition ranging from 44 to 72% was seen in H23, H157 and H1299 NSCLC cell lines. In contrast, the control vector rAAV-GFP had no inhibitory effect demonstrating the specific effect of rAAV-2-mediated wt-p53 gene transfer. As expected, the inhibitory effect of rAAV-p53 was mediated by apoptosis.[27]

Encouraged from the results that *wild-type* AAV-2 itself as well as p53 can enhance the sensitivity to chemotherapy, we were interested if *recombinant* AAV-2 vectors have the same ability. Combined treatment of NSCLC cell lines with cisplatin and *recombinant* AAV-p53 led to additive or overadditive inhibitory effects on lung tumor cells with a growth inhibition between 81 and 91%. In addition, the surviving tumor cells were significantly hampered to form colonies without any further treatment showing a long-term effect even after removement of the cytotoxic drugs. However, no growth inhibitory effects were seen for a combination of cisplatin and the control vector rAAV-GFP in comparison to cisplatin alone. The results implicate that *recombinant* AAV-2 vectors have lost the ability to sensitize NSCLC tumor cells to chemotherapy as described for *wild-type* AAV-2. The lack of rep/cap genes in *recombinant* AAV-2 vectors is the most likely explanation for the missing sensitizing effect on tumor cells. The overadditive synergistic effect of cisplatin and recombinant *AAV-p53* in NSCLC cell lines can be explained by a sustained expression of proapoptotic p53 during the clonogenic assay and DNA damage induced by cisplatin during pretreatment.

Despite the encouraging results, rAAV-2 vector delivery might be difficult. Tropism of rAAV-2 is so far too broad for intravenous application. Moreover, more than 90% of humans have been exposed to wild-type AAV-2 and, therefore, carry antibodies against the virus. Thus, administration or readministration of rAAV-2 in humans could be problematic. Next to direct intratumoral injection, new ways of applications such as an effective aerosolic vector inhalation for local administration would be beneficial or, alternatively, rAAV-2 mutants could be designed mediating a specific tropism in NSCLC cells.

In summary, we have demonstrated for the first time to our knowledge that NSCLC cells are prime targets for AAV-2. A new recombinant AAV-2 vector containing the cDNA for p53 induced a significant growth inhibition and had a chemosensitizing effect. The extent of rAAV-2 mediated p53 tumor cell death and the synergy with DNA-damaging agents such as cisplatin exemplifies the potential of rAAV-2 vectors for cancer therapy. The results encourage future efforts to develop additional rAAV-based vectors containing other tumor suppressor genes such as p16 or FHIT for lung cancer gene therapy.

## Acknowledgments

This work was supported by the Leukämie Liga Duesseldorf.

## References

1. Landis SH, Murray T, Bolden S, Wingo PA. Cancer statistics, 1999. *CA Cancer J Clin*. 1999;49:8–31.
2. Wang X, Liu Y, Chow LS, et al. Cisplatin-induced p53-independent growth arrest and cell death in cancer cells. *Int J Oncol*. 1999;15:1097–1102.
3. Lowe SW, Ruley HE, Jacks T, Housman DE. p53-dependent apoptosis modulates the cytotoxicity of anticancer agents. *Cell*. 1993;74:957–967.
4. Rusch V, Klimstra D, Venkatraman E, et al. Aberrant p53 expression predicts clinical resistance to cisplatin-based chemotherapy in locally advanced non-small cell lung cancer. *Cancer Res*. 1995;55:5038–5042.
5. Horio Y, Takahashi T, Kuroishi T, et al. Prognostic significance of p53 mutations and 3p deletions in primary resected non-small cell lung cancer. *Cancer Res*. 1993;53:1–4.
6. Horster A, Teichmann B, Hormes R, Grimm D, Kleinschmidt J, Sczakiel G. Recombinant AAV-2 harboring gfp-antisense/ribozyme fusion sequences monitor transduction, gene expression, and show anti-HIV-1 efficacy. *Gene Therapy*. 1999;6:1231–1238.
7. Samulski RJ, Chang LS, Shenk T. Helper-free stocks of recombinant adeno-associated viruses: normal integration does not require viral gene expression. *J Virol*. 1989;63:3822–3828.
8. Grimm D, Kern A, Rittner K, Kleinschmidt JA. Novel tools for production and purification of recombinant adenoassociated virus vectors. *Hum Gene Ther*. 1998;9:2745–2760.
9. Zolotukhin S, Byrne BJ, Mason E, et al. Recombinant adeno-associated virus purification using novel methods improves infectious titer and yield. *Gene Therapy*. 1999;6:973–985.
10. Rohr UP, Kronenwett R, Grimm D, Kleinschmidt J, Haas R. Primary human cells differ in their susceptibility to rAAV-2-mediated gene transfer and duration of reporter gene expression. *J Virol Methods*. 2002;105:265–275.
11. Rohr UP, Wulf MA, Stahn S, Steidl U, Haas R, Kronenwett R. Fast and reliable titration of recombinant adeno-associated virus type-2 using quantitative real-time PCR. *J Virol Methods*. 2002;106:81–88.
12. Horio Y, Hasegawa Y, Sekido Y, Takahashi M, Roth JA, Shimokata K. Synergistic effects of adenovirus expressing wild-type p53 on chemosensitivity of non-small cell lung cancer cells. *Cancer Gene Ther*. 2000;7:537–544.

*Int. J. Cancer:* **111,** 259–263 (2004)


Publication of the International Union Against Cancer

# EXPRESSION OF THE TYROSINE KINASE C-KIT IS AN INDEPENDENT PROGNOSTIC FACTOR IN PATIENTS WITH SMALL CELL LUNG CANCER

Ulrich-Peter ROHR[1]*, Nina REHFELD[1], Lucy PFLUGFELDER[1], Helene GEDDERT[2], Wolfram MÜLLER[2], Ulrich STEIDL[1], Roland FENK[1], Thorsten GRÄF[1], Matthias SCHOTT[1], Klaus-Peter THIELE[1], Helmut Erich GABBERT[2], Ulrich GERMING[1], Ralf KRONENWETT[1] and Rainer HAAS[1]

[1]*Klinik für Hämatologie, Onkologie und klinische Immunologie, Heinrich-Heine-Universität Düsseldorf, Düsseldorf, Germany*
[2]*Institut für Pathologie, Heinrich-Heine-Universität, Düsseldorf, Germany*

**In a retrospective analysis of 203 patients with small cell lung cancer (SCLC), we examined the prognostic value of c-kit expression on survival. Expression of c-kit was examined immunohistochemically in formalin-fixed, paraffin-embedded tissue sections. c-kit was observed in 87.7% of SCLC tumors. Using the Kaplan-Meier model, we found that lack of c-kit expression was associated with significantly shorter survival time compared to the presence of c-kit expression (mean survival 151 ± 27 *vs.* 358 ± 49 days, $p = 0.0084$). Moreover, the proportion of c-kit$^+$ cells within the tumor was also related to survival time. Patients with tumors in which >75% of cells stained positive for c-kit had a mean overall survival time of 424 (±72) compared to 295 (±67) days for patients with 25–75% c-kit$^+$ tumor cells. Patients with tumors containing <25% c-kit$^+$ cells had the worst survival, with 164 (±24) days ($p = 0.0033$). Further parameters associated with short survival times were low performance status, elevated levels of lactate dehydrogenase and higher stage according to the TNM classification. Multivariate analysis using the Cox regression model showed that the proportion of c-kit$^+$ cells within the tumor specimen was one of 3 independent prognostic parameters ($p = 0.004$) for overall survival next to TNM classification ($p = 0.001$) and performance status ($p < 0.001$).**


**Key words:** *small cell lung cancer; c-kit; survival; multivariate analysis*

The ongoing progress of cancer research on the molecular level led to a greater understanding of growth-stimulatory signaling in the development of small cell lung cancers (SCLC). Beside growth factors such as platelet-derived growth factor and gastrin-releasing peptide, there is increasing evidence that proliferation of malignant cells in SCLC is mediated by an autocrine loop between the transmembrane c-kit receptor and its ligand, stem cell factor (SCF).[1] Between 79% and 88% of SCLC cell lines were found to express c-kit and 57–76% of the cell lines expressed both c-kit receptor and the ligand SCF.[1,2] After binding of the ligand dimer, 2 adjacent kit receptors form a homodimer, leading to activation of the intracellular kit kinase domains. As a result, tyrosine residues are cross-phoshorylated by the activated kinases of the opposed homodimer partner. Phosphotyrosines are binding sites for cell-signaling proteins, including the Jak/Stat, Ras/Raf and PDK1/AKT cascades, which mediate various cell functions such as proliferation, adhesion, chemotaxis and apoptosis.[3] The potential role of c-kit in the carcinogenesis of SCLC is suggested by *in vitro* findings showing that increased proliferation and migration of SCLC cells can be induced when c-kit$^+$ cell lines are exposed to SCF.[4–7] Further, growth of SCLC cell lines is inhibited by antisense-mediated suppression of c-kit receptor.[8] Although the stimulating role of c-kit in proliferation is obvious, it should be kept in mind that the results are derived from *in vitro* cell culture experiments or xenograft mouse models. There are only few reports addressing the role of c-kit in SCLC *in vivo.* At the moment, the reports are somehow inconsistent, particularly with respect to c-kit expression and prognostic relevance. In the literature, proportions between 27.9%[9] and 78%[10] of c-kit$^+$ SCLC tumors are described. Further, c-kit has been associated with both unfavorable prognosis[11,12] and favorable prognosis[9] and has not been a predictor of survival at all.[13] In the present study, we examined the prognostic value of c-kit expression on survival in 203 patients with SCLC. The influence of c-kit staining intensity (negative, weak, intermediate and strong) and the proportion of c-kit$^+$ cells within a tumor were taken into consideration for univariate and multivariate survival analyses.

## MATERIAL AND METHODS

### *SCLC patients*

Formalin-fixed, paraffin-embedded tissue sections from 203 patients with primary SCLC were used for immunohistochemical examination of c-kit. Specimens were obtained from the Institute of Pathology, University of Duesseldorf. The collection period was 1983–2002. Biopsies from the primary tumor site were taken at initial clinical presentation. The original diagnosis of SCLC was confirmed by 2 different pathologists before the biopsy was accepted for this study. Clinical data of the patients were collected from chart review. Survival time in days was calculated from the date of histologic diagnosis, and the performance status of the patient was evaluated by WHO criteria [graded from fully active (grade 0) to completely disabled (grade IV)]. The grouping of the TNM subsets into the SCLC stages I–IV was based on the revised version of the International System for Staging Lung Cancer (adopted by the American Joint Committee on Cancer and the UICC).[14] The baseline characteristics at diagnosis of the patients with SCLC are summarized in Table I. In 85.1% of evaluable SCLC patients, chemotherapy was performed as a first-line treatment, with an average of 4 cycles (mean 4.26 cycles, range 1–12). The preferred chemotherapeutic regimen was a combination of cyclophosphamide, doxorubicin (Adriamycin) and vincristine (73.2%), followed by a platinum-based combination with etoposide (11.4%) or cyclophosphamide, etoposide and vincristine (4.9%); other combinations were given in 10.5% of patients.

### *Immunohistochemistry*

As described by Naeem *et al.*[11] and Micke *et al.*,[12] immunohistochemical staining was performed for standardized c-kit detection, using a primary antibody against c-kit that targets the COOH-terminal domain of the intracellular part of the c-kit receptor (catalogue 4502; Dako, Hamburg, Germany).

Grant sponsor: Leukämie Liga; Grant sponsor: Novartis Inc.

*Correspondence to: Klinik für Hämatologie, Onkologie und klinische Immunologie, Heinrich-Heine-Universität Düsseldorf, Moorenstrasse 5, D-40225 Düsseldorf, Germany. Fax: +49211-8118853.
E-mail: urohr-uni-duesseldorf@gmx.de

Received 20 August 2003; Revised 25 November 2003; Accepted 19 January 2004

DOI 10.1002/ijc.20252
Published online 12 April 2004 in Wiley InterScience (www.interscience.wiley.com).

**TABLE I** – BASELINE CHARACTERISTICS OF SCLC PATIENTS ($n$ = 203)

| | Evaluated patients (%) |
|---|---|
| Age (years) | 62.8 ± 9.8 |
| Sex | |
| Male | 149 (73.4%) |
| Female | 54 (26.6%) |
| Performance status | |
| WHO 0 | 60 (35.1%) |
| WHO I | 78 (45.6%) |
| WHO II | 25 (14.6%) |
| WHO III | 8 (4.7%) |
| Stage | |
| Ia,b | 5 (3.3%) |
| IIa,b | 11 (7.4%) |
| IIIa,b | 38 (25.3%) |
| IV | 96 (64.0%) |
| LDH (units/l) | 376 ± 355[1] |
| Hemoglobin (g/dl) | 13.7 ± 1.8[1] |
| Thrombocytes (nl) | 319,173 ± 111,091[1] |
| Leukocytes (nl) | 9,741 ± 3,522[1] |

[1]Mean ± SD.

Briefly, fresh tumor tissue specimens were immediately formalin-fixed following bronchoscopy or surgery. Samples were paraffin-embedded and cut in 2–4 μm sections on poly-L-lysine–coated slides. Following deparaffinization with xylene (15 min), sections were rehydrated through decreasing concentrations of ethanol (100%, 96% and 70%) and washed for 5 min. For antigen retrieval, specimens were heated in citrate buffer (pH 6) using a pressure cooker for 15 min. Endogenous peroxidase activity was eliminated by incubation with 3% $H_2O_2$ for 15 min, and unspecific binding of biotin and avidin was blocked using a blocking solution (Dako) for 15 min on each slide. After intensive washing for 5 min, slides were incubated with 1% BSA (Sigma, St. Louis, MO) to block unspecific binding of the primary antibody. Purified anti-c-kit antibody (Dako) was diluted 1:100 using the antibody dilution kit (Dako), and slides were incubated with anti-c-kit antibody for 1 hr. After washing, a streptavidin–horseradish peroxidase detection kit (Dako) containing 3,3-diaminobenzidine solution as substrate was used for immunohistochemical staining, according to the manufacturer's instructions. Appropriate negative controls (normal lung tissue) and positive controls (gastrointestinal stromal tumor, GIST) were additionally evaluated in each run. All slides were simultaneously assessed by 2 investigators using a double-headed discussion microscope. The result was confirmed by a third investigator. Staining intensity for c-kit was evaluated semiquantitatively and classified in 4 groups. The first group showed equal staining intensity compared to the GIST$^+$ control. The second group showed intermediate intensity of c-kit staining, which was lower than the GIST$^+$ control. The third group showed weak staining intensity, while the fourth group showed no immunohistochemical evidence of c-kit expression. Generally, staining intensity was uniform within the slide. For those rare cases where there was a difference in staining intensity, the strongest intensity was chosen for the assessment of c-kit. In contrast to staining intensity, heterogeneity in the proportion of cells expressing c-kit within a tumor was observed. Therefore, tumors were divided into 4 categories: no tumor cells expressing c-kit, c-kit expression in <25% of tumor cells, c-kit expression in 25–75% and c-kit expression in >75% of SCLC cells. The percentage of positive cells was estimated in agreement with all 3 observers. For the estimation, the whole slide was included, containing different tumor areas of 1–4 biopsies from bronchoscopy.

*Statistical methods*

Immunohistochemical staining was performed without prior knowledge of clinical parameters. Means and SEs are reported for several clinical parameters. To compare clinical parameters with c-kit expression, Kaplan-Meier survival analysis with log-rank test was performed. A 2-sided $t$-test was performed to compare clinical variables of c-kit$^+$ and c-kit$^-$ groups. For multivariate analysis, a Cox regression model with a forward stepwise selection was used. Pearson's bivariant correlation analysis was performed, to evaluate a correlation between c-kit expression or proportion of c-kit-expressing cells and clinical parameters. Statistical analysis was performed using SPSS (Chicago, IL) software, version 10.1. Significance was defined as $p < 0.05$.

## RESULTS

*Immunostaining of c-kit in SCLCs*

c-kit expression was observed in 178 of 203 patients (87.7%). Tumors of 37 patients (18.2%) showed weak, 61 (30.1%) intermediate and 80 (39.4%) strong staining intensity of c-kit. No c-kit expression was seen in 25 cases (12.3%) of SCLC (Fig. 1). Since the staining pattern was heterogeneously distributed within the tumor, the proportion of positive tumor cells for each sample was assessed. As shown in Figure 2, 25 SCLCs (12.3%) were negative for c-kit expression in all tumor cells. Proportions of c-kit$^+$ cells of <25%, 25–75% and >75% were observed in 7 (3.5%), 82 (40.4%) and 89 (43.8%) of all patients with SCLC, respectively.

*Prognostic value of c-kit*

To evaluate the prognostic value of c-kit, data from all 203 patients with SCLC were analyzed using Kaplan-Meier survival curves. Mean survival of all patients was 335 (±44) days, and 1- and 5-year survival rates were 23% and 2%, respectively. Survival curves of patients with SCLC showing different staining intensities (negative, low, intermediate and strong) of c-kit were compared. Lack of c-kit expression was associated with significantly shorter survival time compared to presence of c-kit expression, independent from staining intensity ($0.016 < p < 0.021$). There were no statistically significant differences in survival times ($0.77 < p < 0.88$) between patients with SCLC showing weak, intermediate or strong c-kit expression. The respective mean survival times were

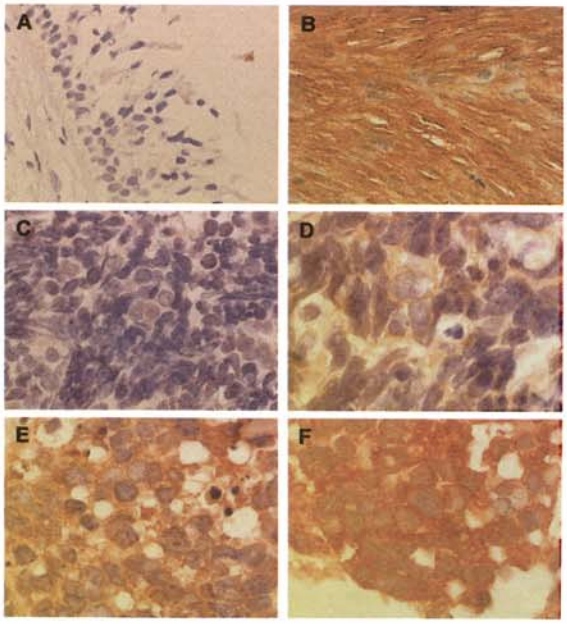


**FIGURE 1** – Immunohistochemical staining of c-kit in SCLC. *(a)* Negative control of normal lung epithelium. *(b)* Positive control of a GIST. *(c)* SCLC with lack of c-kit expression. *(d)* SCLC showing weak c-kit staining. *(e)* SCLC with intermediate c-kit staining. *(f)* SCLC showing strong c-kit expression.

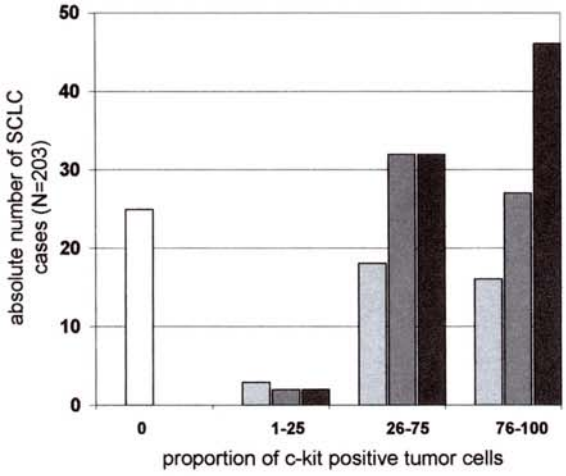


FIGURE 2 – Proportion of c-kit$^+$ tumor cells and c-kit staining intensities of SCLC ($n$ = 203). White bars represent c-kit$^-$ cases; light gray, dark gray and black bars represent weakly, intermediately and strongly stained SCLC tumors, respectively.

376 ± 104, 381 ± 94 and 326 ± 64 days (Fig. 3*a*). Therefore, all patients with c-kit expression, regardless of staining intensity, were grouped together for further analysis.

Lack of c-kit expression was associated with significantly shorter mean survival of 151 ± 27 days compared to 358 ± 49 days ($p$ = 0.0084) for patients with c-kit$^+$ tumors (Fig. 3*b*). There was no significant difference between patients of the c-kit$^+$ and c-kit$^-$ groups with respect to mean age (63.0 ± 10.0 *vs.* 64.4 ± 8.5 years, $p$ = 0.335), mean hemoglobin level (13.7 ± 1.8 *vs.* 14.1 ± 1.6 g/dl, $p$ = 0.412), mean lactate dehydrogenase (LDH) level (377.4 ± 368 *vs.* 367.9 ± 227, $p$ = 0.871), TNM classification[14] (stage I *vs.* II *vs.* III *vs.* IV, $p$ = 0.496), performance status (WHO 0/I *vs.* II/III, $p$ = 0.462) or number of cycles of chemotherapy (4.3 ± 3.2 *vs.* 3.1± 2.6 cycles, $p$ = 0.096), respectively.

Further, the influence of the proportion of c-kit-expressing cells on survival was examined. Interestingly, survival times were also correlated to the proportion of c-kit-expressing cells ($p$ = 0.0033). SCLC patients with tumors containing <25% c-kit$^+$ cells (including c-kit$^-$ cases), 25–75% and >75% c-kit$^+$ cells had mean survival of 164 (±24), 295 (±67) and 424 (±72) days, respectively (Fig. 4). With respect to age, hemoglobin level, LDH, TNM classification, performance status and number of cycles of chemotherapy, no significant differences were seen within the 3 different patient groups.

*Clinical parameters, survival and c-kit expression in multivariate analysis*

Among the clinical parameters, performance status (WHO 0/I *vs.* II/III), LDH (serum levels <240 units/l *vs.* ≥240 units/l), leukocyte count (<3,500/nl, 3,500–11,000/nl, >11,000/nl) and TMN classification (stage I *vs.* II *vs.* III *vs.* IV) were also related to survival time using Kaplan-Meier analysis (data not shown). To examine whether c-kit is an independent prognostic factor, multivariate analysis was performed using a forward selection model of the Cox regression. Eleven variables were included in the multivariate analysis: performance status, gender, age, TNM classification, LDH, smoking status, hemoglobin, thrombocytes, leukocytes, the proportion of c-kit$^+$ cells and the qualitative presence of c-kit expression. None of the clinical parameters was related to c-kit expression or the proportion of c-kit-expressing cells as assessed by Pearson's bivariant correlation analysis. As shown in Table II, only proportion of c-kit$^+$ cells ($p$ = 0.004), TNM stage ($p$ =

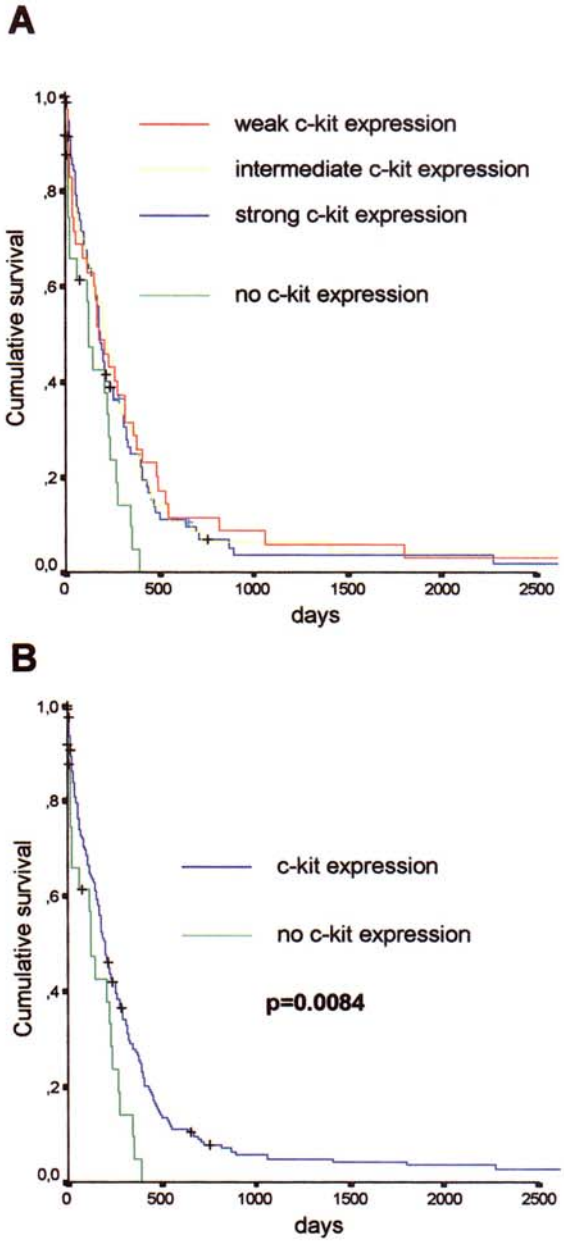


FIGURE 3 – Association of c-kit expression and survival. *(a)* No statistical differences in survival time between patients with SCLC of weak, intermediate and strong c-kit expression were seen. In comparison, lack of c-kit expression was significantly associated with poorer survival compared to positive staining (weak *vs.* no expression, $p$ = 0.021; intermediate *vs.* no expression, $p$ = 0.016; strong *vs.* no expression, $p$ = 0.019). *(b)* All cases with c-kit expression (weak, intermediate and strong) were regarded as positive. Lack of c-kit expression was associated with significantly shorter mean survival of 151 ± 27 days compared to 358 ± 49 days for patients with c-kit$^+$ tumors.

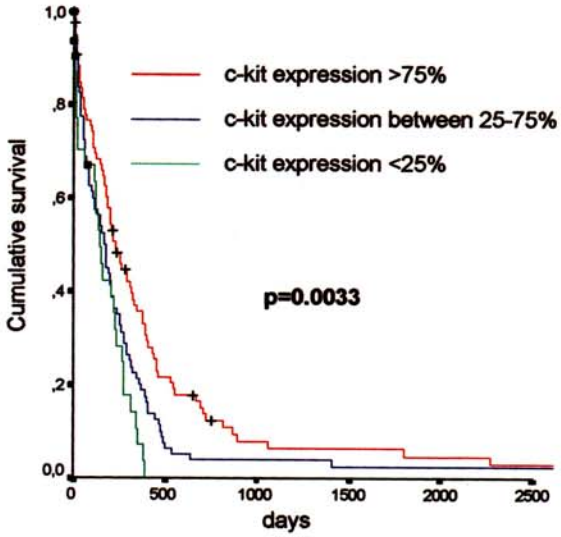


FIGURE 4 – Association of the proportion of c-kit$^+$ cells within SCLC tumor and survival. Patients with <25% (including c-kit$^-$ cases), 25–75% and >75% c-kit$^+$ tumor cells had mean survival of 164 (±24), 295 (±67) and 424 (±72) days, respectively.

TABLE II – VARIABLES ACCEPTED IN THE FORWARD SELECTION MODEL OF THE COX REGRESSION AS EXPLANATORY FACTORS

| | p-value[a] |
|---|---|
| Percentage of tumor cells expressing c-kit[b] | 0.004 |
| Stage[c] | 0.001 |
| Performance status[d] | <0.001 |

[a]according to the score test–[b]proportion of c-kit positive cells within SCLC tumor of 0–24% vs. 25–75% vs. 76–100%–[c]according to TNM-system: stage I vs. II vs. III vs. IV–[d]performance status according to WHO 0, I vs. II, III

0.001) and performance status ($p < 0.001$) were independent, explanatory prognostic factors accepted in the forward selection model of the Cox regression. In contrast to hemoglobin level, thrombocyte count, gender, age and smoking status, which were irrelevant with regard to survival time, the qualitative presence of c-kit, leukocyte count and LDH level were of significance ($p < 0.05$) but not chosen as explanatory, independent variables in the Cox regression model (Table III).

## DISCUSSION

In our study, 87.7% of 203 SCLC tumors examined by immunohistochemistry were positive for the receptor tyrosine kinase c-kit. This finding is in line with other reports demonstrating c-kit expression in 77%, 81% or 100%[1,15,16] of primary human SCLCs. In these studies, Northern and Southern blot analyses were performed for c-kit detection. Other groups using an immunohistochemical staining method have reported proportions of 27% and 78% of c-kit$^+$ SCLC tumors.[9–12] The reported differences can be explained by the use of different criteria to rate tumors as c-kit$^+$ or not. For example, Naem *et al.*[11] found 53% of 30 SCLC tumors to be c-kit$^+$; in their definition, only tumors with >50% c-kit-expressing cells were regarded as c-kit$^+$. In contrast, in the study of Micke *et al.*,[12] a tumor was accepted as c-kit$^+$ if >10% of all tumor cells had "strict, clear-cut positive expression" of c-kit. Based on this criterion, tumor cells which were weakly stained

TABLE III – VARIABLES NOT ACCEPTED AS EXPLANATORY FACTORS OF THE COX REGRESSION FORWARD SELECTION MODEL

| | Score[a] | p-value[b] |
|---|---|---|
| Smoker[c] | 0.79 | 0.38 |
| Age[d] | 1.82 | 0.18 |
| Leukocytes[e] | 7.42 | 0.01 |
| Thromocytes[f] | 1.90 | 0.17 |
| LDH[g] | 7.70 | 0.01 |
| c-kit[h] | 5.08 | 0.02 |
| Haemoglobin[i] | 0.09 | 0.77 |
| Gender[j] | 0.25 | 0.61 |

[a]according to the likelihood ratio test–[b]according to the score test–[c]smoker or formerly smoker vs. non-smoker–[d]age ≤60 years vs. > 60 years–[e]leukocytes <3500/nl vs 3500–11000/nl vs >11000/nl–[f]thrombocytes <150.000/nl vs. 150.000–400.000/nl vs. >400.000/nl–[g]LDH serum levels ≤240 U/liter vs. >240 U/liter–[h]c-kit positive vs. c-kit negative SCLC tumors–[i]haemoglobin levels ≤12g/dl vs. >12g/dl–[j]male vs. female

were not included, resulting in a proportion of only 37% c-kit$^+$ tumors. Consequently, staining intensity and percentage of positively stained tumor cells are crucial points in the definition of a tumor as c-kit$^+$ or c-kit$^-$. Applying different criteria to define whether a tumor is c-kit$^+$ or not for survival analysis, it becomes clear why c-kit has been associated with both better and worse median survival as well as with no impact on survival. To circumvent the c-kit grading problem, we assessed the proportion of c-kit$^+$ cells and their staining intensity for a large group of 203 patients with primary SCLC tumors and correlated the results with survival of the patients.

First, the relationship between c-kit staining intensity and survival was compared. Better overall survival with a mean survival time of 358 *vs.* 151 days was observed for patients whose SCLC tumors expressed c-kit, independent of the expression level, compared to those with no c-kit expression, respectively ($p = 0.0084$). However, there was no statistical difference in the survival of patients with weakly, intermediately or strongly c-kit-stained tumors. These results suggest that the expression level of c-kit in SCLC$^+$ cells is irrelevant with respect to survival but, for the appropriate use of c-kit as a prognostic marker, even weak c-kit expression must be considered as c-kit$^+$.

Next, the prognostic value of the proportion of c-kit$^+$ cells within the tumor was examined. The proportion of c-kit-expressing cells was associated with survival time of SCLC patients ($p = 0.0033$). Patients with tumors containing <25% c-kit$^+$ cells had the worst survival time with 164 days compared to patients with 25–75% or >75% of cells stained positive for c-kit, who had mean overall survival times of 295 and 424 days, respectively.

This result was confirmed by multivariate analysis using the Cox forward selection model to identify prognostic factors. As a result, only the proportion of c-kit expressing cells within the tumor was an independent explanatory prognostic factor of survival in this model next to TNM classification and performance status. Similar to our results, Potti *et al.*[9] found improved median survival in c-kit-expressing, extended-disease SCLC patients. Survival times was 16.5 months compared to the c-kit$^-$ population, in which survival was only 14 months although the result was not statistically significant in multivariate analysis. Interestingly, Onn *et al.*[17] examined the influence of c-kit on survival in early-stage non-small lung cancer (NSCLC) and found c-kit to be the only independent predictive factor of improved prognosis using multivariate analysis.

The association of c-kit expression with better prognosis appears to contradict the expected growth advantage of c-kit-expressing tumor cells since tumor cell growth is mediated by an autocrine loop between the c-kit receptor and its ligand, SCF.[1,5] An explanation could be that c-kit$^+$ SCLC cells are more susceptible to cytotoxic treatment since more tumor cells are in the cell cycle and, consequently, more sensitive to systemic therapy. This view

is not entirely hypothetical since >50% of initially c-kit$^+$ SCLC tumors became negative after combination chemotherapy.[10]

The presence of c-kit in SCLC suggests that it could be a suitable target for novel therapies, *e.g.*, the tyrosine kinase inhibitor imatinib. This drug was initially designed to inhibit the bcr-abl tyrosine kinase in patients with chronic myeloid leukemia. It also inhibits the tyrosine kinase domain of platelet-derived growth factor receptor and c-kit. The inhibitory effect of imatinib has already been used in the treatment of GISTs, in which c-kit mutations in the juxtamembrane domain of exon 11 lead to constitutive activation of the tyrosine kinase domain (TKD) of the receptor.[18] Inhibition of the TKD of c-kit in GISTs using imatinib was the first effective treatment for patients with metastatic disease, resulting in an overall response rate of 82%.[19] Based on these results, the growth-inhibitory effects of imatinib on c-kit$^+$ cell lines have been examined by different groups. Treatment of SCLC cells with imatinib *in vitro* resulted in dose-dependent inhibition of proliferation of 10–50% at a concentration of 1 μM.[20,21] These *in vitro* data are promising, though the possible potential of imatinib for patients with c-kit$^+$ SCLC remains unclear. The therapeutic effect is certainly dependent on c-kit mutations and the expression level of c-kit during therapy. In contrast to GISTs, no receptor activating exon 11 c-kit mutations have been observed so far in SCLC,[22] and the data from Tamberi *et al.*[10] indicate that the c-kit$^-$ SCLC clone might be responsible for tumor recurrence, which is associated with poor prognosis. Therefore, inactivation of c-kit in SCLC patients might lead to the same poor prognosis as for patients in whom c-kit is not expressed.

In conclusion, a high incidence of c-kit positive SCLC tumors was observed, and the qualitative and quantitative presence of c-kit was correlated with improved outcome in these patients.

## REFERENCES


1. Hibi K, Takahashi T, Sekido Y, Ueda R, Hida T, Ariyoshi Y, Takagi H, Takahashi T. Coexpression of the stem cell factor and the c-*kit* genes in small-cell lung cancer. Oncogene 1991;6:2291–6.
2. Rygaard K, Nakamura T, Spang-Thomsen M. Expression of the proto-oncogenes c-*met* and c-*kit* and their ligands, hepatocyte growth factor/scatter factor and stem cell factor, in SCLC cell lines and xenografts. Br J Cancer 1993;67:37–46.
3. Heinrich MC, Rubin BP, Longley BJ, Fletcher JA. Biology and genetic aspects of gastrointestinal stromal tumors: KIT activation and cytogenetic alterations. Hum Pathol 2002;33:484–95.
4. Hida T, Ueda R, Sekido Y, Hibi K, Matsuda R, Ariyoshi Y, Sugiura T, Takahashi T, Takahashi T. Ectopic expression of c-kit in small-cell lung cancer. Int J Cancer Suppl 1994;8:108–9.
5. Papadimitriou CA, Topp MS, Serve H, Oelmann E, Koenigsmann M, Maurer J, Oberberg D, Reufi B, Thiel E, Berdel WE. Recombinant human stem cell factor does exert minor stimulation of growth in small cell lung cancer and melanoma cell lines. Eur J Cancer 1995; 31A:2371–8.
6. Krystal GW, Hines SJ, Organ CP. Autocrine growth of small cell lung cancer mediated by coexpression of c-kit and stem cell factor. Cancer Res 1996;56:370–6.
7. Sekido Y, Takahashi T, Ueda R, Takahashi M, Suzuki H, Nishida K, Tsukamoto T, Hida T, Shimokata K, Zsebo KM. Recombinant human stem cell factor mediates chemotaxis of small-cell lung cancer cell lines aberrantly expressing the c-*kit* protooncogene. Cancer Res 1993; 53:1709–14.
8. Yamanishi Y, Maeda H, Hiyama K, Ishioka S, Yamakido M. Specific growth inhibition of small-cell lung cancer cells by adenovirus vector expressing antisense c-kit transcripts. Jpn J Cancer Res 1996;87:534–42.
9. Potti A, Moazzam N, Ramar K, Hanekom DS, Kargas S, Koch M. CD117 (c-KIT) overexpression in patients with extensive-stage small-cell lung carcinoma. Ann Oncol 2003;14:894–7.
10. Tamberi S, Longo L, Rossi G, Migaldi M, Crino L, Cavazza A, Marchioni A, Bavieri M, Petruzzelli S. Loss of c-kit expression after chemotherapy in small cell lung cancer: therapeutic implications. Proc ASCO 2003;22. Abstract 2607.
11. Naeem M, Dahiya M, Clark JI, Creech SD, Alkan S. Analysis of c-kit protein expression in small-cell lung carcinoma and its implication for prognosis. Hum Pathol 2002;33:1182–7.
12. Micke P, Basrai M, Faldum A, Bittinger F, Ronnstrand L, Blaukat A, Beeh KM, Oesch F, Fischer B, Buhl R, Hengstler JG. Characterization of c-kit expression in small cell lung cancer: prognostic and therapeutic implications. Clin Cancer Res 2003;9:188–94.
13. Blackhall FH, Pintilie M, Michael M, Leighl N, Feld R, Tsao MS, Shepherd FA. Expression and prognostic significance of kit, protein kinase B, and mitogen-activated protein kinase in patients with small cell lung cancer. Clin Cancer Res 2003;9:2241–7.
14. Mountain CF. The international system for staging lung cancer. Semin Surg Oncol 2000;18:106–15.
15. Sekido Y, Obata Y, Ueda R, Hida T, Suyama M, Shimokata K, Ariyoshi Y, Takahashi T. Preferential expression of c-*kit* protooncogene transcripts in small cell lung cancer. Cancer Res 1991;51: 2416–9.
16. Natali PG, Nicotra MR, Sures I, Santoro E, Bigotti A, Ullrich A. Expression of c-kit receptor in normal and transformed human non-lymphoid tissues. Cancer Res 1992;52:6139–43.
17. Onn A, Correa AM, Gilcrease M, Moran C, Roach JS, Isobe T, Bucana CD, Hong WK, Putnam JB, Herbst RS. Epidermal growth factor receptor, HER2,, and c-Kit as predictors of outcome in stage I non-small cell lung cancer. Proc ASCO 2003;22. Abstract 2553.
18. Lasota J, Jasinski M, Sarlomo-Rikala M, Miettinen M. Mutations in exon 11 of c-Kit occur preferentially in malignant versus benign gastrointestinal stromal tumors and do not occur in leiomyomas or leiomyosarcomas. Am J Pathol 1999;154:53–60.
19. Joensuu H, Fletcher C, Dimitrijevic S, Silberman S, Roberts P, Demetri G. Management of malignant gastrointestinal stromal tumors. Lancet 2002;3:655–64.
20. Wang WL, Healy ME, Sattler M, Verma S, Lin J, Maulik G, Stiles CD, Griffin JD, Johnson BE, Salgia R. Growth inhibition and modulation of kinase pathways of small cell lung cancer cell lines by the novel tyrosine kinase inhibitor STI 571. Oncogene 2000;19:3521–8.
21. Krystal GW, Honsawek S, Litz J, Buchdunger E. The selective tyrosine kinase inhibitor STI571 inhibits small cell lung cancer growth. Clin Cancer Res 2000;6:3319–26.
22. Burger H, den Bakker MA, Stoter G, Verweij J, Nooter K. Lack of c-kit exon 11 activating mutations in c-KIT/CD117-positive SCLC tumour specimens. Eur J Cancer 2003;39:793–9.

# Prognostic Relevance of Fragile Histidine Triad Protein Expression in Patients with Small Cell Lung Cancer

**Ulrich-Peter Rohr,[1] Nina Rehfeld,[1] Helene Geddert,[2] Lucy Pflugfelder,[1] Ingmar Bruns,[1] Judith Neukirch,[1] Astrid Rohrbeck,[1] Hans J. Grote,[3] Ulrich Steidl,[1] Roland Fenk,[1] Bertram Opalka,[4] Helmut E. Gabbert,[2] Ralf Kronenwett,[1] and Rainer Haas[1]**

[1]Klinik für Hämatologie, Onkologie und klinische Immunologie, [2]Institut für Pathologie, and [3]Zytopathologisches Institut, Heinrich-Heine-Universität Düsseldorf, Düsseldorf, Germany and [4]Innere Klinik und Poliklinik (Tumorforschung), Universitätsklinikum Essen, Essen, Germany

## ABSTRACT

***Purpose:*** **The fragile histidine triad protein (FHIT) is a putative tumor suppressor in patients with lung cancer. In this study, we examined the prognostic value of FHIT expression for survival in patients with small cell lung cancer (SCLC).**

***Experimental Design:*** **As assessed by immunohistochemistry using formalin-fixed, paraffin-embedded tissue sections, tumors of 225 patients with SCLC were retrospectively evaluated for FHIT expression. The influence of FHIT staining intensities as well as the proportion of FHIT-positive cells within a tumor was taken into consideration for univariate and multivariate survival analysis.**

***Results:*** **FHIT expression was observed in 61.8% of the SCLC tumors. Lack of FHIT was significantly associated with a shorter survival time for the patients with a median of 157 ± 18 days compared with 210 ± 18 days for those patients with FHIT-positive tumors ($P = 0.0061$). Furthermore, the proportion of FHIT-positive cells within the tumor was related to survival. Patients with tumors of <25% FHIT-positive cells had the worst survival of 155 ± 21 days compared with 217 ± 19 days for patients with a proportion of ≥25% of FHIT-expressing tumor cells ($P = 0.0016$). In contrast to the proportion of FHIT-positive cells within the tumor, no significant difference in survival was observed when different FHIT staining intensities (weak versus strong) were considered (median survival of 208 ± 17 versus 234 ± 34 days, $P = 0.665$). Multivariate analysis using Cox regression including 11 variables confirmed the prognostic significance of FHIT expression next to performance status, tumor stage, and lactate dehydrogenase.**

***Conclusion:*** **The presence of FHIT was correlated with a better prognosis for patients with SCLC.**

## INTRODUCTION

Recent advances in cancer research resulted in a better understanding of the pathophysiology of small cell lung cancers (SCLC). Molecular analysis has shown that between 90% and 100% of SCLC and between 50% and 80% of non–small cell lung cancer (NSCLC) tumors have loss of heterozygosity on chromosome arm 3p (1, 2). At least three distinct regions of loss of heterozygosity (3p25, 3p21.3, and 3p14) have been reported. The fragile histidine triad (*FHIT*) gene, located on 3p14.2, has been proposed to be involved in the development of lung cancers. The 16.8-kDa FHIT protein consists of 146 amino acids and is a human orthologue of the fission yeast *Schizosaccharomyces pombe* protein, a diadenosine 5′,5-$P_1P_4$-tetraphosphate hydrolase (3). Whereas the exact molecular pathway of FHIT signaling is unknown, the FHIT substrate complex seems to act as a signaling molecule (4) involved in the regulation of p53-independent apoptosis (5) and cell cycle control (6). Restoration of FHIT expression induced apoptosis and suppressed tumorigenicity of lung cancer cells *in vitro* (7) and *in vivo* (8). Within primary NSCLC tumors, immunohistochemical analysis of FHIT expression revealed greater frequency of FHIT loss in squamous cell carcinomas in comparison with adenocarcinomas. In contrast to NSCLC, only 19 primary SCLCs and 28 SCLC cell lines were systematically examined for FHIT expression. Between 30% and 50% of primary SCLC tumors and 20% and 47% of SCLC cell lines were FHIT positive (9–11). Because of the relatively small number of patients examined, there are no data with regard to the relationship between FHIT expression and patient survival. In this study, we examined the prognostic value of FHIT expression for survival in 225 patients with SCLC. The influence of FHIT staining intensities as well as the proportion of FHIT-positive cells within a tumor was taken into consideration for univariate and multivariate survival analysis.

## PATIENTS AND METHODS

**Patients with SCLC.** Formalin-fixed, paraffin-embedded tissue sections from 225 patients with primary SCLC were used for immunohistochemical examination of FHIT. The specimens were obtained from the Institute of Pathology of the University of Duesseldorf. Biopsies from the primary lung tumor were taken at initial clinical presentation before treatment. The original diagnosis of SCLC was confirmed by two different experienced pathologists (W.M. and H.G.) before the biopsy was accepted for

Received 7/19/04; revised 10/11/04; accepted 10/14/04.
**Grant support:** Leukämie Liga e. V. Duesseldorf.
The costs of publication of this article were defrayed in part by the payment of page charges. This article must therefore be hereby marked *advertisement* in accordance with 18 U.S.C. Section 1734 solely to indicate this fact.
**Requests for reprints:** Ulrich-Peter Rohr, Klinik für Hämatologie, Onkologie und klinische Immunologie, Heinrich-Heine-Universität Düsseldorf, Moorenstraße 5, D-40225 Düsseldorf, Germany. Phone: 49-211-811-7720; Fax: 49-211-811-8853; E-mail: urohr-uni-duesseldorf@gmx.de.

this study. The histopathologic diagnosis was based on H&E stains as well as immunohistochemical stains (cytokeratin and chromogranin A). The patients enrolled in the study were patients from the University of Duesseldorf and associated academic hospitals of the University of Duesseldorf between 1983 and 2003. Clinical data of the patients were collected from chart review with given approval from the ethics committee of the University of Duesseldorf. The baseline characteristics of the patients are presented in Table 1. The survival time in days was calculated from the date of histopathologic diagnosis and the performance status of the patient was evaluated by WHO criteria [graded from fully active (grade 0) to completely disabled (grade IV)]. The grouping of the tumor-node-metastasis (TNM) subsets (T, primary tumor; N, regional lymph nodes; M, distant metastasis) into the SCLC stages I to IV was based on the revised version of the International System for Staging Lung Cancer adopted by the American Joint Committee on Cancer and the Union Internationale Contre le Cancer (12). Chemotherapy was done as a first-line treatment with an average of four chemotherapy cycles (median, 5.0±2.8 cycles; range, 1-12) in 87.3% of evaluable SCLC patients. Patients were uniformly treated using a combination of etoposide 120 mg/m$^2$ d1, adriamycin 45 mg/m$^2$ d1, or epirubicin 65 mg/m$^2$ d1 and cyclophosphamide 1000 mg/m$^2$ d1 (every 3 weeks), which was the preferred chemotherapeutic regimen (62.4%). A platinum-based combination (either cisplatin 90 mg/m$^2$ d1 or carboplatin 300 mg/m$^2$ d1) with etoposide (150 mg/m$^2$ d1-3; every 3 weeks) was given in 15.2%, whereas other combinations were given in 9.7% of patients.

**Immunohistochemistry.** As previously described by Ramp et al. (13), a standardized immunohistochemical staining procedure was done for FHIT detection using a polyclonal antibody raised against full-length human FHIT (Zymed, San Francisco, CA). Briefly, fresh tumor tissue specimens were immediately formalin-fixed following bronchoscopy or computer-tomographic–supported thoracal puncture. Samples were paraffin-embedded, cut in 2- to 4-μm sections on poly-L-lysine–coated slides. Following deparaffinization with xylene (15 minutes), sections were rehydrated through decreasing concentrations of ethanol (100%, 96%, and 70%) and washed for 5 minutes. For antigen retrieval, the specimens were heated in citrate buffer (pH 6) using a pressure cooker for 15 minutes. Endogenous peroxidase activity was eliminated by incubation with 3% hydrogen peroxide for 15 minutes and unspecific binding of biotin and avidin was blocked using a blocking solution (Dako, Hamburg, Germany) for 15 minutes on each slide. After intensive washing for 5 minutes, slides were incubated with 1% bovine serum albumin (Sigma, St. Louis, MO) to block unspecific binding of the primary antibody. The anti-FHIT antibody (Zymed, San Francisco, CA) was diluted 1:200 to a final concentration of 1.25μg/mL and slides were incubated with anti-FHIT antibody for 1 hour. After washing, a streptavidin horseradish peroxidase detection kit (Dako) containing 3,3′-diaminobenzidine solution as substrate was used for immunohistochemical staining according to the manufacturer's instructions. Appropriate positive controls (kidney) were additionally evaluated in each run. All slides were simultaneously assessed by two investigators (N.R. and L.P.) using a double-headed discussion microscope. In a final discussion round all slides were reviewed and the results were confirmed by a third investigator (H.G.). The staining intensities for FHIT were evaluated semiquantitatively and classified into three groups. The first group showed equal or stronger cytoplasmic staining intensity compared with the positive control. The second group showed weaker staining intensity of FHIT compared with the positive control. The third group showed no immunohistochemical evidence of FHIT expression. Generally, the staining intensity and the proportion of FHIT-positive cells was uniform within the slide. For those cases with a difference in staining intensity, the strongest intensity was chosen for the assessment of FHIT. Furthermore, to evaluate the prognostic influence of the proportion of FHIT-positive cells in contrast to their expression level, tumors were divided into five categories: none of the tumor cells expressed FHIT, FHIT positive tumor cell number between 1% and 25%, >25% and 50%, >50% and 75%, and >75%. The percentage of positive cells was estimated in agreement with all three observers. For the estimation, all tumor areas of one to four biopsies from bronchoscopy were included.

*Table 1* Baseline characteristics of patients with SCLC ($N$ = 225)

| | Patients (%) |
|---|---|
| Mean age (years) | 62.6 ± 9.9 (range, 40-87) |
| Sex | |
| Male | 162 (72) |
| Female | 63 (28) |
| Smoking status | |
| Smoker/former smoker | 171 (76) |
| Nonsmoker | 22 (9.8) |
| Not evaluable | 32 (14.2) |
| WHO performance status | |
| 0 | 60 (26.7) |
| I | 89 (39.6) |
| II | 33 (14.7) |
| III | 9 (4.0) |
| Not evaluable | 34 (15) |
| Stage | |
| Ia, b | 5 (2.2) |
| IIa, b | 10 (4.4) |
| IIIa, b | 41 (18.2) |
| IV | 115 (51.1) |
| Not evaluable | 54 (24) |
| LDH (units/L) | 376 ± 339* |
| Hemoglobin (g/dL) | 13.6 ± 1.8* |
| Thrombocytes (μL) | 322410 ± 115270* |
| Leukocytes (μL) | 9614 ± 3448* |

*Mean ± SD.

**Statistical Methods.** The Kaplan-Meier survival analysis with log rank test was done to compare clinical parameters with FHIT expression. Two sided $t$ test was done to compare clinical variables of FHIT-positive and -negative groups. For multivariate analysis, a Cox regression model with a forward stepwise selection was used. Pearson bivariant correlation analysis was done to evaluate a correlation between FHIT expression or proportion of FHIT-expressing cells to clinical parameters. Statistical analysis was done using SPSS software 12.0. Significance is defined as $P < 0.05$ and the respective values are given in the text. Immunohistochemical stains were done without prior knowledge of clinical parameters.

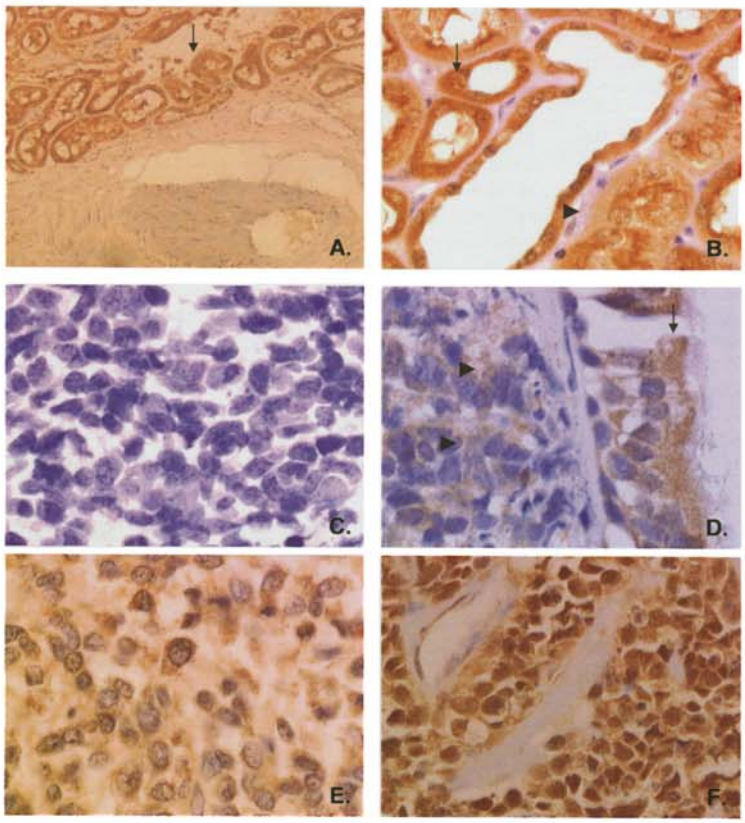


*Fig. 1* Immunohistochemical staining of FHIT in SCLCs. *A* and *B*, positive control of uropoietic tubuli of the kidney (*black arrows*). Uropoietic stromal cells between the tubuli were FHIT negative (*arrowhead*). *C*, SCLC with lack of FHIT expression. *D* and *E*, SCLC showing weak FHIT staining (*arrowhead*). Note the positive cytoplasmic staining of normal bronchial epithelium (*arrows*). *F*, SCLC showing strong FHIT expression.

## RESULTS

**Immunostaining of FHIT in SCLCs.** FHIT expression was observed in 139 (61.8%) of 225 examined tumors, whereas a weak and strong cytoplasmic staining intensity was found in 71 (51.1%) and 68 (48.9%) of 139 FHIT-positive SCLCs, respectively. No FHIT expression was seen in 86 (38.2%) cases ( Fig. 1).

Because an inhomogeneous staining pattern was observed in 21% of the SCLCs, the proportion of positive tumor cells was assessed for each sample of 225 SCLC tumors. Proportions of FHIT-positive cells between 1% and 25%, between >25% and 50%, between >50% and 75%, and >75% were observed in 6 (2.7%), 12 (5.3%), 30 (13.3%), and 91 (40.5%) of all patients with SCLC, respectively, whereas 86 cases (38.2%) were FHIT negative (Fig. 2). For SCLC cases with a heterogeneous staining pattern no biopsy-to-biopsy variation concerning the absolute percentage of cells staining positive for FHIT was observed.

**Prognostic Value of FHIT Expression Using Kaplan-Meier Survival Curves.** In an attempt to evaluate the prognostic value of FHIT expression in patients with SCLC Kaplan-Meier survival curves were chosen for survival analysis. Median and mean survival rates for all 225 patients were 194 ± 16 and 321 ± 43 days; 1- and 5-year survival rates were 23.9% and 2.6%, respectively. To evaluate the impact of different FHIT staining intensities on survival, the survival curves of the three groups showing no, weak, or strong FHIT staining intensities were compared.

A complete lack of FHIT expression was associated with worst prognosis compared with patients with FHIT expression independently from staining intensity ($0.012 < P < 0.033$). No significant differences were observed between the survival curves of the patients with weak and strong FHIT staining (median survival, 208 ± 17 versus 234 ± 34 days; $P = 0.665$), respectively. Therefore, positive stained cases were grouped together for further analysis. Patients with lack of FHIT-expressing tumors had a significant ($P = 0.0061$) shorter median survival of 157 ± 18 days compared with 210 ± 18 days for those patients with FHIT-positive tumors.

No differences between FHIT-negative and FHIT-positive patient group was observed with respect to gender (male versus female, $P = 0.563$), age (mean, 63.3 versus 62.2 years; $P = 0.447$) smoking status (nonsmokers versus smokers, $P = 0.605$), performance status (WHO 0 versus I versus II versus III, $P = 0.809$), tumor stage (I versus II versus III versus IV, $P = 0.441$), mean cycles of chemotherapy (3.51 ± 3.06 versus 4.35 ± 3.1 cycles, $P = 0.11$), mean hemoglobin level (13.47 ± 1.8 versus 13.72 ±

1.68 g/dL, $P = 0.383$), mean platelet count (319,770 ± 115,450 versus 323,940 ± 115,630 cells/μL, $P = 0.812$), mean leukocyte count (9,490 ± 3,360 versus 9,690 ± 3,510 cells/μL, $P = 0.696$) and mean lactate dehydrogenase (LDH) level (394 ± 329 versus 365 ± 346 units/L, $P = 0.595$).

Next, a possible influence of the proportion of FHIT-positive tumor cells was examined. Patients with 1% to 25% FHIT-expressing tumor cells had a similar poor prognosis as those patients with a complete lack of FHIT with a median survival of 87 ± 80 and 157 ± 18 days ($P = 0.165$), respectively. In contrast, median survival of the patients was improved when more than 25% of the tumor cells were FHIT positive. Similar median survival of 203 ± 40, 210 ± 52, and 217 ± 25 days was found for those tumors showing a FHIT-positive cell proportion of >25 to 50%, >50 to 75%, and >75% ($0.644 < P < 0.934$), respectively (Fig. 3*A*). Consequently, two groups were compared to evaluate the quantitative impact of FHIT expression in SCLC: tumors with a FHIT-positive cell proportion of ≤25% and >25%. A significant difference in median survival of 155 ± 21 versus 217 ± 19 days was observed for the two groups ($P = 0.0016$), respectively (Fig. 3*B*). Both groups did not show statistical differences with respect to parameters such as patients' gender, age, smoking status, performance status, tumor stage, cycles of chemotherapy, hemoglobin level, platelet or leukocyte count, or level of LDH.

**Clinical Parameters and FHIT Expression in Multivariate Analysis.** Next to FHIT status, other clinical parameters were also related to survival such as performance status, LDH, leukocyte count, and TNM classification using Kaplan-Meier analysis (data not shown). To evaluate whether FHIT is an independent prognostic parameter, a multivariate analysis was done using the forward selection model of the Cox regression. According to Pearson bivariant correlation analysis FHIT expression was not correlated to any other clinical variable and no statistical differences were found between the patients with FHIT-positive and FHIT-negative tumors using two-sided *t* test. The following 11 variables were included for multivariate analysis: gender (male versus female), age (≤60 versus >60 years), smoking status (smokers versus nonsmokers), performance status (classified into WHO 0 versus 1 versus 2 versus 3), tumor stage (classified into stage I versus II versus III versus IV), hemoglobin level (<12 versus ≥12 mg/dL), platelet count (<150,000/μL, 150,000-400,000/μL, and >400,000/μL) and leukocyte count (<3,500/μL, 3,500-11,000/μL, >11,000/μL), LDH (classified into serum levels <240 versus ≥240 units/L) as well as qualitative (FHIT positive versus negative) and quantitative FHIT expression (FHIT-expressing tumor cell proportion of <25% versus ≥25%). As a result, only FHIT-positive tumor cell proportion ($P = 0.028$), LDH ($P = 0.012$), tumor stage ($P = 0.001$), and performance status ($P < 0.0001$) were identified as independent prognostic parameters by the Cox regression model (Table 2). Of interest, the qualitative presence of FHIT was significant ($P < 0.05$) but not chosen as an explanatory, independent variable in the Cox regression model, whereas hemoglobin level, thrombocyte count, gender, age or smoking status were irrelevant with regard to survival time ($P > 0.05$).

## DISCUSSION

In this study we show that 61.8% of 225 SCLC tumors examined by immunohistochemistry were positive for FHIT expression. To our knowledge, only three reports refer to the presence of FHIT in SCLC. Sozzi et al. (11) examined 13 primary SCLC tumors and 10 cell lines with 4 (30%) primary cases and 2 (20%) cell lines showing FHIT expression using Western blot or immunohistochemical methods. Two other reports by Pylkkänen et al. (9) and Otterson et al. (10) found higher percentages of FHIT-expressing tumors: 13 (46.4%) of 28 SCLC cell lines and 2 (50%) of 4 primary SCLCs were positive. Our study, which is in line with the results of Pylkkänen et al. and Otterson et al., indicate that the percentage of FHIT-expressing tumors in SCLC is similar to the group of adenocarcinomas of NSCLC ranging between 43% and 71% (14–17). Interestingly, in NSCLCs FHIT expression is related to tumor histology with significant lower FHIT expression in squamous cell carcinomas that were 3.6% to 42% FHIT positive (14–17).

Next, the impact of FHIT on survival in SCLC was examined. Loss of FHIT expression was significantly associated with poorer prognosis for patients with SCLC showing a median survival of 157 ± 18 days compared with 210 ± 18 days for patients with FHIT-positive tumors. Of interest, comparing survival of the patient group with weak and strong FHIT tumor expression, no statistical difference with regard to median survival was seen. This result indicates that the expression level of FHIT was irrelevant for prognosis. As a result, weakly expressing FHIT tumor cells must be graded as positive to use FHIT as a prognostic marker. Furthermore, the proportion of FHIT-positive tumor cells within the tumor had an impact on survival. Patients with ≤ 25% of FHIT-positive tumor cells had unfavorable prognosis, showing a median survival of 155 ± 21 days compared with 217 ± 19 days for patients with a FHIT-positive cell proportion of >25%. The prognostic significance of FHIT expression and survival was confirmed using Cox regression multivariate analysis. The presence of FHIT expression was an independent prognostic factor ($P = 0.028$) next to performance status, tumor stage, and LDH. Although the mean survival difference of 2 months between the FHIT-positive and FHIT-negative patient group seems marginal on first glance, one has to consider that the overall mean survival time of all patients with SCLC is 6.5 months. In this context, a predictive marker like FHIT might be

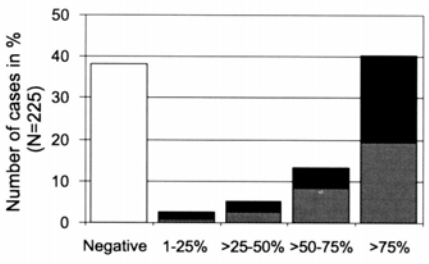


*Fig. 2* Proportion of FHIT-positive tumor cells and FHIT staining intensities of SCLC in percent ($N = 225$). *White column,* FHIT-negative cases; *light gray and black bars,* weakly and strongly stained SCLC tumors, respectively.

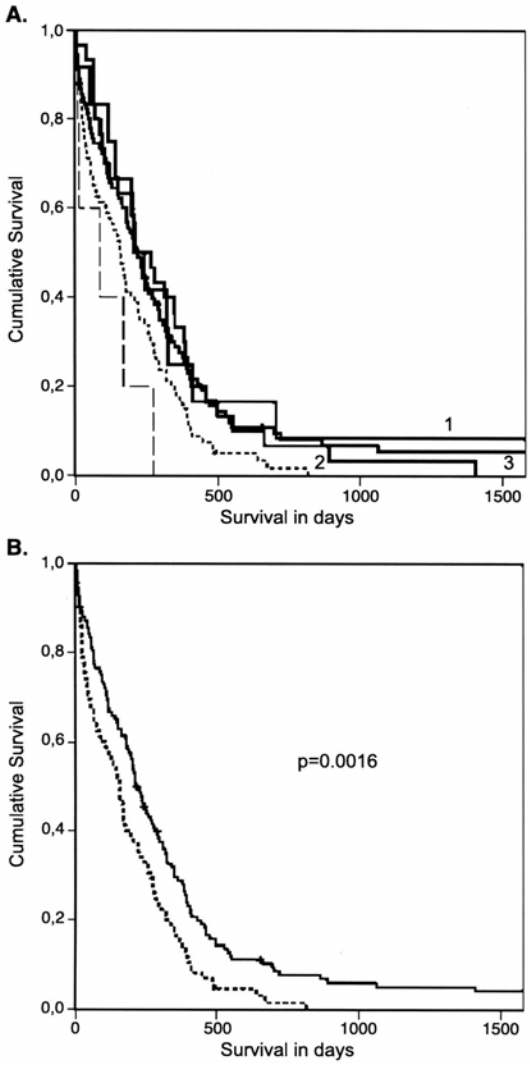


*Fig. 3* Association of the proportion of FHIT-positive cells within the SCLC tumor and survival. *A,* different survival curves of patients were shown with regard to proportion of FHIT-expressing cells. Patients with a complete lack (*dotted line*) or with ≤ 25% FHIT-expressing cells (*dashed line*) had the worst survival of 157 ± 18 and 87 ± 80 days ($P = 0.165$), respectively. Survival was improved when the proportion of FHIT-expressing tumor cells were >25% (*solid lines*). For those tumors showing a FHIT-positive cell proportion of >25% to 50% (*solid line 1*), >50% to 75% (*solid line 2*), and >75% (*solid line 3*), no differences in median survival of 203 ± 40, 210 ± 52, and 217 ± 25 days were found, respectively ($0.644 < P < 0.934$). *B,* comparison of survival curves for patients with a tumor proportion of FHIT-expressing cells of ≤ 25% including negative cases (*dotted line*) and >25% (*solid line*).

valuable to come to a decision on the still controversially discussed question of whether a patient with very limited stage SCLC should be treated with adjuvant chemotherapy or radiation after a histologically confirmed R0 resection of the tumor. Similar to our results, Toledo et al. (15) recently examined 98 primary NSCLCs with regard to FHIT expression and found a poorer survival of patients with lack of FHIT for patients with NSCLCs. Tomizawa et al. (17) reported a significant correlation between FHIT expression and improved survival in 105 NSCLC stage I tumors. These and our data underline the role of *FHIT* as an important gene in lung cancer biology with impact on survival, irrespective of histologic lung tumor subtype.

Several recent studies provide support for a functional activity of *FHIT* as a tumor-suppressing gene. Fifty-three percent of homozygous (−/−) FHIT-deficient mice developed spontaneous tumors within 2 years of follow-up compared with 8% of animals expressing wild-type FHIT (18). Further evidence supporting the hypothesis that FHIT has tumor-suppressing activity is based on gene transfer experiments. Adenoviral vector–mediated replacement of wild-type *FHIT* gene (Ad-FHIT) in lung cancer cell lines that lacked endogenous *FHIT* gene expression significantly reduced cell growth up to 80%, whereas normal human bronchial epithelial cells remained unaffected. Furthermore, lung tumor growth in nude mice that received intratumoral injections of Ad-FHIT was suppressed by 85% to 90% compared with control vector (8). Although FHIT-mediated growth suppression was associated with a $G_0$-$G_1$ arrest of lung cancer tumor cells and an induction of apoptosis (6) the exact molecular pathway of FHIT action is still unclear. Recently it was shown that FHIT is the physiologic target of the protein kinase Src (19). Furthermore, the apoptotic, p53-independent function of FHIT is mediated by the disruption of the inner mitochondrial transmembrane potential with the release of cytochrome *c* protein (5). FHIT protein is a diadenosine-tetraphosphate hydrolase and hydrolyzes diadenosine nucleotides into ADP and AMP. All conserved histidines are required for full activity and the central histidine of the triad is essential for hydrolase activity (20). Surprisingly, a hydrolase "dead" mutant gene also suppressed tumorigenicity in cancer cells and nude mice (21). Therefore, it has been suggested that FHIT binding to a thus far unknown effector or interacting protein forms a complex that acts as the tumor-suppressor molecule (4) possibly involved in apoptosis (6, 19), DNA cytoskeleton assembly (22), and repair machinery (23).

*Table 2* Variables accepted in the forward selection model of the Cox regression as explanatory factors

| | *P** |
|---|---|
| Percentage of tumor cells expressing FHIT† | 0.028 |
| Stage‡ | 0.001 |
| Performance status§ | <0.0001 |
| LDH‖ | 0.012 |

*According to the score test.

†Proportion of FHIT-positive cells within SCLC tumor of 0% to 25% versus >25% to 100%.

‡According to the TNM system: stage I versus II versus III versus IV.

§Performance status according to WHO: 0 versus I versus II versus III.

‖LDH serum levels ≤240 versus >240 units/L.

In conclusion, our data show that FHIT expression is present in 61% of SCLCs. The presence of FHIT was associated with a significant improved outcome for patients with SCLC, indicating that FHIT signaling plays an important role in lung cancer biology.

## REFERENCES


1. Wistuba II, Behrens C, Virmani AK, et al. High resolution chromosome 3p allelotyping of human lung cancer and preneoplastic/preinvasive bronchial epithelium reveals multiple, discontinuous sites of 3p allele loss and three regions of frequent breakpoints. Cancer Res 2000;60:1949–60.

2. Wistuba II, Gazdar AF, Minna JD. Molecular genetics of small cell lung carcinoma. Semin Oncol 2001;28:3–13.

3. Ohta M, Inoue H, Cotticelli MG, et al. The FHIT gene, spanning the chromosome 3p14.2 fragile site and renal carcinoma-associated t(3;8) breakpoint, is abnormal in digestive tract cancers. Cell 1996;84:587–97.

4. Pace HC, Garrison PN, Robinson AK, et al. Genetic, biochemical, and crystallographic characterization of Fhit-substrate complexes as the active signaling form of Fhit. Proc Natl Acad Sci U S A 1998;95:5484–9.

5. Askari MD, Vo-Dinh T. Implication of mitochondrial involvement in apoptotic activity of fragile histidine triad gene: application of synchronous luminescence spectroscopy. Biopolymers 2004;73:510–23.

6. Sard L, Accornero P, Tornielli S, et al. The tumor-suppressor gene FHIT is involved in the regulation of apoptosis and in cell cycle control. Proc Natl Acad Sci U S A 1999;96:8489–92.

7. Roz L, Gramegna M, Ishii H, Croce CM, Sozzi G. Restoration of fragile histidine triad (FHIT) expression induces apoptosis and suppresses tumorigenicity in lung and cervical cancer cell lines. Proc Natl Acad Sci U S A 2002;99:3615–20.

8. Ji L, Fang B, Yen N, Fong K, Minna JD, Roth JA. Induction of apoptosis and inhibition of tumorigenicity and tumor growth by adenovirus vector-mediated fragile histidine triad (FHIT) gene overexpression. Cancer Res 1999;59:3333–9.

9. Pylkkänen L, Wolff H, Stjernvall T, et al. Reduced Fhit protein expression and loss of heterozygosity at FHIT gene in tumours from smoking and asbestos-exposed lung cancer patients. Int J Oncol 2002;20:285–90.

10. Otterson GA, Xiao GH, Geradts J, et al. Protein expression and functional analysis of the FHIT gene in human tumor cells. J Natl Cancer Inst 1998;90:426–32.

11. Sozzi G, Tornielli S, Tagliabue E, et al. Absence of Fhit protein in primary lung tumors and cell lines with FHIT gene abnormalities. Cancer Res 1997;57:5207–12.

12. Mountain CF. Revisions in the international system for staging lung cancer. Chest 1997;111:1710–7.

13. Ramp U, Caliskan E, Ebert T, et al. FHIT expression in clear cell renal carcinomas: versatility of protein levels and correlation with survival. J Pathol 2002;196:430–6.

14. Sozzi G, Pastorino U, Moiraghi L, et al. Loss of FHIT function in lung cancer and preinvasive bronchial lesions. Cancer Res 1998;58:5032–7.

15. Toledo G, Sola JJ, Lozano MD, Soria E, Pardo J. Loss of FHIT protein expression is related to high proliferation, low apoptosis and worse prognosis in non-small-cell lung cancer. Mod Pathol 2004;17:440–8.

16. Tseng JE, Kemp BL, Khuri FR, et al. Loss of Fhit is frequent in stage I non-small cell lung cancer and in the lungs of chronic smokers. Cancer Res 1999;59:4798–803.

17. Tomizawa Y, Nakajima T, Kohno T, Saito R, Yamaguchi N, Yokota J. Clinicopathological significance of Fhit protein expression in stage I non-small cell lung carcinoma. Cancer Res 1998;58:5478–83.

18. Zanesi N, Fidanza V, Fong LY, et al. The tumor spectrum in FHIT-deficient mice. Proc Natl Acad Sci U S A 2001;98:10250–5.

19. Pekarsky Y, Garrison PN, Palamarchuk A, et al. Fhit is a physiological target of the protein kinase Src. Proc Natl Acad Sci U S A 2004;101:3775–9.

20. Barnes LD, Garrison PN, Siprashvili Z, et al. Fhit, a putative tumor suppressor in humans, is a dinucleoside 5′,5‴-P1,P3-triphosphate hydrolase. Biochemistry 1996;35:11529–35.

21. Siprashvili Z, Sozzi G, Barnes LD, et al. Replacement of Fhit in cancer cells suppresses tumorigenicity. Proc Natl Acad Sci U S A 1997;94:13771–6.

22. Chaudhuri AR, Khan IA, Prasad V, Robinson AK, Luduena RF, Barnes LD. The tumor suppressor protein Fhit. A novel interaction with tubulin. J Biol Chem 1999;274:24378–82.

23. Andachi H, Yashima K, Koda M, et al. Reduced Fhit expression is associated with mismatch repair deficiency in human advanced colorectal carcinoma. Br J Cancer 2002;87:441–5.